UNIVERSIDADE FEDERAL DO AMAZONAS

DEPARTAMENTO DE QUÍMICA

PÓS-GRADUAÇÃO EM QUÍMICA

ÁREA DE CONCENTRAÇÃO: QUÍMICA ORGÂNICA

RMN COMO FERRAMENTA PARA AVALIAR A INFLUÊNCIA DA SAZONALIDADE NO PERFIL METABOLÔMICO DE *EUGENIA PUNICIFOLIA* (KUNTH) DC. (MYRTACEAE)

KIDNEY DE OLIVEIRA GOMES NEVES

Doutorado

Manaus - AM

2025

KIDNEY DE OLIVEIRA GOMES NEVES

RMN COMO FERRAMENTA PARA AVALIAR A INFLUÊNCIA DA SAZONALIDADE NO PERFIL METABOLÔMICO DE *EUGENIA PUNICIFOLIA* (KUNTH) DC. (MYRTACEAE)

Tese de Doutorado ao Programa de Pós-Graduação em Química da Universidade Federal do Amazonas exigida para o título de doutorado em Química, com ênfase na linha de pesquisa em Produtos Naturais e Biomoléculas.

ALAN DIEGO DA CONCEIÇÃO SANTOS

Orientador

MARCOS BATISTA MACHADO

Coorientador

Manaus - AM

2025

Ficha Catalográfica

Elaborada automaticamente de acordo com os dados fornecidos pelo(a) autor(a).

N518r Neves, Kidney de Oliveira Gomes
RMN como ferramenta para avaliar a influência da sazonalidade no perfil metabolômico de Eugenia punicifolia (Kunth) DC. (Myrtaceae) / Kidney de Oliveira Gomes Neves. - 2025.
123 f. : il., color. ; 31 cm.

Orientador(a): Alan Diego da Conceição Santos.
Coorientador(a): Marcos Batista Machado.
Tese (doutorado) - Universidade Federal do Amazonas, Programa de Pós-Graduação em Química, Manaus, 2025.

1. Eugenia punicifolia. 2. Sazonalidade. 3. RMN. 4. Análise multivariada. 5. Atividades farmacológicas. I. Santos, Alan Diego da Conceição. II. Machado, Marcos Batista. III. Universidade Federal do Amazonas. Programa de Pós-Graduação em Química. IV. Título

---

RMN como ferramenta para avaliar a influência da sazonalidade no perfil metabolômico de Eugenia punicifolia (Kunth) DC. (Myrtaceae)

KIDNEY DE OLIVEIRA GOMES NEVES

Tese de Doutorado submetida ao Programa de Pós-Graduação em Química, do Instituto de Ciências Exatas da Universidade Federal do Amazonas como requisito parcial para a obtenção do Grau de Mestre (a) em Química.

Aprovado em, 28 de fevereiro de 2025.

ALAN DIEGO DA CONCEIÇÃO SANTOS (PPGQ/UFAM)
Presidente/Orientador

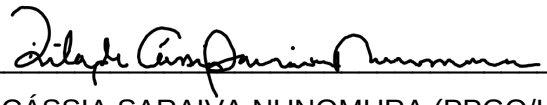

RITA DE CÁSSIA SARAIVA NUNOMURA (PPGQ/UFAM)
Membro Interno

GLAUCIA BRAZ ALCANTARA (UFMS)
Membro Externo

MARCO ANTONIO DOS SANTOS FARIAS (UFSCAR)
Membro Externo

ANDERSSON BARISON (UFPR)
Membro Externo

Universidade Federal do Amazonas
Manaus, 28 de fevereiro de 2025.

Dedico esta tese a todos que estiveram ao meu lado ao longo desta jornada.

AGRADECIMENTOS

Agradeço, acima de tudo, a Deus, que me concedeu o dom da vida.

Aos meus pais, Ediney Neves e Elianay Neves, que sacrificaram seus sonhos para que eu pudesse realizar os meus.

À minha amada esposa, Carla Santos, que, com sua companhia, me mostrou que há luz mesmo nos dias mais escuros.

Aos meus irmãos, Kiandro Neves, Kilder Neves e Kedson Neves, por sempre acreditarem em mim.

Ao meu orientador, Prof. Dr. Alan Diego da Conceição Santos, por acreditar no meu potencial, pela paciência, dedicação, pelos ensinamentos e, principalmente, pela oportunidade de realizar este sonho.

Ao meu coorientador, Prof. Dr. Marcos Batista Machado, por todos os ensinamentos, paciência e, acima de tudo, pela amizade.

Aos meus grandes amigos, Samuel Oliveira e Marinildo Silva, por todos os momentos divertidos.

Ao Prof. Dr. Francisco Célio, que sempre auxiliou na coleta do material botânico.

Ao Prof. Dr. Cláudio Tormena e sua equipe, que me receberam com grande acolhimento em seu laboratório.

À Profa. Dra. Jaqueline de Araújo e sua equipe, pelo inestimável apoio e colaboração.

À Universidade Federal do Amazonas, ao Programa de Pós-Graduação em Química e à Central Analítica, pela oportunidade de realizar esta tese.

À Coordenação de Aperfeiçoamento de Pessoal de Nível Superior (CAPES), à Fundação de Amparo à Pesquisa do Estado do Amazonas (FAPEAM), à Financiadora de Estudos e Projetos (FINEP) e ao Conselho Nacional de Desenvolvimento Científico e Tecnológico (CNPq), pelo suporte financeiro a esta tese.

A todas as pessoas que contribuíram para a realização deste trabalho.

RESUMO

A *Eugenia punicifolia* (Kunth) DC., uma espécie da família Myrtaceae, é amplamente utilizada como fitoterápico para o tratamento de doenças associadas a processos oxidativos. Estudos sobre sua composição química indicam um perfil metabólico complexo e rico em compostos fenólicos bioativos, os quais variam significativamente sob a influência de fatores ambientais. Avaliar o perfil metabólico em função da sazonalidade é um desafio, pois as variações podem ocorrer qualitativa e/ou quantitativamente, tornando necessário o uso de técnicas analíticas versáteis e reprodutíveis, como a Ressonância Magnética Nuclear (RMN). Nesse contexto, o presente estudo teve como objetivo verificar, por meio da RMN associada a análises multivariadas, o impacto da sazonalidade sobre o perfil metabólico e os potenciais antioxidante, antiviral e antiglicante de diferentes extratos das folhas de *Eugenia punicifolia*. Os perfis metabólicos foram obtidos utilizando RMN e CLAE-DAD-EM. As análises de PCA e PLS-DA foram realizadas utilizando os espectros de RMN de ^{1}H. As propriedades farmacológicas dos extratos foram avaliadas em relação à viabilidade celular, capacidade de eliminação dos radicais livres ($DPPH^{\bullet}$ e $ABTS^{\bullet+}$), inibição da formação dos produtos finais da glicação avançada (AGEs) e da infecção pelo vírus Zika. A análise do perfil químico permitiu a identificação de 19 compostos pertencentes às classes dos ácidos orgânicos, flavonoides e carboidratos. A partir da análise de PCA, juntamente com o modelo de PLS-DA validado, foi possível classificar as amostras com base no período de coleta (seca, chuvoso e de transição), permitindo identificar como fatores ambientais desempenham um papel crucial na regulação da biossíntese de compostos fenólicos. A análise dos potenciais antioxidante, antiglicante e antiviral evidenciou que o sistema extrator é determinante para a resposta observada, com as amostras coletadas no período chuvoso e extraídas com o sistema metanol:etanol:água (MEA) apresentaram os melhores resultados. Portanto, este estudo fornece descobertas significativas sobre o perfil metabólico e farmacológico das folhas de *Eugenia punicifolia*, ao mesmo tempo em que oferece uma base para otimizar os períodos de coleta, visando maior rendimento de compostos bioativos.

Palavras-chave: *Eugenia punicifolia*, sazonalidade, RMN, análise multivariada, atividades farmacológicas.

ABSTRACT

Eugenia punicifolia (Kunth) DC., a species of the Myrtaceae family, is widely used as a phytotherapeutic agent for the treatment of diseases associated with oxidative processes. Studies on its chemical composition indicate a complex metabolic profile rich in bioactive phenolic compounds, which vary significantly under the influence of environmental factors. Evaluating the metabolic profile in relation to seasonality is challenging, as variations can occur qualitatively and/or quantitatively, making it necessary to use versatile and reproducible analytical techniques such as Nuclear Magnetic Resonance (NMR). In this context, the present study aimed to verify, through NMR associated with multivariate analyses, the impact of seasonality on the metabolic profile and the antioxidant, antiviral, and antiglycant potentials of different extracts from *Eugenia punicifolia* leaves. The metabolic profiles were obtained using NMR and HPLC-DAD-MS. PCA and PLS-DA analyses were performed using ^{1}H NMR spectra. The pharmacological properties of the extracts were evaluated in relation to cell viability, free radical scavenging capacity ($DPPH^{\bullet}$ and $ABTS^{\bullet+}$), inhibition of advanced glycation end-products (AGEs) formation, and Zika virus infection. The chemical profile analysis allowed the identification of 19 compounds belonging to the classes of organic acids, flavonoids, and carbohydrates. Through PCA analysis, along with the validated PLS-DA model, it was possible to classify the samples based on the collection period (dry, rainy, and transition), enabling the identification of how environmental factors play a crucial role in regulating the biosynthesis of phenolic compounds. The analysis of antioxidant, antiglycant, and antiviral potentials highlighted that the extraction system is a determining factor in the observed response, with samples collected during the rainy season and extracted using the methanol:ethanol:water (MEW) system showing the best results. Therefore, this study provides significant findings on the metabolic and pharmacological profile of *Eugenia punicifolia* leaves while offering a foundation for optimizing collection periods to achieve higher yields of bioactive compounds.

Keywords: *Eugenia punicifolia*, seasonality, NMR, multivariate analyses, pharmacological activities.

LISTA DE ABREVIATURAS E SIGLAS

1D - Unidimensional

2D - Bidimensional

$ABTS^{\bullet+}$ - Ácido 2,2′-azino-bis(3-etilbenzotiazolina-6-sulfônico)

AGEs - produtos finais de glicação avançada

AQ - *Acquisition Time*

CLAE-DAD-EM - Cromatografia Líquida de Alta Eficiência com Detecção por Arranjo de Diodos e Espectrometria de Massas

COSY - *COrrelation SpectroscopY*

D1 – tempo de relaxação

d - Dubleto

dd - Duplo dupleto

D_2O - Óxido de deutério

DMSO - Dimetilsulfóxido

DMSO-*d*6 - Dimetilsulfóxido deuterado

$DPPH^{\bullet}$ - 2,2-difenil-1-picrilhidrazil

EM - Espectrometria de Massas

ESI-MS - *Electrospray Ionization Mass Spectrometry*

EtOH - Etanol

HMBC - *Heteronuclear Multiple Quantum Correlation*

HSQC edit - *Heteronuclear Single Quantum Coherence edited*

J - Constante de acoplamento

m - Multipleto

MeOD - Metanol deuterado

MeOH - Metanol

MS/MS - *Tandem Mass Spectrometry*

m/z - Relação massa/carga

NS - *Number of Scans*

P1 - Pulso de 90º

PCA - *Principal Component Analysis*

PLS-DA - *Partial Least Squares Discriminant Analysis*

qNMR – *quantitative Nuclear Magnetic Resonance*

RMN - Ressonância Magnética Nuclear

RG - *Receiver Gain*

s - *Sinpleto*

SW - *Spectral Width*

T1 - Tempo de relaxação longitudinal

TD - *Time Domain*

TMS - Tetrametilsilano

TMSP-*d*4 – TriMetilSilil-2,2,3,3-*d*4 Propionato de sódio

ZIKV - vírus Zika

zg - Sequência de único pulso de 90º (convencional)

zgpr - Sequência de pulso de 90º com supressão de um sinal

LISTA DE FIGURAS

SUMÁRIO

1. INTRODUÇÃO

A família Myrtaceae está entre as maiores e mais relevantes das angiospermas encontradas no Brasil.[1] Suas espécies apresentam um vasto potencial econômico, pois seus frutos, como os de *Psidium guajava* (goiabeira) e *Eugenia uniflora* (pitanga), são amplamente comercializados na forma de sucos, geleias, sorvetes e *in natura*.[2] Além disso, as folhas de algumas espécies são utilizadas na produção de medicamentos fitoterápicos, como as de *Eugenia punicifolia* (Kunth) DC. e *Myrcia citrifolia* (Lam) DC.[3]

Na região amazônica, um grupo de espécies de Myrtaceae, popularmente conhecido como "pedra-ume-caá", é amplamente comercializado como medicamento fitoterápico para o tratamento da diabetes.[4] Esse grupo inclui as espécies *Myrcia multiflora* (Lam.) DC., *Myrcia guianensis* (Aubl.) DC., *Myrcia citrifolia* (Aubl.) Urb., *Myrcia uniflora* DC., *Eugenia uniflora* L., *Eugenia biflora* (L.) DC. e *Eugenia punicifolia* (Kunth) DC.[3; 5]

Dentre essas espécies, estudos sobre o perfil químico e o potencial farmacológico das folhas de *Eugenia punicifolia* (Kunth) DC. indicam que suas atividades antioxidante, anti-inflamatória e antiglicante estão associadas à presença de compostos fenólicos pertencentes às classes dos ácidos orgânicos e flavonoides.[4; 6; 7] Entretanto, a concentração e/ou a presença desses compostos variam em função de fatores bióticos e abióticos relacionados à sazonalidade, tornando essencial o desenvolvimento de abordagens que permitam monitorar a variação dos metabólitos secundários ao longos das estações e, quando necessário, determinar os períodos de coleta com alta produção dos compostos bioativos.[8; 9]

Do ponto de vista biossintético, quando expostas a diferentes tipos de estresse abiótico, as plantas tendem a produzir metabólitos que contribuem para seus mecanismos de defesa.[10; 11; 12] Dentre esses, os compostos fenólicos desempenham um papel fundamental na resistência a condições ambientais extremas. Flavonoides, amplamente reconhecidos por suas propriedades farmacológicas, são essenciais para mitigar o estresse oxidativo induzido por fatores ambientais, protegendo as células vegetais. Sua capacidade de neutralizar radicais livres, estabilizar membranas celulares e regular vias de resposta ao estresse minimiza danos causados por condições adversas.[10; 13; 14]

Compreender a influência dos fatores ambientais no perfil metabólico das plantas é um desafio, pois, dependendo do tipo de estresse (abiótico e/ou biótico) ao qual

elas são submetidas, sua composição química pode apresentar variações qualitativas e quantitativas. Para isso, o uso de técnicas analíticas avançadas, como a espectroscopia de Ressonância Magnética Nuclear (RMN), é essencial na caracterização e quantificação de metabólitos em matrizes vegetais.[15; 16; 17] A integração dessa técnica com abordagens estatísticas permite explorar, de forma mais eficiente, a influência dos fatores ambientais na biossíntese de compostos bioativos. [10; 18; 19]

Dentre essas abordagens, destaca-se o uso de análises multivariadas, que desempenham um papel fundamental na interpretação dos dados de RMN ao identificar padrões e tendências específicas. Nesse contexto, a análise de componentes principais (PCA) e a análise discriminante por mínimos quadrados parciais (PLS-DA) são amplamente empregadas para avaliar a influência da sazonalidade no perfil metabolômico de plantas. A PCA reduz a dimensionalidade dos dados espectrais, facilitando a identificação de padrões sazonais.[20] Enquanto isso, a PLS-DA, quando corretamente construída e validada, aprimora a discriminação entre amostras coletadas em diferentes períodos, identificando metabólitos diferenciadores com maior precisão.[21; 22] A combinação dessas técnicas proporciona uma interpretação mais robusta dos dados, auxiliando na correlação entre fatores ambientais e a biossíntese de compostos bioativos.

Portanto, este estudo teve como objetivo utilizar a RMN associada à análise multivariada para avaliar a influência da sazonalidade sobre o perfil metabólico e as potenciais bioatividades (antioxidante, antiglicante e antiviral) dos extratos das folhas de *Eugenia punicifolia* (Kunth) DC. coletadas em diferentes meses dos anos de 2021 e 2023, a fim de fornecer uma abordagem eficaz para otimizar os períodos de colheita e maximizar o rendimento de compostos fenólicos bioativos.

2. OBJETIVOS

2.1. Objetivo Geral

Avaliar a influência da sazonalidade sobre o perfil metabolômico de extratos das folhas de *Eugenia punicifolia* (Kunth) DC., utilizando experimentos qualitativos e quantitativos de RMN associados a análises multivariadas, bem como determinar a relação desses perfis metabólicos com os respectivos potenciais antioxidante, antiglicante e antiviral.

2.2. Objetivos específicos

- Avaliar a eficiência dos sistemas de solventes na extração dos compostos presentes nas folhas de *E. punicifolia*;
- Identificar, por ressonância magnética nuclear e cromatografia líquida acoplada à espectrometria de massas, os principais constituintes presentes nos diferentes extratos das folhas de *E. punicifolia*;
- Determinar a viabilidade celular e os potenciais antioxidante, antiglicante e antiviral dos diferentes extratos das folhas de *E. punicifolia*.
- Determinar a concentração, por RMN de ^{1}H (PULCON), dos principais compostos associados às atividades antioxidante, antiglicante e antiviral nos diferentes extratos das folhas de *E. punicifolia*;
- Desenvolver um modelo quimiométrico capaz de classificar as amostras em função dos períodos de coleta e identificar quais metabólitos podem ser utilizados como possíveis marcadores químicos em resposta aos fatores ambientais;
- Determinar como os fatores ambientais influenciam a produção de compostos bioativos nas folhas de *E. punicifolia*.

3. REVISÃO BIBLIOGRÁFICA

3.1. Myrtaceae e as espécies de pedra-ume-caá

Representando uma das maiores famílias da flora brasileira, Myrtaceae está distribuída em 26 gêneros, com aproximadamente 1000 espécies já catalogadas.[1] Entre as regiões do Brasil, a Floresta Atlântica e as áreas de Restinga apresentam a maior diversidade de espécies, sendo estas predominantemente dos gêneros *Marlierea*, *Gomidesia*, *Myrcia* e *Eugenia*. Devido à sua ampla distribuição e composição química diversificada, suas espécies são amplamente empregadas na produção de alimentos e medicamentos fitoterápicos, agregando alto valor comercial à família.

Nesse contexto, dentro da família Myrtaceae, um grupo de espécies denominado pedra-ume-caá é utilizado na formulação de medicamentos fitoterápicos voltados para o tratamento e prevenção de diversas condições, incluindo diabetes, diarreia, hemorragia, febre, reumatismo, colesterol alto, leucemia, herpes e úlceras bucais.[4] Esse grupo é composto pelas espécies *Myrcia multiflora* (Lam.) DC., *Myrcia guianensis* (Aubl.) DC., *Myrcia citrifolia* (Aubl.) Urb., *Myrcia uniflora* DC., *Eugenia uniflora* L., *Eugenia biflora* (L.) DC. e *Eugenia punicifolia* (Kunth) DC. (**Figura 1**).[3; 23]

Figura 1. Espécies de pedra-ume-caá.

Estudos farmacológicos têm associado a presença de triterpenos pentacíclicos, flavonoides e ácidos orgânicos às atividades biológicas relatadas para as espécies de *pedra-ume-caá*, tais como atividades antidiabética, antisséptica, anti-inflamatória, antimicrobiana e antioxidante, além de outras descritas na **Tabela 1**.

Tabela 1. Propriedades biológicas das espécies de pedra-ume-caá.

Espécie	Propriedades farmacológicas	Referências
Myrcia multiflora (Lam.) DC.	Inibição da aldose redutase e a-glucosidase	24
Myrcia guianensis (Aubl.) DC.	Atividade antifúngica, antioxidante e antibacteriana	25; 26
Myrcia citrifolia (Aubl.) Urb.	Antibacteriana	27
Myrcia uniflora DC.	Antimicrobiana, inseticida e antioxidante	23; 28
Eugenia uniflora L.	Atividade antimicrobiana, anti-inflamatória e anti-hipertensivo	29; 30; 31
Eugenia biflora (L.) DC.	Antioxidante, hipoglicêmica e Citotoxicidade	26; 32
Eugenia punicifolia DC.	Atividade hipoglicêmica, anti-inflamatória e antioxidante	4; 7; 29; 32

Contudo, ainda há poucos estudos químicos e farmacológicos sobre as espécies de pedra-ume-caá, especialmente sobre *Eugenia punicifolia* (Kunth) DC. De acordo com o levantamento bibliográfico, seus frutos e folhas apresentam uma composição química rica em substâncias diretamente associadas às principais atividades farmacológicas já identificadas para as espécies de pedra-ume-caá.[4; 32; 33]

3.2. Composição química e propriedades farmacológica da *Eugenia punicifolia*.

Eugenia punicifolia (Kunth) DC. é um arbusto nativo encontrado em diversas regiões do Brasil, especialmente na região amazônica. Na cidade de Manaus, suas folhas são utilizadas na medicina tradicional, em forma de decocções ou infusões, como agente terapêutico natural para o tratamento da diabetes mellitus.[4; 7; 34] Estudos comprovam que, além da atividade antidiabética, essa espécie também apresenta atividades anti-inflamatória e antioxidante, e que esse potencial farmacológico se deve à presença de ácidos triterpênicos e compostos fenólicos encontrados em suas folhas e frutos.[4; 6; 30]

A fim de avaliar o perfil químico e os potenciais farmacológicos de *E. punicifolia* (Kunth) DC., o estudo desenvolvido por Teixeira (2021) demonstrou que suas folhas contêm ácido barbinérvico, um composto com efeito vasodilatador e potencial para ser utilizado como modelo no desenvolvimento de novas moléculas para o tratamento de doenças cardiovasculares.[35; 36] Além disso, Ramos (2019) comprovou que os frutos apresentam

atividades antiglicante e antioxidante, que podem estar associadas à presença dos compostos ácido elágico, miricetina-3-O-ramnosídeo, quercetina-3-O-ramnosídeo e kaempferol-3-O-ramnosídeo.[4]

O estudo do extrato hidroalcoólico das folhas evidenciou efeitos antinociceptivos, anti-inflamatórios e gastroprotetores, além de possibilitar a identificação, por CLAE-DAD, dos flavonoides quercetina, miricetina e rutina, bem como de galotaninos e derivados do ácido gálico.[7] No estudo de doutorado realizado por Oliveira (2022), a análise por RMN e CLAE-DAD-EM identificou um total de dezoito compostos, entre os quais catequina, miricitrina e quercitrina foram destacados como os principais marcadores químicos dessa espécie, além de estarem associados à inibição enzimática da α-glucosidase. Os compostos já identificados nas folhas e frutos de *E. punicifolia* (Kunth) DC. são apresentados na **Figura 2**.

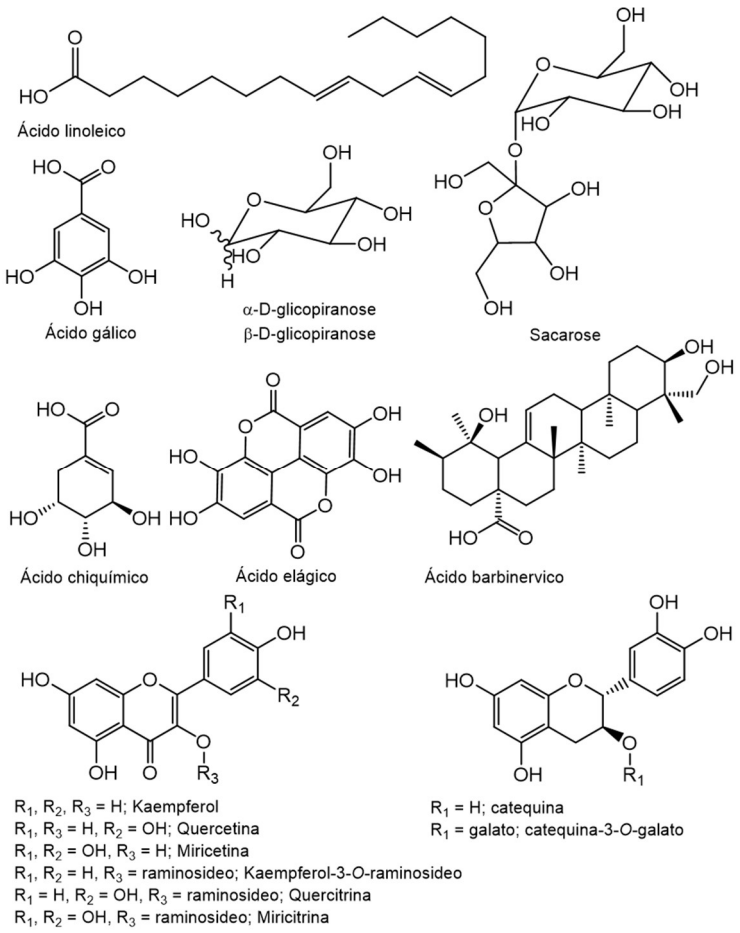

Figura 2. Constituintes químicos identificados nas folhas e frutos de *E. punicifolia* (Kunth) DC.

3.3. Análise do perfil metabólico de matrizes vegetais

O estudo de matrizes vegetais por meio da análise do perfil metabólico tem se mostrado uma abordagem eficiente até os dias atuais, resultando na identificação de substâncias inéditas com potencial para aplicação na área de alimentos ou no desenvolvimento de medicamentos fitoterápicos.[4; 37] Diversas metodologias são empregadas para estudar o perfil metabólico de plantas, sendo a desreplicação e a metabolômica as mais descritas na literatura.[4; 37; 38; 39]

A desreplicação é uma etapa crucial no processo de triagem de extratos brutos, tendo como objetivo determinar o grau de ineditismo das substâncias presentes nesses extratos, evitando, assim, o isolamento e a determinação estrutural de compostos já conhecidos.[4; 37] Já o estudo do perfil metabolômico de extratos brutos de espécies vegetais, utilizando técnicas multivariadas, possibilita a análise de um grande volume de dados, permitindo a correlação entre a composição química das matrizes estudadas, suas atividades farmacológicas e as respostas metabólicas a diferentes estresses ambientais e condições patológicas.[38; 39]

Uma abordagem relevante na área da metabolômica é a investigação da influência da sazonalidade sobre o perfil químico de matrizes vegetais, uma vez que fatores ambientais sazonais, como temperatura, umidade e pluviosidade, impactam diretamente a variação qualitativa e/ou quantitativa dos constituintes químicos presentes nas plantas, influenciando, consequentemente, seus potenciais farmacológicos.[40; 41; 42] Dessa forma, a avaliação da sazonalidade torna-se essencial quando a matriz de interesse possui valor econômico agregado. Nesse contexto, o estudo do perfil químico de *Eugenia punicifolia* (Kunth) DC. em função da sazonalidade pode permitir a identificação do período de coleta ideal para obter a maior concentração de metabólitos responsáveis por seus potenciais farmacológicos.

No entanto, *E. punicifolia* (Kunth) DC. apresenta um perfil metabólico diversificado e complexo, tornando necessário o uso de técnicas analíticas capazes de identificar e quantificar seus constituintes. Dentre as técnicas empregadas para identificação, caracterização e quantificação de compostos orgânicos, a espectroscopia de ressonância magnética nuclear (RMN) destaca-se.[15; 38; 43; 44] Além disso, a análise estatística de dados de RMN de misturas complexas pode direcionar a identificação de compostos bioativos

presentes nas matrizes de interesse, tornando a RMN uma técnica analítica amplamente aplicada no estudo de matrizes vegetais.[45]

3.4. A Ressonância Magnética Nuclear

A espectroscopia de RMN é uma técnica analítica que permite a determinação da estrutura molecular e da composição química de uma amostra por meio da interação da radiação eletromagnética com a matéria. O princípio da técnica baseia-se no fato de que, quando analisados por RMN, os núcleos atômicos com spin diferente de zero ($I \neq 0$) são influenciados pelo campo eletromagnético estático (B_0) gerado pelo equipamento, resultando na mudança da orientação dos spins em relação a B_0, fazendo com que eles precessem em torno do campo magnético principal.[46]

A frequência de precessão (ou frequência de Larmor) dos spins (ν) depende da constante magnetogírica (γ) e da intensidade do campo magnético estático (B_0) aplicado, podendo ser determinada pela **Equação 1**.

Equação 1. $$\nu = \frac{\gamma}{2\pi} Bo$$

Utilizando o átomo de hidrogênio (spin = ½) como exemplo, na ausência de B_0, seus spins nucleares encontram-se em estados degenerados de energia. No entanto, ao serem submetidos a B_0, ocorre a separação desses estados degenerados, resultando na quantização dos níveis de energia e na orientação espacial dos spins. Nesse contexto, os spins passam a adotar dois estados distintos de energia: estado de spin β (maior energia) e estado de spin α (menor energia), conforme exemplificado na **Figura 3**.[46; 47]

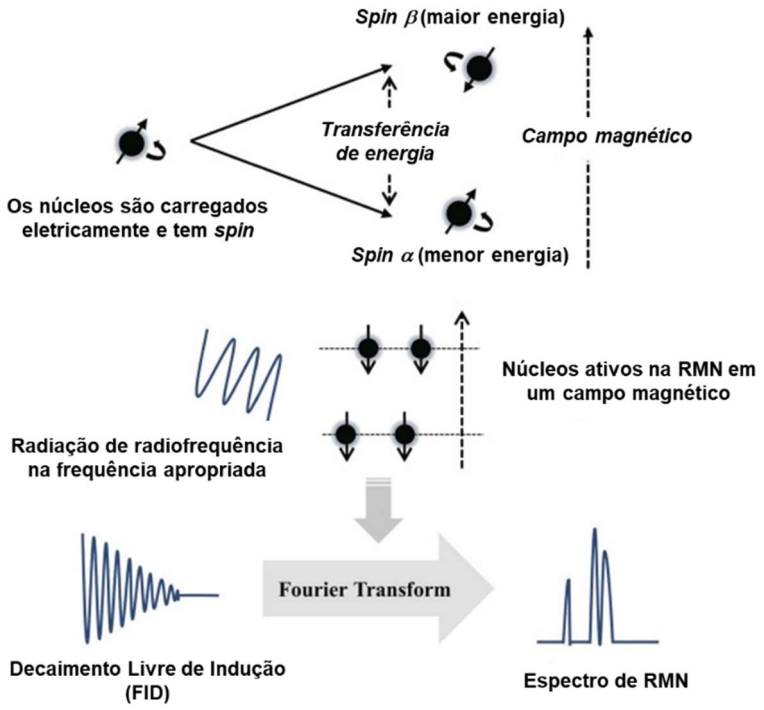

Figura 3. Representação gráfica do princípio da RMN aplicada ao átomo de hidrogênio (adaptado de Nascimento, 2016).

No entanto, o fenômeno da RMN ocorre quando os spins em excesso no estado de menor energia são excitados para o estado de maior energia ao receberem um pulso de radiofrequência. Esse pulso é gerado por um campo oscilante (B_1), perpendicular ao campo magnético principal aplicado, e possui a mesma frequência de precessão determinada pela **Equação 1**.[46]

Após a cessação do campo oscilante, os spins passam por dois mecanismos simultâneos de relaxação: relaxação transversal (T_2, Spin-Spin) e relaxação longitudinal (T_1, Spin-Rede). Esses mecanismos são responsáveis pelo processo de decaimento de energia, denominado Decaimento Livre de Indução (*Free Induction Decay* – FID). O sinal gerado é armazenado no domínio do tempo e convertido para o domínio da frequência por meio da equação matemática conhecida como Transformada de Fourier, permitindo a obtenção de informações essenciais sobre a estrutura dos átomos e moléculas analisadas, como o deslocamento químico e a multiplicidade.[46]

3.5. Quantificação de compostos orgânicos por RMN

A RMN é uma técnica espectroscópica amplamente utilizada na química de produtos naturais, pois, além de fornecer informações estruturais detalhadas, também permite a quantificação de compostos orgânicos de maneira não destrutiva.[48] Diferentemente de outras técnicas quantitativas, a RMN dispensa a necessidade de padrões internos, tornando-se uma alternativa robusta para a determinação absoluta da concentração de analitos. [49; 50; 51]

O princípio da quantificação por RMN baseia-se no fato de que a intensidade do sinal (área do pico de ressonância) é proporcional ao número de núcleos de um determinado elemento na amostra.[49] Essa relação direta entre intensidade e quantidade de núcleos possibilita a determinação quantitativa sem a necessidade de calibração complexa. No entanto, a intensidade do sinal também é influenciada por fatores como tempo de relaxação nuclear, homogeneidade do campo magnético e parâmetros instrumentais, exigindo métodos precisos para garantir a confiabilidade dos resultados.[52; 53]

A dependência da intensidade do sinal em relação ao tempo de relaxação destaca a necessidade de métodos de quantificação que levem em conta essas variáveis. Nesse contexto, o PULCON (*Pulse Length-Based Concentration Determination*) surge como uma abordagem eficiente e amplamente utilizada na quantificação absoluta por RMN.[54] O método PULCON elimina a necessidade de padrões internos ao utilizar um padrão externo previamente quantificado. Esse padrão é registrado sob as mesmas condições experimentais da amostra em análise, permitindo a comparação direta das áreas dos picos de ressonância. Dessa forma, a quantificação absoluta é realizada com base na razão entre as intensidades do sinal da amostra e do padrão, considerando fatores como tempo de relaxação longitudinal (T_1), largura de pulso de radiofrequência e sensibilidade do espectrômetro.[50; 55]

Uma das principais vantagens do PULCON é sua reprodutibilidade e precisão, tornando-o uma ferramenta essencial em diversas áreas. Além disso, a RMN quantitativa, aliada a análises multivariadas, se torna uma abordagem valiosa em estudos metabolômicos de matrizes vegetais.

3.6. Análise Multivariada aplicada aos dados de RMN de ^{1}H

Entre as diversas abordagens das análises multivariadas, a quimiometria se destaca pelo uso de técnicas estatísticas e matemáticas, permitindo uma interpretação mais refinada e precisa dos dados químicos. Essa disciplina é utilizada para tratar problemas complexos em química, onde há uma grande quantidade de informações ou variáveis inter-relacionadas. As técnicas quimiométricas incluem métodos multivariados, como Análise de Componentes Principais (PCA), Análise Discriminante (DA), Regressão Linear Múltipla, Análise Hierárquica de Clusters (HCA), Calibração Multivariada, entre outras. Essas ferramentas permitem a identificação de padrões, redução de dimensionalidade, tratamento de ruído e interferências, além de possibilitar a interpretação de resultados de maneira mais robusta e precisa.[22; 56; 57]

Para análise do perfil metabolômico de plantas, PCA, HCA e PLS-DA (Mínimos Quadrados Parciais - Análise Discriminante) são amplamente utilizadas.[15; 58] A PCA reduz a dimensionalidade dos dados ao projetá-los em um novo espaço formado por componentes principais, permitindo uma visualização e análise dos padrões dos dados. O HCA pode ser utilizada para classificação de amostras em diferentes grupos com base em suas características e, o PLS-DA que é uma extensão do método PLS (*Partial Least Squares*), é frequentemente utilizado para a análise de regressão em dados multivariados que tem como objetivo encontrar componentes que maximizem a variação explicada entre os grupos e minimizem a variação dentro de cada grupo, permitindo uma discriminação mais eficiente que a observada na análise por PCA.[22; 57; 59]

Quanto às técnicas utilizadas para a aquisição de dados na análise quimiométrica, diversos estudos comprovam que a RMN possui vantagens significativas, como a simplicidade no preparo das amostras, já que, na maioria dos casos, não é necessário submetê-las a processos químicos. Além disso, a técnica permite uma aquisição de dados eficiente, reprodutível e de fácil execução.[15, 60] Devido esses fatores, análises quimiométricas utilizando dados de RMN são aplicadas no controle de qualidade de alimentos, na avaliação da influência de fatores biológicos em organismos vivos, e na verificação da influência de fatores sazonais na composição química de matrizes vegetais.[19; 40; 41]

No controle de qualidade de alimentos oriundos de matrizes vegetais, o estudo de Daolio (2007) foi pioneiro ao descrever um método baseado em ressonância magnética

nuclear de ângulo mágico (^{1}H-HR-MAS RMN) associado à análise de componentes principais (PCA) para a análise metabolômica de amostras comerciais de Catuaba. Essa abordagem reduziu significativamente o tempo necessário para analisar um sistema complexo fundamentado em marcadores químicos, permitindo a classificação das amostras com base no tipo de matéria-prima utilizada em sua fabricação[61] Além disso, a combinação da espectroscopia de RMN de ^{1}H com método quimiométrico também permitiu as análises qualitativas e quantitativas de extratos de medicamentos fitoterápicos chineses, resultando na identificação de ácidos fenólicos, saponinas, sacarídeos, ácidos orgânicos e aminoácidos, e na definição dos valores limite para avaliação da qualidade do produto em função de sua composição química.[18]

A fim de avaliar a influência da sazonalidade sobre a composição química e as propriedades medicinais da espécie *Leucosidea seria*, os dados de RMN de ^{1}H foram submetidos a análise de PCA e análise discriminante parcial ortogonal supervisionada por mínimos quadrados (OPLS-DA), onde a PCA mostrou clara separação das estações e o OPLS-DA determinou os compostos que diferenciaram as amostras de primavera das de inverno. Além disso, foi constatado que a variação de suas propriedades medicinais é resultado da diferenciação em sua composição química em função do período do ano.[62]

Portanto, estudos quimiométricos de matrizes vegetais utilizando a RMN, mostra-se como uma importante abordagem para avaliar como a composição química e as propriedades farmacológicas dessas matrizes são influenciados por diferentes fatores ambientais.

3.7. Atividade antioxidante de produtos naturais

Os ensaios antioxidantes são uma forma simples e eficiente de verificar se substâncias e extratos provenientes de matrizes vegetais apresentam a capacidade de inibir substâncias responsáveis por processos oxidativos. A determinação da atividade antioxidante, resultado de reações que envolvem a inibição de substâncias oxidantes e radicais livres presentes em sistemas biológicos, os quais são apontadas como causadores do envelhecimento precoce e de doenças degenerativas relacionadas ao envelhecimento, como câncer, doenças cardiovasculares, declínio do sistema imune e disfunções cerebrais.[63; 64; 65]

Os ensaios de capacidade antioxidante podem ser divididos de acordo com os tipos de reações envolvidas no processo: ensaios baseados nas reações de transferência de átomo de hidrogênio (HAT) e ensaios baseados nas reações de transferência de elétrons (ET).[64; 66] Os ensaios baseados em ET medem a capacidade de um antioxidante em reduzir um oxidante, que, ao ser reduzido, adquire uma coloração diferente. A maioria dos ensaios baseados em HAT aplica um esquema de reações competitivas, nas quais antioxidantes e substratos competem por radicais gerados termicamente através da decomposição de compostos azos.[64] De acordo com o método proposto para analisar a atividade antioxidante, os ensaios ET e HAT podem ser utilizados para determinar a atividade antioxidante de diferente classe de compostos. Com base nisso, esses ensaios são realizados de diferentes maneiras, mas com basicamente a mesma finalidade. No **Quadro 1**, estão classificados os principais tipos de ensaios antioxidantes de acordo com seus mecanismos químicos.[64; 67; 68]

Quadro 1. Principais tipos de ensaios antioxidante baseados em HAT e ET.

Ensaios baseados em HAT	Ensaios baseados em ET
• Inibição induzida de auto oxidação de lipoproteínas de baixa densidade • Capacidade de absorção de radical oxigênio (ORAC) • Parâmetro antioxidante total de aprisionamento radical (TRAP) • Ensaios de branqueamento da crocina.	• Determinação dos fenóis totais por reagente de Folin-Ciocalteu (RFC) • Poder antioxidante de redução do Ferro (FRAP) • Potencial antioxidante total utilizando o íon Cu (II) como oxidante • Captura do radical DPPH$^{\bullet}$ • Monitoramento do decaimento do cátion radical ABTS$^{\bullet+}$

Na área de produtos naturais, os ensaios mais utilizados para determinar a capacidade antioxidante dos extratos e substâncias são aqueles que envolvem a captura do radical DPPH$^{\bullet}$ (2,2-difenil-1picrilhidrazil) e do cátion radical ABTS$^{\bullet+}$ [Ácido 2,2′-azino-bis(3-etilbenzotiazolina-6-sulfônico)].[69; 70; 71] No ensaio de captura do radical DPPH$^{\bullet}$, é possível observar, por espectrofotometria, que a absorbância a 515 nm diminui como resultado de uma alteração na coloração violeta-escura para violeta-clara, uma vez que o

radical é capturado pelas substâncias antioxidantes presentes na amostra, ocorrendo a doação de um átomo de hidrogênio para formar a molécula estável DPPH-H (**Figura 8**).[66; 72]

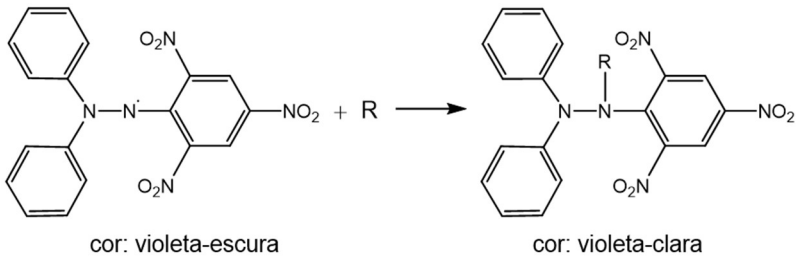

Figura 4. Reação entre a molécula de DPPH• e um antioxidante para formar DPPH reduzido.

O ensaio de descoloração do cátion radical $ABTS^{\bullet+}$ baseia-se na sua redução por substâncias antioxidantes, resultando no decréscimo de sua absorbância ao longo do tempo. A leitura é feita a partir da mistura do radical com o antioxidante em diferentes intervalos de tempo. O valor obtido é conhecido como TEAC (capacidade antioxidante equivalente ao trolox) e fornece uma estimativa da quantidade de moléculas de radicais consumidas pelo antioxidante (**Figura 9**).[64; 66; 73]

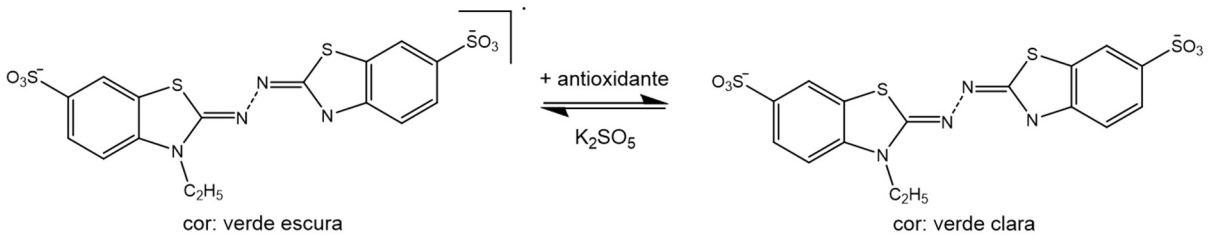

Figura 5. Estabilização do radical ABTS•+ por um antioxidante e sua formação pelo persulfato de potássio.

Devido à sua praticidade e baixo custo, ensaios antioxidantes como a captura do radical $DPPH^{\bullet}$ e o monitoramento do decaimento do cátion radical $ABTS^{\bullet+}$ tornaram-se ferramentas comuns e extremamente necessárias na seleção inicial de substâncias que possam ser utilizadas como fármacos.[74] Além disso, esses ensaios podem auxiliar na escolha das espécies vegetais para estudos químicos e farmacológicos, bem como comprovar a presença de substâncias antioxidantes em alimentos como frutas, legumes e bebidas. Na área de produtos naturais, esses ensaios são amplamente utilizados para determinar a atividade antioxidante de extratos e substâncias isoladas, como compostos fenólicos em geral, fenilpropanoides, flavonoides, cumarinas, antocianinas e carotenoides.[68; 74]

3.8. Atividade Antiglicante

A diabetes mellitus tipo 2 é uma desordem metabólica crônica caracterizada pela hiperglicemia persistente, condição que promove reações de glicação não enzimática envolvendo proteínas e lipídios. Esses processos representam a etapa inicial na formação de produtos finais de glicação avançada (AGEs - *Advanced Glycation End-products*), que desempenham um papel central no desenvolvimento de complicações associadas ao diabetes, como nefropatia, retinopatia e doenças cardiovasculares.[75] Dada a relevância dos AGEs na fisiopatologia dessas complicações, a busca por estratégias que inibam sua formação tem se tornado uma prioridade em diversos estudos farmacológicos.

No organismo, um dos processos de formação dos AGEs tem início a partir de uma reação de adição nucleofílica, na qual ocorre a condensação da cadeia lateral de um aminoácido presente em uma proteína com um grupo carbonila de um carboidrato, resultando em uma carbinolamina intermediária. Esta, por sua vez, sofre desidratação, formando um aduto de imina instável que, devido à sua estrutura, pode sofrer um rearranjo, dando origem a compostos mais estáveis, denominados produtos de Amadori, cuja característica é a geração da função α-amino-carbonila nos açúcares (**Figure 6**).[75; 76]

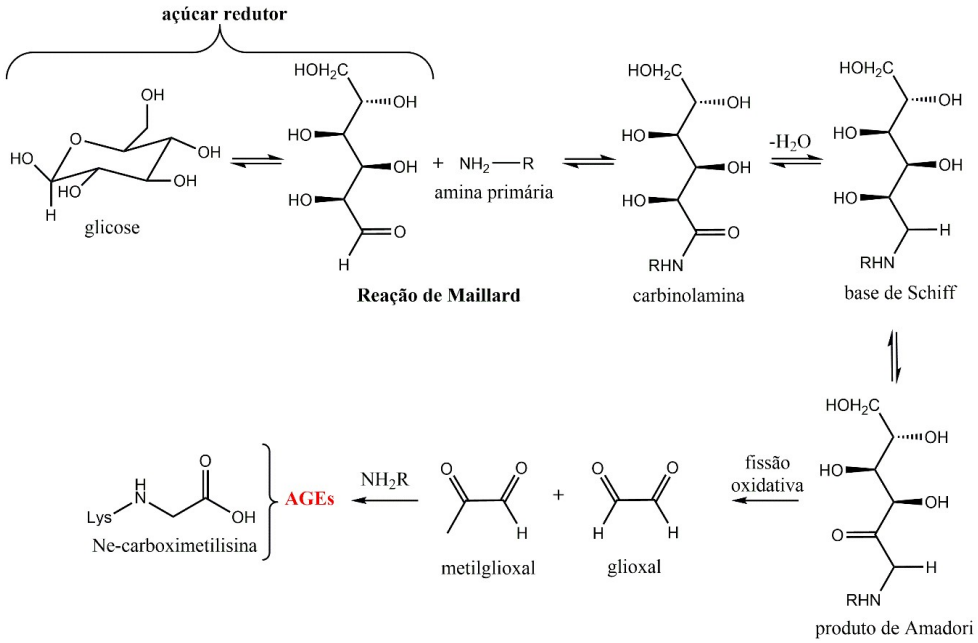

Figura 6. Mecanismo simplificado do processo de formação do AGE, Ne-carboximetilisina (adaptado de Vistoli, 2013).

Por fim, o produto de Amadori sofre o processo de fissão oxidativa dando origem ao glioxal e metilglioxal, que por sua vez podem reagir com um grupo amino dando origem ao Ne-carboximetilisina, principal AGE envolvido na fisiopatologia do diabetes e outras doenças.[76; 77]

Uma abordagem promissora tem sido a investigação de matrizes vegetais ricas em compostos bioativos capazes de inibir a formação de AGEs. Nesse contexto, as folhas de *Eugenia punicifolia* têm se destacado por suas propriedades antioxidantes e seu potencial antiglicante. Estudos recentes avaliaram a capacidade de diferentes extratos dessas folhas de inibir a formação de AGEs pela via não oxidativa, demonstrando resultados expressivos.[33] Contudo, a literatura ainda carece de estudos mais aprofundando sobre o potencial antiglicante dessa matriz.

3.9. Citotoxicidade e atividade antiviral

A investigação da citotoxicidade e da atividade antiviral de extratos vegetais tem se consolidado como uma abordagem relevante em pesquisas farmacológicas, dado seu potencial na inibição e no tratamento de diversas infecções virais.[78] Avaliar a atividade antiviral de extratos vegetais constitui uma etapa essencial na identificação de compostos bioativos com potencial terapêutico, podendo contribuir significativamente para o desenvolvimento de novas estratégias antivirais baseadas em produtos naturais. Nesse contexto, *Eugenia punicifolia*, tradicionalmente utilizada no tratamento do diabetes mellitus tipo 2 devido ao seu potencial antiglicante, apresenta uma composição rica em compostos fenólicos bioativos, o que justifica sua investigação para outras aplicações farmacológicas, incluindo suas possíveis propriedades antivirais.[7; 33; 35; 79]

A citotoxicidade, ou avaliação da viabilidade celular, representa uma etapa essencial na investigação do potencial antiviral de extratos e substâncias vegetais.[80] Esse processo permite determinar a segurança dos compostos e extratos testados, identificando concentrações que não causam danos significativos às células, sendo este, um critério indispensável para a validação de qualquer agente antiviral. Além disso, a análise da viabilidade celular fornece informações valiosas sobre possíveis mecanismos de ação dos compostos bioativos, diferenciando efeitos antivirais diretos de respostas celulares

inespecíficas induzidas pelo estresse citotóxico.[81; 82; 83] Portanto, essa etapa inicial é indispensável para a triagem de novos compostos com potencial farmacológico, garantindo que a atividade antiviral observada não seja decorrente de toxicidade celular, mas sim de uma interação seletiva com o vírus ou com processos essenciais para sua replicação.

A investigação da atividade antiviral de extratos vegetais envolve a avaliação de sua capacidade de inibir a replicação viral sem comprometer a viabilidade celular.[84] No contexto da região Amazônica, o vírus Zika (ZIKV) é particularmente relevante, pois a Amazônia apresenta um ambiente tropical úmido, com temperaturas elevadas e alta pluviosidade, fatores que favorecem a proliferação de mosquitos vetores, especialmente do gênero *Aedes*, como *Aedes aegypti* e *Aedes albopictus*, principais transmissores do ZIKV.[85] Diante disso, a busca por compostos naturais com potencial antiviral contra o ZIKV tem se intensificado, destacando-se espécies vegetais ricas em metabólitos secundários bioativos, como os polifenóis e flavonoides presentes em *Eugenia punicifolia*.

A avaliação da atividade antiviral contra o ZIKV é conduzida por meio de ensaios celulares utilizando linhagens susceptíveis à infecção viral, como as células Vero E6, derivadas do rim de primatas não humanos.[86] Esses ensaios permitem determinar a capacidade dos extratos de interferirem na replicação viral, seja por meio de ação direta sobre as partículas virais, seja pela inibição de etapas do ciclo replicativo dentro das células hospedeiras. Para isso, os extratos são testados em diferentes concentrações previamente estabelecidas como não citotóxicas, garantindo que os efeitos antivirais observados sejam específicos contra o vírus e não resultem de um comprometimento generalizado da viabilidade celular.[87]

Portanto, a identificação de propriedades antivirais em extratos vegetais, como os de *E. punicifolia*, não apenas amplia o conhecimento sobre a biodiversidade química dessas plantas, mas também abre novas perspectivas para o desenvolvimento de medicamentos fitoterápicos voltadas para o combate ao ZIKV e outras arboviroses emergentes.

4. Resultados

4.1. Perfil químico por RMN de ^{1}H e atividade antioxidante de extratos de *Eugenia punicifolia* ao longo das estações: um estudo piloto metabolômico

O presente artigo utilizou técnicas analíticas para caracterizar o perfil químico e avaliar a atividade antioxidante dos extratos das folhas de *Eugenia punicifolia* obtidos ao longo das estações de seca, chuva e transição. Os extratos foram obtidos utilizando dimetilsulfóxido (DMSO-d_6) como solvente e analisados por espectroscopia de ressonância magnética nuclear (RMN) e cromatografia líquida de alta eficiência acoplada à espectrometria de massa de alta resolução. A análise por RMN de ^{1}H forneceu perfis químicos detalhados dos extratos, que foram submetidos às análises de componentes principais (PCA) e discriminante de mínimos quadrados parciais (PLS-DA). Essas análises permitiram diferenciar os extratos com base no período de coleta e identificar compostos-chave responsáveis por essas variações, incluindo sacarose, catequina, epicatequina, quercetina, ácidos graxos e ácido gálico. Os dados de PLS-DA foram validados por métodos estatísticos, incluindo validação cruzada e testes de permutação, garantindo a robustez dos modelos quimiométricos. Os ensaios antioxidantes (DPPH e ABTS) foram realizados para determinar a capacidade de eliminação de radicais livres, com os resultados demonstrando maior atividade antioxidante nos extratos da estação seca. Essa abordagem integrada, que combinou análise química detalhada, ferramentas estatísticas e ensaios farmacológicos, forneceu insights sobre o impacto da sazonalidade na composição química e bioatividade das folhas de *Eugenia punicifolia*, além de estabelecer uma base para futuras investigações.

Situação: Artigo publicado no *Journal of the Brazilian Chemical Society* em 24/01/2024. Disponível em https://doi.org/10.21577/0103-5053.20240010.

Article

Journal of the Brazilian Chemical Society

https://dx.doi.org/10.21577/0103-5053.20240010

J. Braz. Chem. Soc., **2024**, *35*, 7, e-20240010, 1-10

^{1}H NMR Chemical Profile and Antioxidant Activity of *Eugenia punicifolia* Extracts Over Seasons: A Metabolomic Pilot Study

Kidney O. G. Neves,[a] Maria F. C. Santos,[b] Josiana M. Mar,[c] Flávia L. D. Pontes,[d] Claudio F. Tormena,[b] Francisco C. M. Chaves,[e] Francinete R. Campos,[d] Edgar Aparecido Sanches,[c] Jaqueline A. Bezerra,[f] Marcos B. Machado *,[a] ***and Alan D. C. Santos*** *,[a]

[a]*Núcleo de Estudos Químicos de Micromoléculas da Amazônia (NEQUIMA), Universidade Federal do Amazonas, 69067-005 Manaus-AM, Brazil*

[b]*Instituto de Química, Universidade Estadual de Campinas, 13083-862 Campinas-SP, Brazil*

[c]*Laboratório de Polímeros Nanoestruturados (NANOPOL), Departamento de Física de Materiais, Universidade Federal do Amazonas, 69067-005 Manaus-AM, Brazil*

[d]*Departamento de Farmácia, Universidade Federal do Paraná, 80210-170 Curitiba-PR, Brazil*

[e]*Empresa Brasileira de Pesquisa Agropecuária - Embrapa Amazônia Ocidental, 69010-970 Manaus-AM, Brazil*

[f]*Centro Analítico, Instituto Federal de Educação, Ciência e Tecnologia do Amazonas, 69020-120 Manaus-AM, Brazil*

Eugenia punicifolia (Kunth) DC. is a medicinal plant used to treat diseases related to oxidative processes. In this work, ^{1}H nuclear magnetic resonance (NMR) spectroscopy and multivariate analysis have been employed to track the chemical changes and antioxidant activity of dimethyl sulfoxide (DMSO) extracts from *E. punicifolia* leaves over seasons. Principal component analysis (PCA) applied to ^{1}H NMR allowed discriminating DMSO extracts from leaves collected in the dry and rainy seasons and pointed out sucrose, catechin, and epicatechin as responsible for separating dry season samples and quercetin, acid gallic, glucose, and fatty acids contributed for rainy samples grouping. Notably, antioxidant assays revealed that dry season extracts exhibited a higher radical scavenging capacity. When those compounds were submitted to partial least squares-discriminant analysis (PLS-DA) only sucrose and fatty acids presented variable importance projection (VIP) score > 1, both metabolites are related somehow to the defense mechanisms of the plant. This pilot study may suggest new experimental approaches for more effectively monitoring the spectrum-effect relationship of *E. punicifolia* leaf extracts.

Keywords: Myrtaceae, medicinal plant, seasonality, PLS-DA, DPPH, ABTS

Introduction

The investigation of medicinal plants through chemical profiling has emerged as an effective approach, leading to the identification of several bioactive compounds with the potential for developing new drugs. However, the chemical profile is susceptible to environmental influences, and among these factors, seasonality stands out as a primary determinant affecting both metabolite identities within plants and their respective concentrations.[1,2]

The therapeutic effect of medicinal plants is closely linked with a specific set of metabolites, and once the contents of these active principles fluctuate, so does the therapeutic effect.[3] Hence, the timing of plant harvest is of paramount importance when considering medical uses, since the abundance of active compounds can vary significantly throughout the year. This phenomenon is well-documented in the literature. For

*e-mail: alandiegormn@gmail.com.br; marcosmachado@ufam.edu.br
Editor handled this article: Ivo M. Raimundo Jr. (Associate)
This manuscript is part of a series of publications in the Journal of the Brazilian Chemical Society by young researchers who work in Brazil or have a solid scientific connection with our country. The JBCS welcomes these young investigators who brighten the future of chemical sciences.

instance, *Calamintha nepeta* and *Phillyrea angustifolia* demonstrated heightened activity and increased levels of active compounds in colder months.[4,5] Conversely, plants like *Croton heliotropiifolius*, *Salvia fruticose*, and *Rosmarinus officinalis* exhibited higher contents of active compounds during summer and spring months.[6-8] In certain species, seasonal variations appear negligible, as evidenced by consistent alkaloid contents in *Duguetia furfuracea*.[9] Therefore, understanding the patterns of metabolite accumulation is crucial for the standardization of cultivation practices, especially in large-scale production or sustainable plant exploitation.

In the Amazon region, leaves of *Eugenia punicifolia* (Kunth) DC., a Myrtaceae species, are widely commercialized as a phytotherapeutic for the treatment of *Diabetes mellitus*.[10,11] Furthermore, studies on *E. punicifolia* leaves have associated the anti-inflammatory, antinociceptive, and gastroprotective potential with the presence of gallic acid, proanthocyanidins, gallotannin, quercetin, myricitrin, and rutin.[12] Fruits of *E. punicifolia* have also been chemically evaluated being reported the presence of sucrose, α and β-glucose, gallic acid, ellagic acid, quercetin 3-*O*-rhamnoside, kaempferol 7-*O*-rhamnoside, as well as antiglycating and antioxidant properties.[10] As *E. punicifolia* is already consumed by the local population and has market potential, investigating seasonality effects on the chemical composition becomes important and can add economic value to this species.

However, monitoring multiple compounds in very complex matrices like natural products is not a simple task. The high diversity and complexity of chemical structures and the expressive differences in metabolite concentrations make it difficult to track relevant chemical information. Despite this, analytical tools, such as nuclear magnetic resonance (NMR) and high-performance liquid chromatography hyphenated with a diode array detector and mass spectrometer (HPLC-DAD-HRMS), along with multivariate and univariate analysis methods have been successfully applied in this context; and progress has been observed on the identification and quantification of primary and secondary metabolites that are modulated by seasonal changes. Several papers dealing with that matter can be seen in the literature.[2,13-15]

Therefore, this study aims to identify the main compounds present in dimethyl sulfoxide (DMSO) extracts of *E. punicifolia* leaves using NMR and HPLC-DAD-HRMS, as well as to use ^{1}H NMR spectroscopy combined with chemometrics analysis to evaluate the influence of seasonality on their chemical composition and antioxidant potential. The results might indicate the most promising time for leaf harvesting, which is essential to explore *E. punicifolia* as herbal medicine and for the development of bioproducts.

Experimental

Materials

Deuterated dimethyl sulfoxide used in extractions and NMR analyzes was purchased from Cambridge Isotope Laboratories Inc. (Andover, Massachusetts, USA). The methanol and formic acid used in the HPLC-DAD-HRMS analyzes were purchased from Sigma-Aldrich (St. Louis, MO, USA). The reagents 6-hydroxy-2,5,7,8-tetramethylchroman-2-carboxylic acid (Trolox), 2,2-diphenyl-1-picrylhydrazyl (DPPH$^{\bullet}$), 2,2'-azino-bis(3-ethylbenzothiazoline-6-sulfonic acid) diammonium salt (ABTS$^{\bullet+}$) and methanol used in the antioxidant assays were obtained from Sigma-Aldrich (St. Louis, MO, USA).

Plant material

Leaves of *Eugenia punicifolia* species were collected at 9 am in different months (August 2021 (dry season), December 2021 (transition period), and March 2022 (rainy season)) at the Brazilian Agricultural Research Corporation-Embrapa Western Amazon, located on AM-010 Highway, km 29 (2°53'23"S 59°58'26"W). Climatic characteristics can be expressed in terms of average temperature, precipitation, solar radiation, and relative humidity reaching values of 27.4 and 26.2 ºC, 4.6 and 11.7 mm, 15,265.4 and 11,930.9 kJ m^{2}, and 72.3 and 81.7% to dry and rainy seasons, respectively, data acquired from the National Institute of Meteorology (INMET).[16] From the plantation composed of 150 individuals, 15 were randomly selected, and their leaves were collected from different parts of the tree to obtain the best representativeness *per* sample (11 leaves from the lower part, 11 from the intermediate part, and 11 from the upper part). The plant material was dried at room temperature for 24 and 48 h in a forced air circulation oven at 40 °C. After drying, each sample was subjected to the cold maceration process with liquid nitrogen, weighed, and stored in a freezer at −80 °C until the extraction procedure.

Chemical profile of the DMSO extract of *E. punicifolia* by HPLC-DAD-HRMS

For the analysis of HPLC-DAD-HRMS, 50 mg of dried leaves from a mix of the samples from the first collection were extracted with 650 µL of deuterated dimethyl sulfoxide in an ultrasonic bath for 20 min. After this time, the sample was centrifuged at 10.000 rpm

for 10 min, the supernatant (550 μL) was removed, lyophilized, and subjected to analysis. Analyses was performed on a high-performance liquid chromatograph (HPLC) (Shimadzu, Tokyo, Japan), with an autosampler maintained at 10 °C, coupled to the quadrupole time of flight high resolution mass spectrometer (Q-TOF-MS) (Bruker Daltonics, Fremont, CA, USA). A reversed-phase Synergi Fusion-RP C18 Phenomenex® column (150 × 2.1 mm, 4 μm particle size) was used with a guard column of the same phase. The mobile phase consisted of water (A) and methanol (B), both containing 0.1% formic acid. Elution was performed in gradient mode, with 0-28 min (20-100% B), 28-38 min (100% B), 38-48 min (100-20% B), 48-55 min (20% B). The flow rate was maintained at 200 μL min^{-1} and the column temperature at 40 °C. The injection volume was 2.0 μL. The parameters of the ionization source (electrospray in positive mode) were as follows: capillary potential of 4.5 kV, end plate offset of 0.5 kV, nebulizer gas pressure (nitrogen) of 2.0 bar, drying gas flow (nitrogen) of 6 L min^{-1}, and gas temperature of 180 °C. The acquisition range was from *m/z* 100 to 1000. The instrument was calibrated with 10 mM sodium formate. Data acquisition was performed with Data Analysis 4.1 software.[17]

Acquisition of NMR spectroscopy data

Fifty milligrams of *E. punicifolia* leaves were extracted with 650 μL of deuterated DMSO in an ultrasonic bath for 20 min. The sample was then centrifuged at 10.000 rpm for 10 min, the supernatant was removed, and transferred to a 5 mm NMR tube. NMR spectra were acquired on a Bruker Avance III NMR spectrometer (Bruker, Billerica, Massachusetts, USA), operating at 9.4 T, equipped with a 5 mm BBI probe with a gradient along the z-axis. NMR spectra were obtained at 25 °C using the *zgpr* pulse sequence with a 90º pulse duration of 8.58 μs. 4 dummy scans, and 64 scans were collected with 64 k data points using a spectral width of 8 kHz, a relaxation time of 1.0 s, and an acquisition time of 4.0 s. The residual water signal of DMSO-d_6 (δ_H 3.36, s) was suppressed using a power of 4.98 10^{-5} W, and the receiver gain was set to 203. Phase and baseline corrections of the spectra were performed manually using TopSpin 3.6.3 software.[18] The chemical shift (in ppm) of ^{1}H NMR spectra was referenced to the methyl signal of tetramethylsilane at δ_H 0.0. The ^{1}H-^{13}C correlations from edited heteronuclear quantum coherence (HSQCedit) and heteronuclear multiple bond correlation (HMBC) NMR experiments were acquired using the coupling constants *J* (H,C, one-bond) and *J* (H,C, long-range) of 145 and 8 Hz, respectively.

Multivariate data analysis

^{1}H NMR spectra of the 45 samples were acquired in triplicate, exported from TopSpin 3.6.3 software in .csv format and transferred to OriginPro 2018 software to build the data matrix.[18,19] Chemometric analysis was carried out using the region of ^{1}H NMR spectra between 0.55 to 7.40 ppm resulting in a matrix (135 samples × 5310 variables). The areas of residual water signal (3.30 to 3.40 ppm) and deuterated dimethyl sulfoxide (2.46 to 2.54 ppm) were excluded.

Principal component analysis (PCA) was performed using the PLS-Toolbox Solo 9.0 software.[20] Spectra preprocessing consisted of baseline correction (Automatic Weighted Least Squares, order = 2), variable alignment (Correlation Optimized Warping: Slack 5, Segment Length 50, and Alignment function Linear of the 1st Order). The data was normalized to the area and mean centered. The scores and loadings graphs were plotted using the algorithm Singular Value Decomposition (SVD).

Data processing and construction of the PLS-DA calibration model

To perform partial least squares-discriminant analysis (PLS-DA), the ^{1}H NMR spectra of the 135 *E. punicifolia* samples were exported to R-Studio software version 2022.07.2.[21] Subsequently, the spectral region from 0.05 to 8.20 ppm was aligned, and the residual water signal region of DMSO-d_6 was excluded. The spectra were then divided into 0.04 ppm buckets with a 50% degree of freedom, resulting in a table of 135 samples and 245 variables. This table was exported to The Unscrambler 10.3 software, where it was normalized based on total intensity (each bucket's intensity was divided by the sum of all bucket intensities in the spectrum), resulting in optimal data optimization for metabolomics studies, as described by Wang *et al.*[22,23]

The intensities of the buckets corresponding to the signals of sucrose (δ_H 5.18, *d*, 3.7 Hz), catechin (δ_H 5.93, d, 2.3 Hz), epicatechin (δ_H 5.89, d, 2.2 Hz), fatty acids (δ_H 1.23, s), α-glucose (δ_H 4.90, d, 3.6 Hz), β-glucose (δ_H 4.27, d, 7.8 Hz), gallic acid (δ_H 6.95, s), and quercetin (δ_H 7.30, d, 2.3 Hz) were exported from The Unscrambler 10.3 software and transferred to MetaboAnalyst 5.0, where they were scaled using the autoscaling method (mean-centered and divided by the standard deviation of each variable).[24,25] After scaling, the data were used to build the PLS-DA calibration model, which underwent cross-validation (method 5-fold CV), permutation testing

(separation distance adjusted to 2000 permutation), and the construction of Vip score plots.

DPPH radical scavenging capacity

The experiments were carried out following the methods described in a previous study.[26] The radical scavenging capacity of *E. punicifolia* sample after various treatment processes was assessed using the DPPH$^{\bullet}$ radical method. A 100 μM methanolic DPPH$^{\bullet}$ solution was prepared. Then, the sample was prepared at a concentration of 1 mg mL^{-1} and mixed with 1900 μL of the methanolic DPPH$^{\bullet}$ radical solution. Trolox was used as a positive control (ranging from 100 to 2000 μM) for comparison. The mixture was incubated in darkness at room temperature for 30 min. Absorbance readings were taken at 515 nm using a microplate reader (Bio Tek Instruments Inc., Winooski, VT, USA). The antioxidant capacity was quantified in Trolox equivalents. The assay was performed in triplicate. The relationship was determined as $y = -0.0004x + 0.7126$, with coefficient of determination (R^2) value of 0.9926, and the results were expressed in micromolar Trolox Equivalents (μM TE mL^{-1}).

ABTS radical cation scavenging capacity

The ABTS$^{\bullet+}$ scavenging assay entails observing the fading of the ABTS$^{\bullet+}$ solution color in the presence of antioxidant extracts.[26,27] Following a reaction period of 6 min between the sample and the radical at a 1:10 ratio, absorbances were recorded at 750 nm using a microplate reader (Bio Tek Instruments Inc., Winooski, VT, USA). Trolox was employed to construct the standard curve ($y = 0.0003x + 0.7216$, $R^2 = 0.9951$), and the results were quantified in micromolar Trolox Equivalents (μM Trolox mL^{-1}).

Statistical analysis

The distribution of antioxidant data for DPPH radical and ABTS radical cation, as well as to the area of the signs of sucrose (δ_H 5.18, d) and fatty acids (δ_H 1.23, s) were assessed using the normality test (Kolmogorov-Smirnov), followed by the Kruskal-Wallis nonparametric test for data with a non-normal distribution. The comparison among multiple data sets with a normal distribution was performed using ANOVA (variance analysis) with the Tukey's test, at a significance level of 95%. Pearson correlation coefficients were obtained with a p-value of < 0.05. The analyses were conducted using Minitab™ 18.1 software.[28]

Results and Discussion

Chemical profiles of *E. punicifolia* extracts via HPLC-DAD-HRMS and NMR spectroscopy

HPLC-DAD-HRMS profiles of DMSO-d_6 extracts from *E. punicifolia* revealed the presence of 10 flavonoids (Table 1). The identification of these compounds was achieved through an analysis of their ion fragmentation patterns (Figures S1-S18, Supplementary Information (SI) section), as well as by comparison with mass spectrometry (MS) data previously documented in the literature for *Eugenia* species. DMSO extracts were submitted to NMR spectroscopy, and spectra of hydrogen revealed a typical complex profile with signals in the aliphatic, carbinolic, and aromatic regions (Figures S19-S21, SI section). To endorse the compound identities in ^{1}H NMR spectra, 2D NMR experiments, such as (^{1}H-^{1}H) correlated spectroscopy (COSY), (^{1}H-^{13}C) HSQCedit, and (^{1}H-^{13}C) HMBC, were also obtained (Figures S22-S30, SI section).

Characteristic signals of fatty acids (**1**) and carbohydrates (**2-4**) were observed, as previously reported.[10] Also, three flavonoids were identified: catechin (**5**), epicatechin (**6**), and quercetin (**7**). For catechin, the signals at δ_H 5.83 (d, 2.3 Hz), δ_H 5.93 (d, 2.3 Hz), δ_H 6.86 (d, 2.3 Hz), δ_H 6.66 (d, 8.1 Hz) and δ_H 6.75 (dd, 2.3 and 8.1 Hz), related to position 6, 8, 2', 5' and 6' of rings A and B were assigned.[29] The epicatechin A-ring showed resonances at δ_H 5.89 (d, 2.2 Hz) and δ_H 5.88 (d, 2.2 Hz).[30] While for quercetin, the signals attributed were δ_H 7.30 (d, 2.1 Hz), δ_H 7.25 (dd, 2.1 Hz and 8.4 Hz), and δ_H 6.87 (d, 8.4 Hz), related to quercetin C-ring, as well as signals at δ 6.40 (d, 2.1 Hz) and δ_H 6.21 (d, 2.1 Hz), characteristic of ring A of quercetin.[28] Finally, signals at δ_H 6.95 (s) and δ_H 6.82 (s) showed correlations to δ_C 165.9, δ_C 108.6, δ_C145.7, and δ_C 138.3 in the HMBC experiment indicating the presence of gallic acid (**8**) and derivatives.[31] Figure 1 depicts the compounds identified.

Multivariate NMR data analysis

^{1}H NMR spectra of *E. punicifolia* were submitted to PCA analysis aiming to discriminate the sample groups by season and to track the compounds responsible for such grouping. Scores and loadings plots are depicted in Figures 2 and 3. The two first principal components explained 65.82% of the total variance. Samples from drought and rainy periods occupied the positive and negative sides of PC1, respectively. Samples collected in the transition season could be found spread all over the

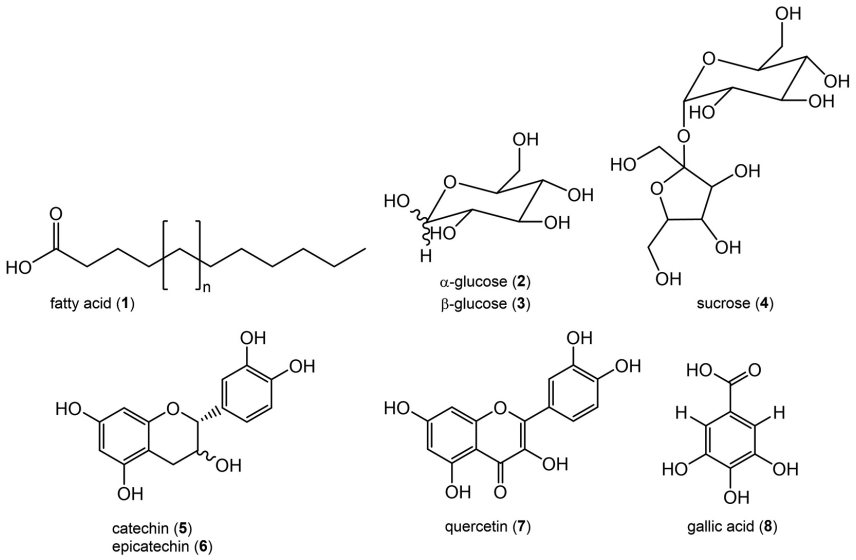

Figure 1. Compounds identified by NMR spectroscopy analysis of DMSO-d_6 extracts from *E. punicifolia*.

Table 1. Compounds identified in DMSO extract from *E. punicifolia* leaves by HPLC-DAD-HRMS

t_r / min	Compound	Molecular formula	Meas.[a] (*m*/*z*)	Calcd.[b] (*m*/*z*)	Error / ppm	MS/MS[c]	Reference
5.0	epicatechin	$C_{15}H_{14}O_6^+$	291.086571	291.086315	0.88	139	32,33
5.2	epigallocatechin gallate	$C_{22}H_{18}O_{11}^+$	459.090472	459.092188	–3.74	289, 139	34,35
7.0	catechin gallate	$C_{22}H_{18}O_{10}^+$	443.097327	443.097273	0.12	291, 273, 139	33,36
8.7	epicatechin 3-*O*-(3-*O*-methylgallate)	$C_{23}H_{20}O_{10}^+$	457.112003	457.112923	–2.01	273, 167, 151, 139	37,38
10.2	Myricitrin myricetin	$C_{21}H_{20}O_{12}^+$ $C_{15}H_{10}O_8^+$	465.102519 319.045936	465.102753 319.044844	–0.50 3.42	319, 303, 153 153	29,39 40,41
12.1	Quercitrin quercetin	$C_{21}H_{20}O_{11}^+$ $C_{15}H_{10}O_7^+$	449.108278 303.050967	449.107838 303.049929	0.98 3.43	303 229, 153	34,42 36,43
13.7	kaempferol-7-rhamnoside kaempferol	$C_{21}H_{20}O_{10}^+$ $C_{15}H_{10}O_6^+$	433.112825 287.055621	433,112923 287.055014	–0.23 2.11	287 153	10,44 45,46

[a]Measured; [b]calculated; [c]main fragments.

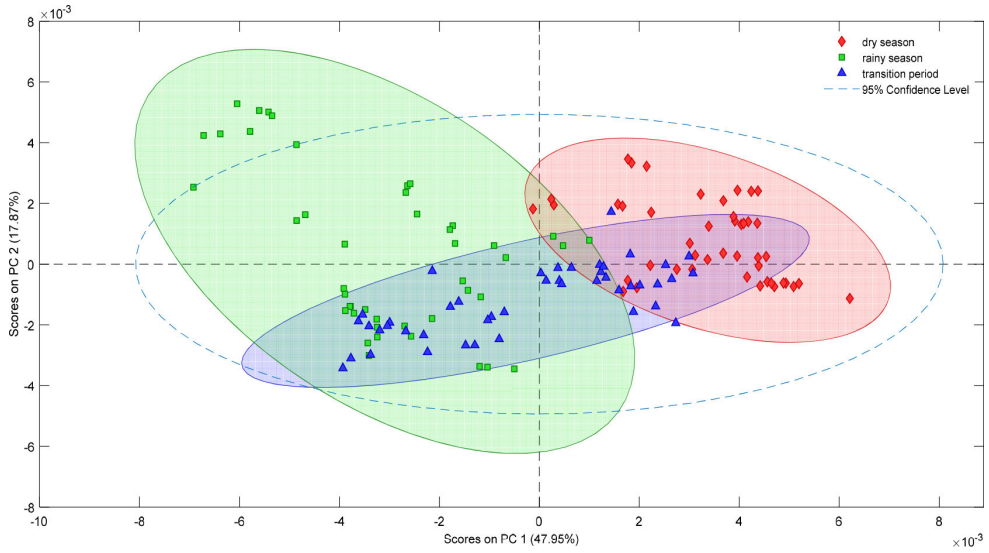

Figure 2. Principal components analysis (PCA) of DMSO extracts of *E. punicifolia*. Scores plot of PC1 (47.95%) *versus* PC2 (17.87%). Samples falling outside the 95% confidence level were not designated as outliers, as there were no identified issues with sample collection, extraction procedures, or data acquisition and processing. These samples exhibited lower sucrose contents compared to the remaining samples collected during the dry season.

scores plot, some of them having chemical profiles like rainy samples and others more like drought samples.

According to the loadings plot (Figure 3), sucrose (δ_H 5.18, d, 3.7 Hz), catechin (δ_H 5.93, d, 2.3 Hz) and epicatechin (δ_H 5.89, d, 2.2 Hz) influenced the discrimination of drought period samples, while fatty acids (δ_H 1.23, s), α-glucose (δ_H 4.90, d, 3.6 Hz), β-glucose (δ_H 4.27, d, 7.8 Hz), gallic acid (δ_H 6.95, s), and quercetin (δ_H 7.30, d, 2.3 Hz) were responsible for the grouping of samples of rainy period in the negative region of PC1. Of note, the transition samples mostly occupied the negative side of PC2, yet shared similar chemical characteristics with certain rainy and drought samples. Upon examining the loadings plot of PC2, it was possible to identify the α-glucose (δ_H 4.90, d, 3.6 Hz) as responsible for samples in the negative side of PC2, while β-glucose, gallic acid, sucrose, and predominantly fatty acids were identified in positive PC2 (Figure S32, SI section).

PLS-DA calibration model

The PLS-DA model was constructed using normalized and autoscaled intensities of buckets from the compounds indicated by PCA analysis: sucrose (δ_H 5.18, d, 3.7 Hz), catechin (δ_H 5.93, d, 2.3 Hz), epicatechin (δ_H 5.89, d, 2.2 Hz), fatty acids (δ_H 1.23, s), α-glucose (δ_H 4.90, d, 3.6 Hz), β-glucose (δ_H 4.27, d, 7.8 Hz), gallic acid (δ_H 6.95, s), and quercetin (δ_H 7.30, d, 2.3 Hz). PLS-DA has been used as a discriminative variable selection, allowing tracking of the contribution of each input information to the prediction model.[47,48] Once samples from the transition period had chemical features similar to samples from dry and rainy seasons, we kept them out in this part of the study.

Component 1 (57.3%) of the PLS-DA model was responsible for separating samples collected during the dry and rainy periods, as illustrated in Figure 4a. Estimation of the model's quality was performed using the cross-validation method through values of accuracy, Q^2, and R^2.[49-51] Q^2 indicates the predictive capability of the model, while R^2 represents the model's ability to explain the data and predict new observations.[50,51] Based on Table 2, one can be observed that Q^2 and R^2 have similar magnitudes for all calculated components, indicating the absence of overfitting, and accuracy values above 90%. To demonstrate that the values obtained from the cross-validation method were not acquired by chance, a permutation test was conducted. In this test, *p*-values < 0.05 suggest that the obtained data is significant. Q^2 was chosen as the statistical parameter for the permutation test, resulting in a *p*-value < 0.0005, which confirms the validity of the model.

After validating the model, the variable importance projection (VIP) scores were used to judge the importance of a compound (bucket area) in explaining the chemical variation over the seasons (Figure 4b). Normally, variables with VIP score greater than 1 are considered relevant to the model with an important contribution to explaining the dependent variable.[52] It becomes evident that sucrose and fatty acids emerge as responsible for discriminating samples from the dry and rainy periods, respectively. Conversely, the remaining compounds exhibited VIP scores below 1.

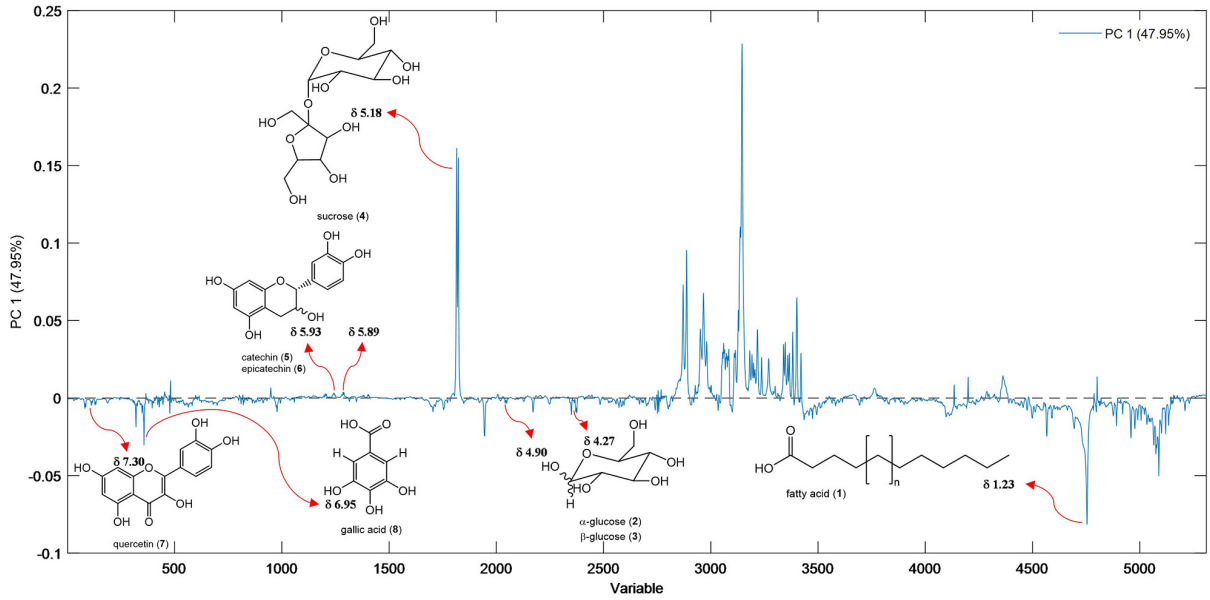

Figure 3. Loadings plot of PC1 discriminating the compounds responsible for the grouping of samples of *E. punicifolia*. Data obtained by [1]H NMR (400 MHz, DMSO-d_6).

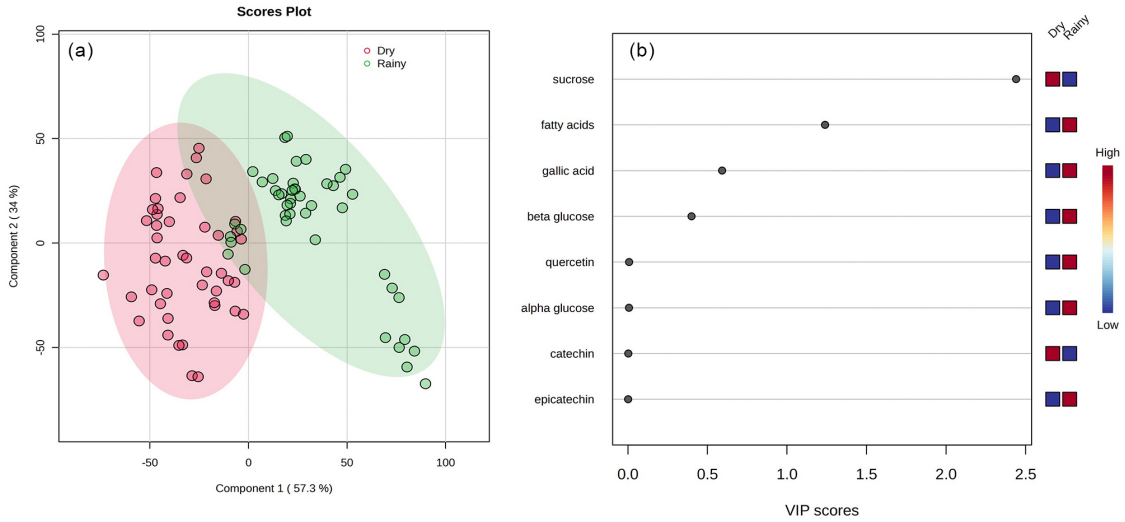

Figure 4. PLS-DA score plot showing the separation of dry and rainy samples (a), and graph of VIP scores (b).

Table 2. Accuracy, R^2, and Q^2 values obtained in the cross-validation of the PLS-DA model as a function of the number of components (comps) used

Measure	1 comps	2 comps	3 comps	4 comps	5 comps
Accuracy	0.9333	0.9333	0.9333	0.9333	0.9444
R^2	0.6613	0.7469	0.8011	0.8049	0.8414
Q^2	0.6481	0.7342	0.7831	0.7853	0.7966

Q^2: predictive capability of the model; R^2: model's ability to explain the data and predict new observations.

Table 3. Scavenging capacity of the free radical DPPH$^{\bullet}$ and the cation radical ABTS$^{\bullet+}$

Season	DPPH$^{\bullet}$ SC ± SD / (μM TE g^{-1})	ABTS$^{\bullet+}$ SC ± SD / (μM TE g^{-1})
Dry	1208.0 ± 112.6^{a}	1641.2 ± 147.5^{a}
Transition	1160.7 ± 108.8^{ab}	1567.6 ± 145.6^{b}
Rainy	1132.1 ± 114.6^{b}	1465.3 ± 120.6^{c}

^{a,b,c}Clustering for DPPH$^{\bullet}$ and ABTS$^{\bullet+}$ assay using Tukey's method and 95% confidence interval; SC: scavenging capability expressed in micromolar Trolox Equivalents (μM TE mL^{-1}); SD: standard deviation; DPPH•: 2,2-diphenyl-1-picrylhydrazyl; ABTS•+: 2,2'-azino-bis(3-ethylbenzothiazoline-6-sulfonic acid) diammonium salt.

Antioxidant potential of DMSO extracts from leaves of *E. punicifolia*

DMSO extracts from *E. punicifolia* leaves were submitted to assays for scavenging the free radical DPPH and the cation radical ABTS. Fifteen samples from each period were employed in those experiments. The analysis of DPPH$^{\bullet}$ data variance resulted in the formation of two groups: group A, composed of samples from dry and transition periods, and group B, comprising samples from transition and rainy periods. While for the ABTS$^{\bullet+}$ assay, three groups were observed, corresponding to each collection period (Table 3). Notably, despite the slight differences between the assays, samples obtained during the dry period exhibited a superior scavenging capacity in both assays. The Pearson correlation between the DPPH$^{\bullet}$ and ABTS$^{\bullet+}$ assays was 0.85 ($p < 0.05$) which indicates a moderate and positive correlation and strengthens the presence of antioxidant properties of DMSO extracts from *E. punicifolia* leaves.

[1]H NMR chemical profiles and antioxidant activities of DMSO extracts

The environmental stress, provoked by the water scarcity and higher indexes of solar radiation and temperatures, inherent to the dry seasons, intensifies the oxidative stress in plants, which in turn, triggers their defense mechanisms to minimize oxidative damage to cells.

As reviewed by Liebelt *et al.*,[53] seasonal effects on antioxidants are diverse. Small water-soluble sugars, such as sucrose, have been recognized as crucial in orchestrating plant developmental responses under oxidative stress, not only as a consequence of remodeling carbon metabolism or signaling, but acting as an antioxidant itself, or serving as a substrate to the synthesis of oligosaccharides also with antioxidant properties.[54,55] According to Uemura and Steponkus,[56] at low concentrations, sucrose might serve as a substrate or signal for stress-induced alterations, while, at high concentrations, it can directly play a protective agent role. That might explain the increase in sucrose content and antioxidant activity in the DMSO extracts of *E. punicifolia* leaves obtained in the dry season.

Furthermore, literature underscores sucrose's role in the accumulation of phenolic compounds and the improvement of antioxidant activity.[57-59] Unfortunately, the chemical

profiles acquired in our work did not allow us to visualize such a trend. To overcome that, a target extraction method should be investigated which can lead to the acquisition of phenolic-rich NMR profiles enabling the correlation between secondary metabolites and antioxidant activity. A closer look at MS data indicates a richer phenolic composition than that registered by NMR data, and those compounds, even in lower concentrations, can contribute significantly to the bioactivity observed. That is quite reasonable once the antioxidant activity of a compound depends on its chemical structure, for example, phenolic compounds glycosylated have shown stronger activity than not glycosylated ones.[55]

Conversely, during the rainy season, there was an increase in the normalized area of fatty acids suggesting an alteration in the lipid metabolism. At high average relative humidity and rainfall rates, plants become more susceptible to pathogen attacks, like fungi.[60] Oxylipins and unsaturated fatty acids play an important role in signaling functions during plant-pathogen interaction. Besides that, the very long chain fatty acid (VLCFA) biosynthesis pathway has been associated with plant defense through different aspects, including the biosynthesis of sphingolipids, which is a signaling component, and the production of the plant cuticle, which can change its composition because of the pathogen attack. Of note, one of the ways plants synthesize VLCFA is through the elongation of the C16 and C18 fatty acids, which can explain the increase in fatty acid production.[61,62]

Conclusions

Through HPLC-DAD-HRMS and NMR spectroscopy, fifteen compounds were identified in DMSO extracts from *E. punicifolia* leaves. The chemical information obtained via ^{1}H NMR spectroscopy was enough to discriminate *E. punicifolia* leaves collected in dry and rainy seasons via PCA. Also, antioxidant assays showed extracts from the dry season with higher radical scavenging capacity. PLS-DA of the metabolites pointed out sucrose and fatty acids as mainly responsible for the grouping of samples. These results suggest that the dry season had an impact on carbon metabolism as a consequence of the oxidative stress and the triggering of antioxidant mechanisms. Similarly, the rainy season appeared to influence lipid metabolism, which is related to plant protection against pathogen attacks. This preliminary investigation will provide a foundation for our forthcoming study, wherein we will examine month-to-month fluctuation in chemical profiles acquired through a phenolic-driven extraction method. Our aim is to enhance the methodology capacity to uncover correlations between secondary metabolites and bioactivity. Knowledge of this spectrum-effect relationship aggregates value to *E. punicifolia* and might suggest the most appropriate season for developing *E. punicifolia* leaves-based bioproducts and exploring it as herbal medicine.

Supplementary Information

Supplementary data (HRMS spectra and NMR spectra) are available free of charge at http://jbcs.sbq.org.br as PDF file.

Acknowledgments

The authors would like to thank Fundação de Amparo à Pesquisa do Estado do Amazonas-FAPEAM (EDITAL No. 013/2022-PRODUTIVIDADE-CT&I), Resolução No. 002/2023-PROSGRAD 2023/2024-Coordenador/Auxílio Financeiro/PPGQ) the Postgraduate Program in Chemistry at the Federal University of Amazonas (PPGQ-UFAM), and Nuclear Magnetic Resonance Laboratory (NMRLab) of the Analytical Center of UFAM for the financial support, fellowships, and infrastructure, and Dr Otávio Neto for curating climate date.

Author Contributions

Kidney O. G. Neves, Marcos B. Machado, and Alan D. C. Santos contributed to the conceptualization of the project and manuscript writing; Josiana M. Mar, Edgar A. Sanches, and Jaqueline A. Bezerra provided the materials and reagents necessary for conducting the antioxidant assays, as well as performing the assays themselves; Flávia L. D. Pontes and Francinete R. Campos were responsible for acquiring the HPLC-DAD-HRMS spectra; Francisco C. M. Chaves was in charge of identifying and collecting botanical material, as well as obtaining meteorological data; Maria F. C. Santos and Claudio F. Tormena facilitated the acquisition and interpretation of NMR data.

References

1. Aru, V.; Engelsen, S. B.; Savorani, F.; Culurgioni, J.; Sarais, G.; Atzori, G.; Cabiddu, S.; Marincola, F. C.; *Metabolites* **2017**, *7*, 36. [Crossref]
2. Aves Filho, E. G.; Silva, L. M. A.; Ribeiro, P. R. V.; de Brito, E. S.; Zocolo, G. J.; Souza-Leão, P. C.; Marques, A. T. B.; Quintela, A. L.; Larsen, F. H.; Canuto, K.; *Food Chem.* **2019**, *289*, 558. [Crossref]
3. Zanatta, A. C.; Vilegas, W.; Edrada-Ebel, R.; *Front. Chem.* **2021**, *9*, 710025. [Crossref]
4. Pacifico, S.; Galasso, S.; Piccolella, S.; Kretschmer, N.; Pan, S.-P.; Marciano, S.; Bauer, R.; Monaco, P.; *Food Res. Int.* **2015**, *69*, 121. [Crossref]

5. Scognamiglio, M.; D'Abrosca, B.; Fiumano, V.; Golino, M.; Esposito, A.; Fiorentino, A.; *Phytochem Lett.* **2014**, *8*, 163. [Crossref]
6. de Alencar Filho, J. M. T.; Araújo, L. C.; Oliveira, A. P.; Guimarães, A. L.; Pacheco, A. G. M.; Silva, F. S.; Cavalcanti, L. S.; Lucchese, A. M.; Almeida, J. R. G. S.; Araújo, E. C. C.; *Rev. Bras. Farmacogn.* **2017**, *27*, 440. [Crossref]
7. Sarrou, E.; Martens, S.; Chatzopoulou, P.; *Ind. Crops Prod.* **2016**, *94*, 240. [Crossref]
8. Lemos, M. F.; Lemos, M. F.; Pacheco, H. P.; Endringer, D. C.; Scherer, R.; *Ind. Crops Prod.* **2015**, *70*, 41. [Crossref]
9. Macedo, A. L.; Boaretto, A. G.; da Silva, A. N.; Maia, D. S.; de Siqueira, J. M.; Silva, D. B.; Carollo, C. A.; *J. Braz. Chem. Soc.* **2021**, *32*, 1840. [Crossref]
10. Ramos, A. S.; Mar, J. M.; da Silva, L. S.; Acho, L. D. R.; Silva, B. J. P.; Lima, E. S.; Campelo, P. H.; Sanches, E. A.; de Araujo Bezerra, J.; Chaves, F. C. M.; Campos, F. R.; Machado, M. B.; *Food Res. Int.* **2019**, *123*, 674. [Crossref]
11. de Souza, A. M.; de Oliveira, C. F.; de Oliveira, V. D.; Betim, F. C. M.; Miguel, M. D.; *Planta Med.* **2018**, *84*, 1232. [Crossref]
12. Basting, R. T.; Nishijima, C. M.; Lopes, J. A.; Santos, R. C.; Lucena Périco, L.; Laufer, S.; Bauer, S.; Costa, M. F.; Santos, L. C.; Rocha, L. R. M.; Vilegas, W.; Santos, A. R. S.; dos Santos, C.; Hiruma-Lima, C. A.; *J. Ethnopharmacol.* **2014**, *157*, 257. [Crossref]
13. Larive, C. K.; Barding, G. A.; Dinges, M. M.; *Anal. Chem.* **2014**, *87*, 133. [Crossref]
14. Zhuang, H.; Ni, Y.; Kokot, S.; *Chemom. Intell. Lab. Syst.* **2014**, *135*, 183. [Crossref]
15. Santos, M. F. C.; Rech, K. S.; Dutra, L. M.; Menezes, L. R. A.; Santos, A. D. C.; Nagata, N.; Stefanello, M. É. A.; Barison, A.; *Food Chem.* **2023**, *408*, 135016. [Crossref]
16. National Institute of Meteorology (INMET); *Annual Meteorological Data of Brazil*; https://portal.inmet.gov.br/, accessed on September 9th, 2022.
17. *Data Analysis*, version 4.1; Bruker Daltonics; Billerica, MA, USA, 2017.
18. *TopSpin*, version 3.6.3; Academia License, Bruker Optics GmbH & Co. KG; Ettlingen, Germany, 2021.
19. *OriginPro*, version 2018; OriginLab Corporation; Northampton, MA, USA, 2018.
20. *PLS-Toolbox Solo*, version 9.0; Eigenvector Research Inc.; Wenatchee, WA, USA, 2021.
21. *RStudio: Integrated Development Environment for R*; RStudio, PBC; Boston, MA, USA, 2020.
22. Wang, B.; Goodpaster, A.; Kennedy, M. A.; *Chemom. Intell. Lab. Syst.* **2013**, *128*, 9. [Crossref]
23. *The Unscrambler*, version 10.3; CAMO software AS; Oslo, Norway, 2012.
24. Xia, J.; Psychogios, N.; Young, N.; Wishart, D. S.; *Nucleic Acids Res.* **2009**, *37*, W652. [Crossref]
25. Pang, Z.; Chong, J.; Zhou, G.; Morais, D. A. L.; Chang, L.; Barrette, M.; Gauthier, C.; Jacques, P.-É.; Li, S.; Xia, J.; *Nucleic Acids Res.* **2021**, *49*, W388. [Crossref]
26. Mar, J. M.; da Silva, L. S.; Moreira, W. P.; Biondo, M. M.; Pontes, F. L. D.; Campos, F. R.; Kinupp, V. F.; Campelo, P. H.; Sanches, E. A.; Bezerra, J. A.; *Food Chem.* **2021**, *356*, 129723. [Crossref]
27. Aquino Neto, F. R.; *Cromatografia: Princípios Básicos e Técnicas Afins*, vol. 1, 1st ed.; Interciência: Rio de Janeiro, Brazil, 2003.
28. *Minitab*, version 18.1; Minitab Inc.; State College, PA, USA, 2017.
29. Oliveira, E. S. C.; Acho, L. D. R.; da Silva, B. J. P.; Morales-Gamba, R. D.; Pontes, F. L. D.; do Rosário, A. S.; Bezerra, J. A.; Campos, F. R.; Barcellos, J. F. M.; Lima, E. S.; Machado, M. B.; *J. Ethnopharmacol.* **2022**, *293*, 115276. [Crossref]
30. Napolitano, J. C.; Gödecke, T.; Lankin, D. C.; Jaki, B.; McAlpine, J. B.; Chen, S.-N.; Pauli, G. F.; *J. Pharm. Biomed. Anal.* **2013**, *93*, 59. [Crossref]
31. López-Martínez, L.; Santacruz-Ortega, H.; Navarro, R.; Sotelo-Mundo, R.; González-Aguilar, G. A.; *PLoS ONE* **2015**, *10*, 0140242. [Crossref]
32. Soares, J. C.; Rosalen, P. L.; Lazarini, J. G.; Massarioli, A. P.; da Silva, C. F.; Nani, B. D.; Franchin, M.; de Alencar, S. M.; *Food Chem.* **2019**, *281*, 178. [Crossref]
33. Chang, C.-L.; Wu, R.-T.; *Food Chem.* **2011**, *126*, 710. [Crossref]
34. da Silva, G. L.; Campideli, M. B.; Ferrari, A. B. S.; Mannochio-Russo, H.; Fraige, K.; Dametto, A. C.; Bolzani, V. S.; Zeraik, M. L.; *Nat. Prod. Res.* **2021**, *36*, 4724. [Crossref]
35. Spáčil, Z.; Nováková, L.; Solich, P.; *Food Chem.* **2010**, *123*, 535. [Crossref]
36. Siebert, D. A.; Bastos, J.; Spudeit, D. A.; Micke, G. A.; Alberton, M. D.; *Ver. Bras. Farmacogn.* **2017**, *27*, 459. [Crossref]
37. Tan, J.; Dai, W.; Lu, M.; Lv, H.; Guo, L.; Zhang, Y.; Zhu, Y.; Peng, Q.; Lin, Z.; *Food Res. Int.* **2016**, *79*, 106. [Crossref]
38. Dou, J.; Lee, V. S. Y.; Tzen, J. T. C.; Lee, M.-R.; *J. Agric. Food Chem.* **2007**, *55*, 7462. [Crossref]
39. Hwang, I. W.; Chung, S. K.; *Prev. Nutr. Food Sci.* **2018**, *23*, 341. [Crossref]
40. Borges, K. C.; Bezerra, M. F.; Rocha, P. M.; Silva, E. S. D.; Fujita, A.; Genovese, M. I.; Correia, R. T. P.; *J. Prob. Health* **2016**, *4*, 100145. [Crossref]
41. Mbeunkui, F.; Grace, M. H.; Yousef, G. G.; Ann Lila, M.; *J. Sep. Sci.* **2012**, *35*, 1682. [Crossref]
42. Pacheco, A. G. M.; Branco, A.; Câmara, C. A.; Silva, T. M. S.; Silva, T. M. G.; Oliveira, A. P.; Santos, A. D. C.; Dutra, L. M.; Rolim, L. A.; Oliveira, G. G.; *Nat. Prod. Res.* **2021**, *35*, 2414. [Crossref]
43. Tsimogiannis, D.; Samiotaki, M.; Panayotou, G.; Oreopoulou, V.; *Molecules* **2007**, *12*, 593. [Crossref]

44. Sharaf, M.; El-Ansari, M. A.; Saleh, N. A. M.; *Biochem. Syst. Ecol.* **1997**, *25*, 161. [Crossref]
45. John, K. M.; Ayyanar, M.; Subbiah, J.; Murugesan, S.; Gansukh, E.; Kim, D.; *BioMed Res. Int.* **2014**, *2014*, ID726145. [Crossref]
46. Ma, C.; Lv, H.; Zhang, X.; Chen, Z.; Shi, J.; Lu, M.; Lin, Z.; *Anal. Chim. Acta* **2013**, *795*, 15. [Crossref]
47. Lee, L. C.; Liong, C. Y.; Jemain, A. A.; *Analyst* **2018**, *143*, 3526. [Crossref]
48. Zheng, R.; Chen, Z.; Guan, Z.; Zhao, C.; Cui, H.; Shang, H.; *Chin. Med.* **2023**, *18*, 15. [Crossref]
49. Cruciani, G.; Baroni, M.; Clementi, S.; Costantino, G.; Riganelli, D.; Skagerberg, B.; *J. Chemom.* **1992**, *6*, 335. [Crossref]
50. Szymańska, E.; Saccenti, E.; Smilde, A. K.; Westerhuis, J. A.; *Metabolomics* **2012**, *8*, 3. [Crossref]
51. Westerhuis, J. A.; van Velzen, E. J. J.; Hoefsloot, H. C. J.; Smilde, A. K.; *Metabolomics* **2008**, *4*, 293. [Crossref]
52. Akarachantachote, N.; Chadcham, S.; Saithanu, K.; *Int. J. Pure Apll. Math.* **2014**, *94*, 3. [Crossref]
53. Liebelt, D. J.; Jordan, J. T.; Doherty, C. J.; *Phytochem. Rev.* **2019**, *18*, 1409. [Crossref]
54. Scarpeci, T. E.; Valle, E. M.; *Plant Growth Regul.* **2008**, *54*, 133. [Crossref]
55. Van den Ende, W.; Valluru, R.; *J. Exp. Bot.* **2009**, *60*, 9. [Crossref]
56. Uemura, M.; Steponkus, P. L.; *Plant Cell Environ.* **2003**, *26*, 1083. [Crossref]
57. Nguyen, B. C. Q.; Shahinozzaman, M.; Tien, N. T. K.; Thach, T. N.; Tawata, S.; *J. Cereal Sci.* **2020**, *93*, 102985. [Crossref]
58. Jeong, H.; Sung, J.; Yang, J.; Kim, Y.; Jeong, H. S.; Lee, J.; *J. Funct. Foods* **2018**, *43*, 70. [Crossref]
59. Guo, R.; Yuan, G.; Wang, Q.; *Food Chem.* **2011**, *129*, 1080. [Crossref]
60. Gottlieb, O. R.; *Micromolecular Evolution, Systematics, and Ecology: An Essay into a Novel Botanical Discipline*; Springer-Verlag: Berlin, Germany, 1982.
61. Raffaele, S.; Leger, A.; Roby, D.; *Plant Signaling Behav.* **2009**, *4*, 94. [Crossref]
62. He, M.; Ding, N.-Z.; *Front. Plant Sci.* **2020**, *11*, 562785. [Crossref]

Submitted: October 6, 2023
Published online: January 24, 2024

4.2. Investigação da influência do sistema de extração e da sazonalidade no potencial farmacológico das folhas de *Eugenia punicifolia*

Os dados apresentados neste artigo são resultados da investigação sobre a influência dos sistemas de extração e da sazonalidade no potencial farmacológico das folhas de *Eugenia punicifolia*. Os extratos foram obtidos por maceração exaustiva, utilizando quatro sistemas de extração: metanol (M), etanol (E), etanol/metanol (1:1, EM) e metanol/etanol/água (3:1:1, MEW). O perfil qualitativo e quantitativo dos extratos foi determinado por espectroscopia de ressonância magnética nuclear de hidrogênio (RMN de ^{1}H), empregando o método PULCON para a quantificação de compostos fenólicos, incluindo ácido gálico, catequina, epigalocatequina, quercetina e miricetina. A correlação entre os perfis químicos e as atividades bioativas foi realizada por meio da análise de correlação canônica (CCA). A atividade antioxidante foi avaliada pelos ensaios de eliminação de radicais livres (DPPH e ABTS), enquanto a capacidade antiglicante foi testada pela inibição da formação de produtos finais de glicação avançada (AGEs). O potencial antiviral contra o vírus Zika (ZIKV) foi analisado em células Vero E6, por meio da medição da infectividade viral em ensaios de imunofluorescência. Os resultados indicaram que o sistema MEW foi o mais eficiente na extração de compostos bioativos, especialmente em amostras coletadas na estação chuvosa. A CCA identificou os compostos ácido gálico, catequina, quercetina e miricetina como marcadores químicos para as atividades antioxidante, antiglicante e antiviral, destacando a importância da escolha do solvente e da sazonalidade na otimização do uso farmacológico das folhas de *E. punicifolia*.

Situação: Artigo publicado na *Molecules* em 05/02/2025. Disponível em **https://doi.org/10.3390/molecules30030713**.

molecules

MDPI

Article

Investigation of the Influence of the Extraction System and Seasonality on the Pharmacological Potential of *Eugenia punicifolia* Leaves

Kidney O. G. Neves [1], Samuel O. Silva [1], Marinildo S. Cruz [1], Josiana Moreira Mar [2], Jaqueline A. Bezerra [2], Edgar A. Sanches [2], Natasha Marques Cassani [3], Giovanna A. Antoniucci [3], Ana Carolina Gomes Jardim [3], Francisco C. M. Chaves [4], Leonard D. R. Acho [5], Emersom S. Lima [5], Marcos B. Machado [1,*] and Alan D. C. Santos [1,6,*]

[1] Núcleo de Estudos Químicos de Micromoléculas da Amazônia—NEQUIMA, Universidade Federal do Amazonas, Manaus 69067-005, AM, Brazil; kidneydeoliveira@ufam.edu.br (K.O.G.N.); samuel-oliveira.silva@ufam.edu.br (S.O.S.); marinildo.cruz@ufam.edu.br (M.S.C.)
[2] Laboratório de Polímeros Nanoestruturados (NANOPOL), Departamento de Física de Materiais, Universidade Federal do Amazonas, Manaus 69067-005, AM, Brazil; josimoreira@ufam.edu.br (J.M.M.); jaqueline.araujo@ifam.edu.br (J.A.B.); sanchesufam@ufam.edu.br (E.A.S.)
[3] Laboratory of Antiviral Research, Federal University of Uberlândia, Uberlândia 38405-302, MG, Brazil; natashacassani@ufu.br (N.M.C.); giovanna.antoniucci@ufu.br (G.A.A.); jardim@ufu.br (A.C.G.J.)
[4] Empresa Brasileira de Pesquisa Agropecuária—Embrapa Amazônia Ocidental, Manaus 69010-970, AM, Brazil; celio.chaves@embrapa.br
[5] Laboratório de Atividade Biológica, Faculdade de Ciências Farmacêuticas, Universidade Federal do Amazonas, Manaus 69067-005, AM, Brazil; leonard.rosale@ufam.edu.br (L.D.R.A.); eslima@ufam.edu.br (E.S.L.)
[6] Núcleo de Pesquisa de Produtos Naturais, Universidade Federal de Santa Maria, Santa Maria 97105-900, RS, Brazil
* Correspondence: marcosmachado@ufam.edu.br (M.B.M.); alandiegormn@gmail.com.br (A.D.C.S.)

Academic Editors: Claudio Ferrante, Irwin Rose Alencar Menezes, Henrique Douglas Melo Coutinho, Almir Gonçalves Wanderley and Jaime Ribeiro-Filho

Received: 3 December 2024
Revised: 23 January 2025
Accepted: 27 January 2025
Published: date

Citation: Neves, K.O.G.; Silva, S.O.; Cruz, M.S.; Mar, J.M.; Bezerra, J.A.; Sanches, E.A.; Cassani, N.M.; Antoniucci, G.A.; Jardim, A.C.G.; Chaves, F.C.M.; et al. Investigation of the Influence of the Extraction System and Seasonality on the Pharmacological Potential of *Eugenia punicifolia* Leaves. *Molecules* **2025**, *30*, x. https://doi.org/10.3390/xxxxx

Abstract: The chemical complexity of natural products, such as *Eugenia punicifolia* (Kunth) DC. plant, presents a challenge when extracting and identifying bioactive compounds. This study investigates the impact of different extraction systems and seasonal variations on the chemical profile and pharmacological potential of *E. punicifolia* leaves using NMR spectroscopy for chemical analysis and canonical correlation analysis (CCA) for bioactivity correlation. Extracts obtained with methanol (M), ethanol (E), methanol/ethanol (1:1, ME), and methanol/ethanol/water (3:1:1, MEW) were analyzed for antioxidant, antiglycation, and antiviral activities. Quantitative ^{1}H NMR, combined with the PULCON method, was used to quantify phenolic compounds such as quercetin, myricetin, catechin, and gallic acid. The results showed that the MEW extract obtained in the rainy season exhibited the highest antioxidant and antiglycation activities, with a greater than 93% of advanced-glycation end-products (AGEs) inhibition capacity. Furthermore, our results showed that all the extracts were able to inhibit over 94% of the Zika virus (ZIKV) infection in Vero E6 cells. The CCA established strong correlations between the phenolic compounds and bioactivities, identifying gallic acid, catechin, quercetin, and myricetin as key chemical markers. This study demonstrates the importance of selecting appropriate extraction systems and considering seasonality to optimize the pharmacological potential of *E. punicifolia* leaves and highlights the efficacy of NMR in linking chemical composition with bioactivities.

Keywords: pedra-ume-caá; medicinal plant; solvent extraction; antioxidant; antiglycation; antiviral; Zika virus; phenolic compounds; NMR spectroscopy; CCA

1. Introduction

Eugenia punicifolia (Kunth) DC., a species that is both native and endemic to Brazil, is widely distributed throughout the Amazon region. Commonly known as a "vegetable insulin", this plant is part of a group of species known *as* pedra-ume-caá, which are traditionally used in herbal medicine [1–3]. Research on this matrix has demonstrated that its leaves contain barbinervic acid, a compound with vasodilatory effects. This compound shows significant potential as a template for developing new molecules to treat cardiovascular diseases [4]. Basting et al. (2014) demonstrated that the hydroalcoholic extract from the leaves has significant antinociceptive and anti-inflammatory effects, which may be related to the inhibition of the glutamatergic system, nitric oxide synthesis, and the phosphorylation of p38α MAPK [5]. Furthermore, Oliveira et al. (2022), Sales et al. (2014), and Ramos et al. (2019) showed that the leaves and fruits of this species exhibit antioxidant and antiglycation potential, as well as a chemical composition rich in flavonoids and organic acids with various pharmacological properties, particularly for the treatment of diabetes mellitus [2,6,7]. *E. punicifolia* is frequently marketed in the Amazon for this purpose. Its widespread use in this region has driven scientific interest in exploring its pharmacological potential, especially its ability to manage blood glucose levels in diabetic patients [2,6–9].

In general, natural products are chemically complex and contain a wide variety of bioactive compounds, including alkaloids, flavonoids, terpenes, lignoids, and phenolic acids, each contributing to the plant's overall pharmacological activity. This complexity, coupled with the typically low concentrations of these bioactive compounds, poses significant challenges in the chemical analysis of such matrices, making the choice of extraction methodology crucial. Extraction serves as the initial step to isolate the desired bioactive compounds from the raw material and can provide a clear snapshot of the plant's chemical profile, while the type of extraction used can maximize both the yield and selectivity of active principles [10].

This matter has been exemplified in the work published by Neves et al. (2004), who investigated the influence of seasonal variation (dry, rainy, and transition periods) on the ^{1}H NMR chemical profiles and antioxidant potential of *E. punicifolia* leaf extracts obtained with dimethyl sulfoxide (DMSO) [11]. Although variations in the chemical profiles and antioxidant activities were observed between the seasons, the ^{1}H NMR data did not provide sufficient insight into the correlation between secondary metabolites and bioactivity, since DMSO favored the extraction of primary metabolites. This limitation highlights the need to explore alternative extraction methods to better establish the link between secondary metabolites and bioactivity.

Although several studies have reported extraction methods for analyzing the chemical composition of *E. punicifolia*, only a few have investigated or optimized these processes to assess their impact on biological activity [9,12,13]. Among them, the work of Santos et al. (2020) stands out for its focus on optimizing the recovery of phenolic compounds with enhanced antioxidant and antiproliferative activities. Using a multivariate analytical approach, they developed an optimized extraction method for *E. punicifolia* leaves. Among the solvents tested (ethanol, methanol, and water), ethanolic extracts yielded the highest phenolic content, exhibited the strongest antioxidant activity, and demonstrated moderate antiproliferative activity against HEp-2 cells [9]. Santos et al.'s (2020) study provides a solid foundation for research on extraction methods for *E. punicifolia* and served as the starting point for our current investigation.

Nuclear magnetic resonance spectroscopy (NMR) has played an important role in tracking the qualitative and quantitative profiles of metabolites in plants, offering relevant insight into their complex chemical compositions [14–16]. This technique is essential for establishing correlations between the chemical profiles of plant extracts and their biological activities, often referred to as spectrum–effect relationships [17–19]. By providing detailed molecular information, NMR allows researchers to link specific metabolites to pharmacological effects, aiding in the identification of key bioactive compounds and optimizing the extraction methods for targeted applications.

In this context, the present study aimed to identify the most effective extraction solvent for correlating the quantitative chemical profiles, obtained through NMR spectroscopy, with the pharmacological potential (antioxidant, antiglycation, and antiviral) of *E. punicifolia* leaves collected during different seasonal periods.

2. Results and Discussion

2.1. The Performance of the Extraction Systems Tested

Water, methanol, ethanol, their mixtures, and aqueous acetone solutions are commonly used for the extraction of phenolic compounds [9]. However, the wide diversity of phenolics in plants poses a challenge to the standardization of extraction methods, particularly in selecting the most suitable solvent [9,11].

The efficiency of the extraction system was evaluated by calculating the mean and standard deviation of yield values obtained in triplicate (Table 1). The ternary mixture MEW (methanol/ethanol/water) produced the highest yields, with overall standard deviations ranging from 7.31% to 13.46%. The method's reproducibility was assessed using an ANOVA of the mean yields, considering both the extraction solvent and the collection period. This analysis demonstrated satisfactory reproducibility, as no significant statistical differences in extraction yields were observed across samples collected in different periods as a function of the extraction solvent—except for the samples collected during the dry season and extracted with methanol. This indicates that the extraction efficiency is slightly affected by the season, though it confirms that, overall, the extraction systems are suitable for obtaining *E. punicifolia* leaf extracts.

Table 1. Yields of *E. punicifolia* leaf extracts according to the extraction system and collection period.

Sample	MEW (mg g^{-1} Dry Extract)	M (mg g^{-1} Dry Extract)	EM (mg g^{-1} Dry Extract)	E (mg g^{-1} Dry Extract)
Dry	312.2 ± 13.5 ^{ab}	275.8 ± 5.9 ^{c}	207.4 ± 4.7 ^{e}	117.0 ± 8.9 ^{f}
Transition	334.1 ± 7.3 ^{a}	298.9 ± 8.6 ^{b}	224.9 ± 1.9 ^{ed}	118.9 ± 7.8 ^{f}
Rainy	328.2 ± 8.1 ^{a}	304.2 ± 1.9 ^{b}	242.9 ± 9.1 ^{d}	124.4 ± 7.1 ^{f}

$^{a, b, c, d, e, f}$ Clustering for extraction yield using Tukey's test and a 95% confidence interval. Extract acronyms: MEW—methanol/ethanol/water; M—methanol; EM—ethanol/methanol; and E—ethanol.

2.2. Bioactivities of the E. punicifolia Leaf Extracts

2.2.1. Cytotoxicity of *Eugenia punicifolia* Leaf Extracts

Cytotoxicity, or assessing cell viability, is a critical step in evaluating the antiviral potential of plant extracts and substances, as it indicates the ability of a substance or extract to cause cellular damage or death [20]. In this study, to investigate potential cytotoxicity, Vero E6 cells (kidney tissue derived from a normal, adult African green monkey) were each treated with *E. punicifolia* extracts at the concentrations of 50, 10, and 2 μg mL^{-1}

for 72 h. Then, cell viability was assessed via an MTT assay. DMSO (0.1%) was used as the untreated control. Analyzing the effects of the tested extracts on cell viability, we found that the treatment of Vero E6 cells with extracts at the concentration of 50 μg mL^{-1} presented cell viability over 90% (Figure S1).

2.2.2. Anti-ZIKV Activity

Due to its traditional use in the treatment of type 2 diabetes mellitus, research on *E. punicifolia* has primarily focused on evaluating its antiglycation potential [2,6,7]. However, given the species' diverse chemical composition and its use in regions frequently affected by viruses, including ZIKV, it is crucial to investigate its potential antiviral properties. In this study, the anti-ZIKV activity of the extracts was assessed using Vero E6 cells infected with $ZIKV_{PE243}$ in the presence or absence of the extracts for 72 h. The results showed that the extracts at the established non-cytotoxic concentration were able to inhibit up to 100% of ZIKV infection, with the minimum inhibitory rate of 94.8% under treatment with the M-Transition extract (Figure 1). This is the first study to demonstrate that *E. punicifolia* leaf extracts can inhibit ZIKV replication, which enhances the value of this plant species. However, additional assays should be performed to better understand the mechanism of action of these extracts and their cytotoxic effects, since they were tested in a general MTT and infection assay. The observed reduction in viral replication could be a result of either a virucidal activity or inhibition of viral replication cycle within the host cells.

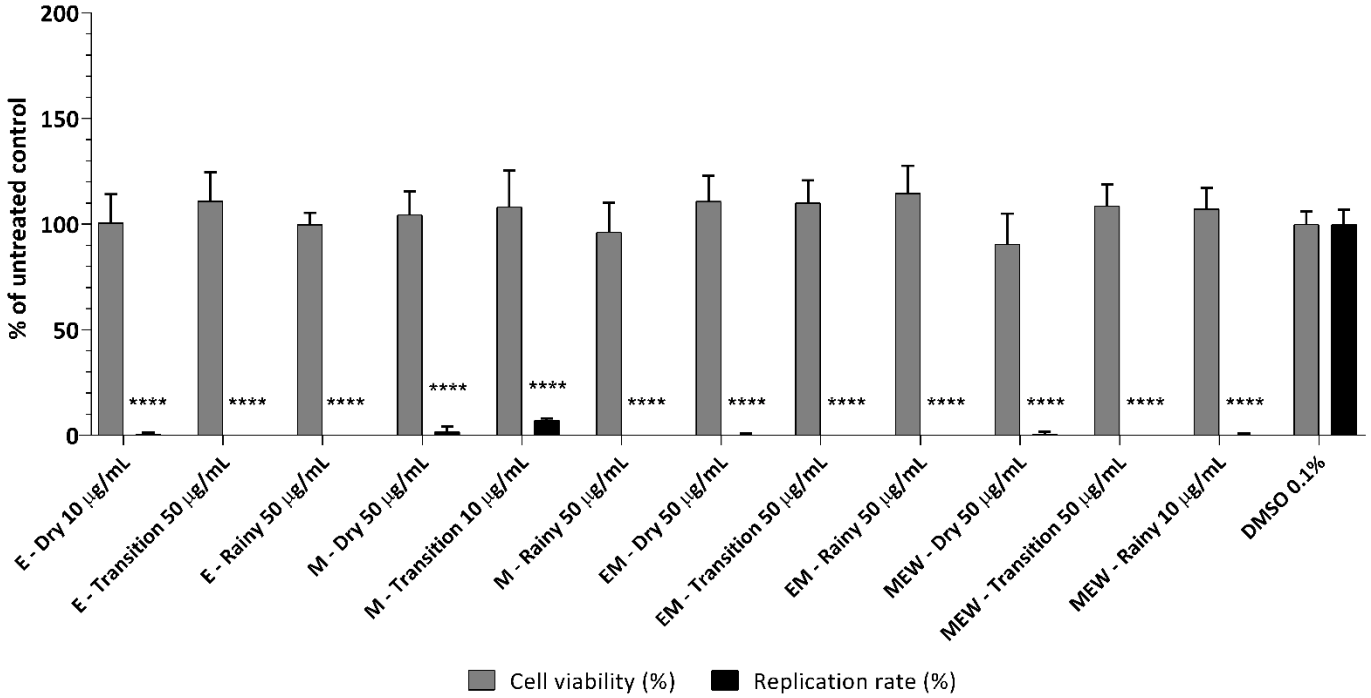

Figure 1. Effect of extracts of *E. punicifolia* leaves on viability of Vero E6 cells and ZIKV infectivity. Vero E6 cells were infected with $ZIKV_{PE243}$ at an MOI of 0.01 in the presence or absence of each extract at the highest non-cytotoxic concentration for 72 h. Then, the cells were fixed, and an immunofluorescence assay was performed. Focus-forming units (FFUs) were counted. The viability assay was performed in parallel by treating Vero E6 cells with each compound at the previously established non-cytotoxic concentration, and absorbance was measured (560 nm). DMSO (0.1%) was used as the untreated control. The mean values of two independent experiments, each performed in triplicate, including the standard error of the mean, are shown. *P* values < 0.05 were considered significant. (****) $p < 0.0001$. Extract acronyms: MEW—methanol/ethanol/water; M—methanol; EM—ethanol/methanol; and E—ethanol.

2.2.3. Antioxidant Activity via DPPH and ABTS Assays

DPPH and ABTS assays provide a low-cost and efficient method for determining the oxidation-inhibiting capacity of plant-derived substances and extracts [21,22]. As such, these assays can be used as probes to assess the impact of external factors on the chemical composition of plant matrices [23,24].

The DPPH and ABTS assays demonstrated that, regardless of the extraction system used, samples collected during the rainy season exhibited the strongest antioxidant responses (Table 2). Among the extraction systems, EM and MEW yielded the best results; however, MEW showed an antioxidant response of 8% to 16%, which is higher than that of the samples extracted with EM. The Pearson correlation for the antioxidant assays was 0.923 ($p < 0.05$), indicating a strong correlation between the assays and confirming the antioxidant potential of the samples collected during the rainy season and extracted using the MEW system.

Table 2. Scavenging capacity of the DPPH$^{\bullet}$ free-radical and the ABTS$^{\bullet+}$ cation radical expressed in μM TE g^{-1}.

Sample	Dry		Transition		Rainy	
	DPPH$^{\bullet}$	ABTS$^{\bullet+}$	DPPH$^{\bullet}$	ABTS$^{\bullet+}$	DPPH$^{\bullet}$	ABTS$^{\bullet+}$
MEW	1317.5 ± 6.6 ^{a}	1848.8 ± 6.9 ^{a}	1449.2 ± 8.8 ^{a}	2008.8 ± 8.4 ^{a}	1530.8 ± 5.2 ^{a}	2121.0 ± 6.7 ^{a}
EM	1139.2 ± 10.1 ^{b}	1702.1 ± 10.7 ^{b}	1213.3 ± 8.0 ^{b}	1766.5 ± 6.9 ^{b}	1343.33 ± 8.0 ^{b}	1919.9 ± 8.4 ^{b}
E	1115.0 ± 9.0 ^{c}	1685.4 ± 6.9 ^{b}	1189.2 ± 8.8 ^{c}	1751.0 ± 6.7 ^{b}	1318.3 ± 6.3 ^{c}	1827.7 ± 6.7 ^{d}
M	1025.8 ± 5.2 ^{d}	1645.4 ± 8.4 ^{c}	1085.8 ± 3.8 ^{d}	1703.2 ± 10.2 ^{a}	1140.8 ± 7.6 ^{d}	1878.8 ± 8.4 ^{c}

$^{a, b, c, d}$ Clustering for scavenging capacity using ANOVA (Tukey's test and 95% confidence interval). Extract acronyms: MEW—methanol/ethanol/water; M—methanol; EM—ethanol/methanol; and E—ethanol.

2.2.4. Antiglycation Activity Assay: Non-Oxidative Pathway

Type 2 diabetes mellitus, characterized by persistent hyperglycemia, leads to non-enzymatic glycation reactions with proteins and lipids, marking the initial stage in the formation of advanced-glycation end-products (AGEs) [25]. Since AGEs play a critical role in diabetic complications, identifying plant matrices rich in compounds that can inhibit the glycation process has become a promising and effective approach. In this study, the ability of various *E. punicifolia* leaf extracts to inhibit AGE formation via the non-oxidative pathway was evaluated (Table 3).

Table 3. Inhibitory capacity of *E. punicifolia* leaf extracts on the formation of advanced-glycation end-products via the non-oxidative pathway.

Sample	MEW (% Inhibition of AGEs)	M (% Inhibition of AGEs)	EM (% Inhibition of AGEs)	E (% Inhibition of AGEs)
Dry	80.5 ± 1.4 ^{b}	90.1 ± 2.0 ^{a}	80.4 ± 3.0 ^{b}	76.0 ± 1.8 ^{b}
Transition	94.3 ± 1.5 ^{a}	82.4 ± 2.4 ^{b}	83.4 ± 1.6 ^{b}	94.0 ± 3.0 ^{a}
Rainy	93.1 ± 3.7 ^{a}	88.2 ± 3.8 ^{ab}	94.8 ± 1.4 ^{a}	87.5 ± 3.0 ^{a}

$^{a, b}$ Clustering for inhibition of AGEs using ANOVA with Tukey's test and 95% confidence interval. Extract acronyms: MEW—methanol/ethanol/water; M—methanol; EM—ethanol/methanol; and E—ethanol.

The results demonstrate that all the extracts exhibited an inhibition potential greater than 75%. Furthermore, with the exception of the methanol extracts, significant differences in inhibition capacities were observed between the samples collected during the dry and rainy seasons. The rainy season samples showed up to 15% higher inhibition

compared to those collected in the dry season. This finding confirms that the collection period is a critical factor when evaluating the antiglycation potential of *E. punicifolia* leaves.

2.3. Identification of Phenolic Compounds in E. punicifolia Leaf Extracts

The four extracts (E, M, EM, and MEW) of *E. punicifolia* leaves were analyzed via NMR spectroscopy, which led to the identification of gallic acid (**1**) and four flavonoids: epigallocatechin (**2**), catechin (**3**), quercetin (**4**), and myricetin (**5**) (Figures S2–S6). Gallic acid was identified by correlating the signal at δ 6.95 (H-2 and H-6, s) with the signals observed at 165.7 (COOH), 108.6 (C-2 and C-6), 145.6 (C-3 and C-5), and 138.2 (C-4) in the long-range ^{1}H-^{13}C HMBC correlation map [26]. While the signals at δ 5.89 (H-8, d, 2.3 Hz), δ 5.72 (H-6, d, 2.3 Hz), and δ 6.38 (H-2′ and H-5′, s) were attributed to rings A and B of epigallocatechin, along with the singlet at δ 4.73 (H-2, s) and the multiplet at δ 4.00 (H-3, m) referring to its C ring [27]. The presence of catechin in the extracts was supported by signals at δ 5.83 (H-6, d, 2.3 Hz), δ 5.93 (H-8, d, 2.3 Hz), δ 6.65 (H-5′, d, 8.1 Hz), δ 6.75 (H-6′, dd, 2.3 Hz and 8.1 Hz), and δ 6.86 (H-2′, d, 2.3 Hz), corresponding to rings A and B, as well as the doublet at δ 5.02 (H-2, d, 1.8 Hz) referring to the C ring [28]. Quercetin and myricetin both exhibited signals at δ 6.41 (H-8, d, 2.1 Hz) and δ 6.22 (H-6, d, 2.1 Hz) belonging to ring A; however, in ring B, myricetin presented a signal at δ 7.01 (H-2′ and H-5′, s), while quercetin displayed signals at δ 7.30 (H-2′, d, 2.1 Hz), δ 7.25 (H-6′, dd, 2.1 and 8.3 Hz), and δ 6.87 (H-5′, d, 8.3 Hz) [28]. The connection of the B ring with the C ring of the flavonoids was assigned based on the correlations observed in the HMBC correlation plot, as shown in Figure 2.

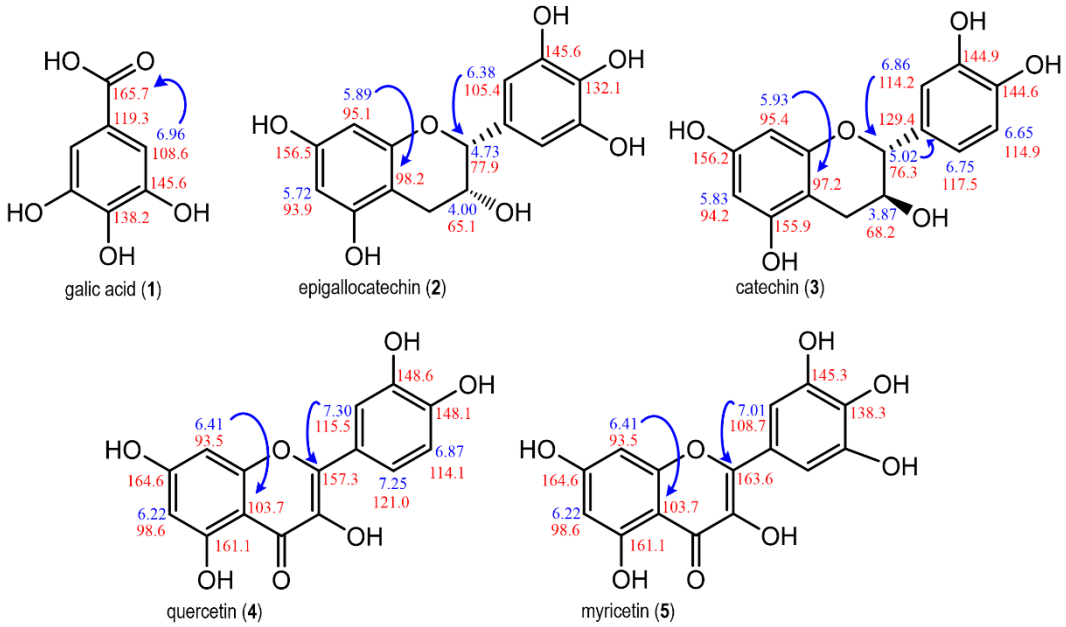

Figure 2. Compounds identified by NMR spectroscopy in different *E. punicifolia* leaf extracts. Blue arrows represent key correlations observed in the long-range HMBC correlation plot.

2.4. qNMR of Phenolic Compounds by PULCON

PULCON (Pulse Length-Based Concentration Determination) is a powerful NMR method for quantifying compounds in complex mixtures without requiring specific standards for the compounds of interest [29,30]. The method is based on the principle of reciprocity, which correlates the absolute intensities in two one-dimensional (1D) NMR spectra [31,32]. Using PULCON, the ^{1}H NMR signals corresponding to gallic acid (δ 6.96, s),

epigallocatechin (δ 5.89, d, 2.3 Hz), catechin (δ 5.93, d, 2.3 Hz), quercetin (δ 7.30, d, 2.1 Hz), and myricetin (δ 7.01, s) were quantified in the different extracts of *E. punicifolia* leaves (Figures S7–S12), as summarized in Table 4. Overall, the concentrations of compounds in the *E. punicifolia* extracts can be categorized into three groups: (I) catechin as the most abundant phenolic compound, (II) gallic acid and epigallocatechin at intermediate concentrations and (III) quercetin and myricetin as the least abundant. The specific ranking within groups II and III depended on the extraction solvent used and the period considered.

Table 4. ^{1}H NMR quantification of the main phenolic compounds of *E. punicifolia* leaf extracts using PULCON.

Sample	Quercetin (mg g^{-1} Dry Extract)	Myricetin (mg g^{-1} Dry Extract)	Gallic acid (mg g^{-1} Dry Extract)	Catechin (mg g^{-1} Dry Extract)	Epigallocatechin (mg g^{-1} Dry Extract)	Sum of Total Phenolics (mg g^{-1} Dry Extract)
E—Dry	1.94 ± 0.01	1.40 ± 0.00	3.49 ± 0.01	5.02 ± 0.01	3.34 ± 0.01	15.24 ± 0.20
E—Transition	2.23 ± 0.01	1.62 ± 0.00	3.54 ± 0.01	4.65 ± 0.02	3.63 ± 0.02	15.75 ± 0.31
E—Rainy	2.23 ± 0.00	1.69 ± 0.00	3.50 ± 0.01	4.54 ± 0.01	3.55 ± 0.01	15.60 ± 0.17
EM—Dry	1.24 ± 0.01	1.45 ± 0.01	3.23 ± 0.01	5.50 ± 0.02	3.60 ± 0.02	15.09 ± 0.37
EM—Transition	1.73 ± 0.00	1.71 ± 0.00	4.04 ± 0.01	6.55 ± 0.01	5.01 ± 0.00	19.13 ± 0.18
EM—Rainy	2.44 ± 0.00	1.87 ± 0.00	3.61 ± 0.01	5.78 ± 0.01	4.47 ± 0.00	18.27 ± 0.07
M—Dry	1.47 ± 0.00	1.75 ± 0.01	3.85 ± 0.02	6.54 ± 0.03	4.28 ± 0.02	17.98 ± 0.43
M—Transition	2.07 ± 0.00	1.60 ± 0.00	4.00 ± 0.02	6.35 ± 0.01	5.55 ± 0.01	19.65 ± 0.18
M—Rainy	2.29 ± 0.01	1.83 ± 0.01	3.91 ± 0.00	5.89 ± 0.02	5.08 ± 0.01	19.11 ± 0.43
MEW—Dry	2.89 ± 0.01	2.13 ± 0.00	3.38 ± 0.03	6.97 ± 0.03	4.87 ± 0.03	20.35 ± 0.35
MEW—Transition	2.70 ± 0.01	1.56 ± 0.01	3.91 ± 0.01	6.67 ± 0.03	5.85 ± 0.02	20.94 ± 0.56
MEW—Rainy	3.16 ± 0.00	1.98 ± 0.00	3.79 ± 0.02	6.12 ± 0.01	5.07 ± 0.01	20.22 ± 0.27

Extract acronyms: MEW—methanol/ethanol/water; M—methanol; EM—ethanol/methanol; and E—ethanol.

Table 4 also presents the NMR-quantified phenolic compounds, representing the sum of all the identified and quantified phenolic compounds. These values clearly demonstrate the influence of the extraction procedure on the selectivity of phenolic compounds, with MEW being the most selective solvent and E the least selective. Notably, the total phenolic content suggested a dependency between the extraction solvent's selectivity and the periods (dry, transition, and rainy). For the MEW samples, no significant statistical differences in total phenolics were observed among the periods. In contrast, extractions with E showed significant seasonal variation.

The phenolic content provided by PULCON can be a valuable tool in understanding the relationship between the chemical composition and biological activity of *E. punicifolia* leaf extracts, especially since their phenolic profiles are qualitatively similar. In such cases, differences in biological activities may be linked to variations in phenolic content.

2.5. Chemical Composition and Bioactivities of the E. punicifolia Leaf Extracts: Searching for Correlations

The correlation between the compounds quantified via ^{1}H NMR and the pharmacological potential of *E. punicifolia* leaf extracts (Figure 3) was assessed using a canonical correlation analysis (CCA), a multivariate statistical technique that identifies and quantifies the relationship between two sets of variables [33]. Pearson's correlation coefficient was applied as the index to evaluate the strength or existence of this correlation (Table S1) [34,35].

An analysis of the Pearson correlation values with the antioxidant assays revealed that 2-epigallocatechin (r = 0.67), quercetin (r = 0.87), and myricetin (r = 0.65) exhibit a moderately positive correlation with the ABTS radical cation scavenging capacity. Additionally, only quercetin (r = 0.85) and myricetin (r = 0.58) were found to correlate with the DPPH radical scavenging capacity (Figure 3). Several studies on these flavonoids have demonstrated their ability to scavenge free radicals in the body [36,37].

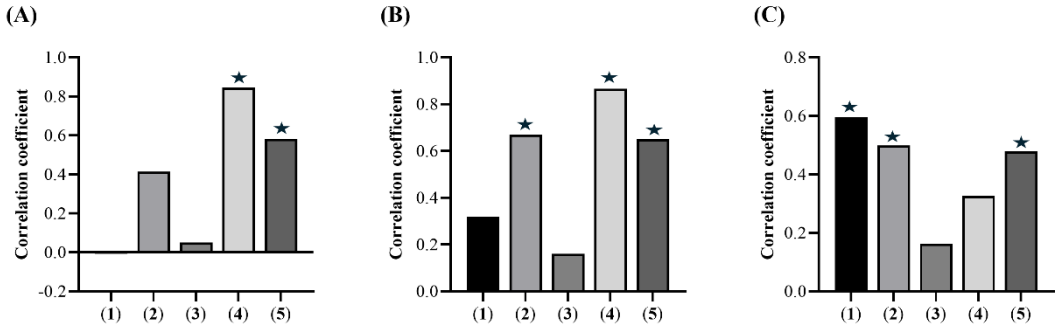

Figure 3. Canonical correlation analysis. Pearson correlation coefficients (★, r > 0.50) between the concentrations determined using ^{1}H NMR and the scavenging capacity of the DPPH radical (**A**), the ABTS radical cation (**B**), and AGE formation inhibition (**C**) **1**—gallic acid, **2**—epigallocatechin, **3**—catechin, **4**—quercetin, and **5**—myricetin.

In 2024, a study on the antioxidant potential of DMSO extracts of *E. punicifolia* leaves revealed that samples collected during the dry period exhibited the strongest antioxidant response [11]. This supports the notion that the extraction system is a key factor since it influences not only the antioxidant activity but also any pharmacological activity of plant matrices. For *E. punicifolia*, DMSO extraction primarily favored carbohydrates and fatty acids, whereas the extraction systems described in this study favored flavonoid compounds. Among the identified flavonoids, myricetin was notably absent in the DMSO-extracted samples. Given myricetin's high antioxidant potential, its presence likely contributes to the differences in antioxidant capacity observed between the various extraction systems [38]. These findings highlight the need to establish a standardized extraction protocol to ensure the chemical profile is consistent and serves as a reliable basis for comparison between studies on plant matrices.

In the AGE formation inhibition assay, the Pearson' correlation analysis revealed that only gallic acid (r = 0.60), 2-epigallocatechin (r = 0.50), and myricetin (r = 0.48) showed a moderately positive correlation (Figure 3). Studies on these compounds demonstrate their crucial role in inhibiting the early stages of glycation, thus preventing the formation of AGEs [39]. Furthermore, Wang et al. (2024) reported that myricetin and its derivatives can completely inhibit products generated by non-enzymatic glycation reactions [40]. Along with their association with the antiglycation activity of *E. punicifolia* leaves, gallic acid, catechin, and myricetin have also been suggested by Oliveira et al. (2024) as key chemical markers for species of *Pedra-ume-caá* [2].

Given that all *E. punicifolia* extracts demonstrated variable cytotoxicity in Vero E6 cells and a ZIKV infection inhibition capacity greater than 95%, this response is likely attributed to the phenolic compounds identified and quantified in the extracts [41,42]. Some components of the extracts enhanced cell viability at certain concentrations, and this might be due to the fact that plant-derived polyphenols, including flavonoids, exhibit antioxidant properties that support cell survival and growth under certain conditions [43,44]. Myricetin has shown concentration-dependent protective effects, enhancing cellular repair and proliferation at optimal levels [44]. Likewise, quercetin has been linked to

improved mitochondrial function and increased metabolic activity, aiding cell viability, especially under stress, which can further be seen by different effects in different concentrations [45].

Regarding the antiviral properties, a study by Lim et al. (2017) showed that myricetin can inhibit 88% of $ZIKV_{NS2B\text{-}NS3}$ activity [46]. Similarly, an in vitro study by Zou et al. (2020) found that, at a concentration of 1.0 mM, myricetin and quercetin can inhibit up to 80% of $ZIKV_{NS1}$ infection, as also found by Ramos et al. (2022), with quercetin inhibiting $ZIKV_{NS5}$ RNA-dependent RNA polymerase (RdRp) with IC_{50} values of 0.5 μM [47]. This inhibitory capacity has been linked to the presence of hydroxyl groups on ring B of these compounds [48].

Thus, the canonical correlation analysis, with the Pearson's correlation coefficient as an index, proved to be an effective approach, allowing for the identification of gallic acid, catechin, quercetin, and myricetin as chemical indicators for monitoring the antioxidant, antiglycation, and antiviral activities of *E. punicifolia* leaf extracts in relation to the collection period.

3. Materials and Methods

3.1. Materials

The methanol (HPLC) and absolute ethanol (99.5% PA) used for plant material extraction were purchased from Sigma-Aldrich (St. Louis, MO, USA). The deuterated dimethyl sulfoxide (DMSO-*d*6, 99.9%) with tetramethylsilane (TMS, 0.05% V/V) for NMR analyses was obtained from Cambridge Isotope Laboratories Inc. (Andover, MA, USA). Dimethyl terephthalate (DMT), a certified reference material, was provided by the Division of Chemical and Thermal Metrology (Inmetro, Rio de Janeiro, Brazil), under certification number DIMCI 1507/2019 (certified purity: 99.988 ± 0.060%). The reagents used in antioxidant assays, including 6-hydroxy-2,5,7,8-tetramethylchroman-2-carboxylic acid (Trolox), 2,2-diphenyl-1-picrylhydrazyl ($DPPH^{\bullet}$), and 2,2′-azino-bis(3-ethylbenzothiazoline-6-sulfonic acid) and ammonium salt ($ABTS^{\bullet+}$), were obtained from Sigma-Aldrich (St. Louis, MO, USA). Similarly, albumin, fructose and sodium azide used in the antiglycation assay were sourced from Sigma-Aldrich (St. Louis, MO, USA). For the cytotoxic and antiviral assay, Dulbecco's Modified Eagle's Medium (DMEM) and 3-(4,5-dimethylthiazol-2-yl)-2,5-diphenyltetrazolium bromide (MTT) were obtained from Sigma-Aldrich (St. Louis, MO, USA), while penicillin, streptomycin, non-essential amino acids, and fetal bovine serum were sourced from Gibco Life Technologies (Carlsbad, CA, USA). The ZIKV rabbit anti-NS3 primary antibody was kindly provided by Professor Andres Merits [49]. Goat anti-rabbit IgG Alexa Fluor 488 was sourced from Invitrogen (Waltham, MA, USA).

3.2. Plant Material

The leaves of *E. punicifolia* were collected during different months [August 2021 (dry period), December 2021 (transition period), and March 2022 (rainy period)] at the Brazilian Agricultural Research Corporation—Embrapa Amazônia Ocidental—located along Rodovia AM-010, Km 29 (2° 53′ 23″ S 59° 58′ 26″ W). Access to genetic heritage was registered (A82BD35) in the National System of Management of Genetic Heritage and Associated Traditional Knowledge (SisGen). From a plantation of 150 individuals, 15 trees were randomly selected, and leaves were gathered from various heights to ensure a representative sample (11 leaves each from the lower, middle, and upper parts of the trees). The collected plant material was dried at room temperature for 24 h, followed by 48 h in a forced air circulation oven at 40 °C. After drying, each sample was subjected to the cold maceration process with liquid nitrogen, weighed, and then stored in a freezer at −80 °C until the extraction procedure.

3.3. Extraction Procedure

The extraction systems used were selected based on the methodology described by Santos et al. (2020) [9]. For the extractions, 1.0 g of the sample mixture from each collection was subjected, in triplicate, to four different extraction systems: [1: methanol (100%)—M; 2: ethanol (100%)—E; 3: ethanol (50%)/methanol (50%)—EM; and 4: methanol (60%)/ethanol (20%)/water (20%)—MEW]. Each extraction was performed four times and sonicated in an ultrasonic bath for 15 min, followed by centrifugation at 4000 rpm for 10 min (4226 *g*). The supernatant was then separated and dried using nitrogen gas. Statistical analysis of the extraction yields was conducted using Minitab 18.1, employing the analysis of variance (ANOVA) with the Tukey's test and a significance level of 95% [50].

3.4. Acquisition and Processing of NMR Data

Twenty milligrams (20.0 mg) of each *E. punicifolia* leaf extract was solubilized in 520 µL of DMSO-d_6, sonicated in an ultrasonic bath for 10 min, and then transferred to a 5 mm NMR tube. NMR spectra were acquired using a Bruker Avance IIIHD NMR spectrometer (Bruker, Billerica, MA, USA), operating at 11.7 T (500 MHz for ^{1}H) and equipped with a 5 mm BBFO Plus SmartProbe™ with a Z-axis gradient. The pulse sequences used were obtained from the Bruker database. The zgpr pulse sequence was used, with the following acquisition parameters: time domain (TD) data points of 32k, spectral width (SW) of 8 kHz, acquisition time (AQ) of 1.64 s, receiver gain (RG) of 90.5, number of scans (NS) equal to 32, dummy scans of 2, FID resolution of 0.30 Hz, central frequency (O1) set to 1667.48 Hz, and suppression power (PLW9) of 8.6289e^{-005}. The P1 value was automatically calculated for each sample using the pulsecal sn command. The D1 values for signals corresponding to the aromatic compounds were calculated using Equation (1). The longitudinal relaxation constant (T1) was determined using an inversion–recovery experiment (t1ir) pulse sequence, and the highest T1 value was used to determine the D1 value (15 s) for the sample acquisition.

$$D1 = 7 \times T1 - AQ \quad (1)$$

The dimethyl terephthalate (DMT) was prepared in triplicate at a concentration of 20.12 mM in DMSO-d_6 (D, 99.9%) with TMS (0.05% v/v) as an internal reference standard (0.00 ppm). For the quantitative ^{1}H NMR spectrum, the 90° pulse of DMT (10.65 µs) was calculated for the signal at δ 8.10 (s, 4H) using the 90° pulse experiment (zg). The determination of T1 was carried out using the t1ir1d experiment for the signal at δ 8.10. After obtaining the T1 value, D1 (16.62 s) was estimated using Equation (1), for which the acquisition time (AQ) was set to 1.64 s. Except for the P1 and D1 parameters, the same acquisition parameters used for the quantitative spectra of the extracts were applied to the acquisition of DMT.

Phase and baseline corrections of the spectra were performed manually using TopSpin 3.6.3 software. The chemical shift (in ppm) of the ^{1}H NMR spectra was referenced to the methyl signal of tetramethylsilane at δ_H 0.00, and the coupling constants (J) were recorded in Hz. HSQC and HMBC NMR experiments were conducted to verify the absence of signal overlap with the signals of interest, with the ^{1}H-^{13}C correlations acquired using coupling constants J (H, C—single bond) and J (H, C—long-range) of 145 and 8 Hz, respectively. Signal integration was performed manually, and the quantification of phenolic compounds using the PULCON method was carried out with the ERETIC2 (electronic reference to access in vivo concentrations) tool in TopSpin 3.6.3 software [51,52].

3.5. Cell Culture

The Vero E6 cells (kidney tissue derived from a normal adult African green monkey, ATCC E6/CRL-1586) were cultured in Dulbecco's modified Eagle's medium supplemented

with 100 U mL^{-1} penicillin, 100 mg mL^{-1} streptomycin, 1% (*v*/*v*) non-essential amino acids, and 10% (*v*/*v*) fetal bovine serum at 37 °C in a humidified 5% CO_2 incubator.

3.6. Cell Viability Assay

Cell viability was measured via the MTT [3-(4,5-dimethylthiazol-2-yl)-2,5-diphenyl tetrazolium bromide] method. The Vero E6 cells were seeded in 96-well plates at a density of 5×10^3 cells per well and incubated overnight at 37 °C in a humidified 5% CO_2 incubator. The drug-containing medium at the concentrations of 50, 10, and 2.0 μg mL^{-1} was added to the cell culture for 72 h at 37 °C. Then, the medium was removed, and a solution containing MTT at the final concentration of 1 mg mL^{-1} was added to each well and incubated for 30 min at 37 °C in a humidified 5% CO_2 incubator, after which media were replaced with 100 μL of DMSO to solubilize the formazan crystals. Absorbance was measured using the optical density (OD) of each well at 560 nm, using a GloMax® microplate reader (Promega, Madison, WI, USA). Cell viability was calculated according to the equation (T/C) × 100%, where T and C represent the mean optical density of the treated group and vehicle control group, respectively.

3.7. Antiviral Assay—ZIKV

A wild-type ZIKV isolate from a clinical sample of a patient in Brazil ($ZIKV_{PE243}$) was amplified employing infected Vero E6 cells in 75 cm^2 flask for 3 days [53]. Then, the viral supernatant was collected and stored at −80 °C. To determine viral titers, 5 x 10^3 Vero E6 cells were seeded in each of the 96-well plates 24 h prior to the infection. Cells were infected with 10-fold serial dilution of $ZIKV_{PE243}$ and incubated for 72 h in a humidified 5% CO_2 incubator at 37 °C. Following this, the cells were fixed with 4% formaldehyde, washed with phosphate-buffered saline (PBS), and a blocking buffer (BB) was added containing 0.10% Triton X-100, 0.20% bovine albumin, and PBS for 30 min. An immunofluorescence assay was performed as previously described [54]. In summary, the cells were incubated with the ZIKV anti-NS3 primary antibody, followed by a second incubation with the goat anti-rabbit IgG Alexa Fluor 488. Images were analyzed using EVOs Cell Imaging Systems Fluorescence Microscopy (Thermo Fisher Scientific), and the foci of infection were counted and measured as focus-forming units (FFUs mL^{-1}) for viral titer determination.

To assess the antiviral activity of each extract, the Vero E6 cells were seeded at a density of 5×10^3 cells per well into 96-well plates for 24 h and infected with $ZIKV_{PE243}$ at a multiplicity of infection (MOI) of 0.01 FFU/cell in the presence of each compound at the established non-cytotoxic concentration. After 72h, the cells were fixed with 4% formaldehyde, incubated for 30 min, washed with PBS, and the BB was added for the immunofluorescence assay for FFU determination. Viral replication was calculated according to the equation (T/C) × 100%, where T and C represent the FFU mean of the treated group and vehicle control group, respectively.

Data were analyzed for normal distribution to demonstrate the applicability of a parametric or nonparametric tests. Subsequently, two-way ANOVA, using GraphPad Prism 10.3.0 software, was employed to compare the treatment of each compound with DMSO (0.1%) as a negative control, with significance set at $p < 0.05$ [55].

All the ZIKV infection assays were performed at a BSL-2 laboratory under the authorization number CBQ: 163/02 and process SEI: 01.245.006267/2022–14 from the CTNBio—National Technical Commission for Biosecurity from Brazil.

3.8. Determination of Antioxidant Potential

3.8.1. DPPH Radical Scavenging Capacity

The experiments were conducted following the methodology of Samaniego-Sánchez et al. (2011) with adaptations by Mar et al. (2021) [56,57]. The free-radical scavenging capacity of *E. punicifolia* leaf extracts was assessed using the DPPH• radical method. A 100 µM methanolic DPPH• solution was prepared. The samples were then prepared at a concentration of 1.0 mg mL^{-1} and mixed with 1900 µL of the methanolic DPPH• solution. Trolox, at a concentration from 100 to 2000, was used as a positive control. The mixture was incubated in the dark at 25 °C for 30 min. Absorbance was measured at 515 nm using a microplate reader (Bio Tek Instruments Inc., Winooski, VT, USA). The antioxidant capacity was quantified in Trolox equivalents, and the assay was performed in triplicate. The relationship between absorbance and Trolox concentration was determined as $y = -0.0004x + 0.731$, with an R^2 value of 0.9944. All measurements were made in triplicate, and the results were expressed in micromolar Trolox equivalents (µM Trolox mL^{-1}).

3.8.2. ABTS Radical Cation Scavenging Capacity

The $ABTS^{\bullet+}$-scavenging assay involves observing the color bleaching of the $ABTS^{\bullet+}$ solution in the presence of antioxidant extracts at a concentration of 1.0 mg mL^{-1}. The methodology of Samaniego-Sánchez et al. (2011) was utilized, with adaptations (Mar et al., 2021) [56,57]. After a 6 min reaction between the sample and the radical at a 1:10 ratio, absorbances were measured at 750 nm using a microplate reader (Bio Tek Instruments Inc., Winooski, VT, USA). Trolox was used to construct the standard curve ($y = 0.0003x + 0.7473$, $R^2 = 0.999$), and the results were expressed as mean ± standard deviation ($n = 3$) of the micromolar Trolox equivalents (µM Trolox mL^{-1}).

3.9. Antiglycation Activity: Non-Oxidative Pathway

The ability to inhibit the formation of advanced-glycation end-products (AGEs) was evaluated according to the method of Kiho et al. (2004), with slight modifications [58]. The reaction was carried out in triplicate using the following concentrations: 10.0 mg mL^{-1} albumin (BSA), 30 mM fructose, and 1.00 mg mL^{-1} of the sample (dissolved in DMSO). The fructose and BSA solutions were prepared in a phosphate buffer (0.20 M, pH 7.4) with 3.0 mM sodium azide as an antimicrobial agent. The 300 µL of the total reaction mixture consisted of BSA (135 µL), fructose (135 µL), and DMSO or sample (30 µL). The mixture was incubated at 37 °C for 48 h under sterile conditions and in the dark. After incubation, each sample was analyzed in a microplate reader for fluorescence intensity (emission λ 330 nm and excitation λ 420 nm). Aminoguanidine was used as a standard, and DMSO served as a negative control. The percentage inhibition was calculated using Equation (2), and the results are expressed as mean % inhibition ± standard deviation ($n = 3$).

$$\% \text{ inhibition} = 100 - [\text{Fluora/p/FLuorC}] \times 100 \quad (2)$$

where: Fluora/p = (White fluorescence − Sample fluorescence); FLuorC = (White fluorescence − Control fluorescence).

3.10. Canonical Correlation Analysis (CCA)

CCA was conducted using Pearson's correlation coefficient as a correlation index between the chemical composition and the bioactivities of the extracts obtained during the dry and rainy periods. The concentrations of the compounds determined using ^{1}H NMR, along with the antioxidant potential and AGE inhibition values, were used as variables. Pearson correlation coefficients were calculated using GraphPad Prism 10.3.0 software, with a 95% confidence interval and significance set at $p < 0.05$ (two-tailed) [55].

4. Conclusions

This investigation revealed that the extraction system and seasonality significantly influence the quantitative chemical profile and the antioxidant, antiglycation, and antiviral activities of *Eugenia punicifolia* leaf extracts. The MEW (methanol/ethanol/water) system proved to be the most efficient for extracting bioactive compounds, showing strong antioxidant and antiglycation potentials, especially in samples collected during the rainy season. The use of quantitative NMR and canonical correlation analysis (CCA) allowed for the identification and quantification of key phenolic compounds, including gallic acid, catechin, quercetin, and myricetin, which were linked to the observed pharmacological effects. These compounds can serve as chemical markers for tracking the antioxidant, antiglycation, and antiviral activities of *E. punicifolia* leaf extracts. Overall, this research highlights the importance of choosing the appropriate extraction methods and season to maximize the pharmacological potential of plant-based extracts.

Supplementary Materials: The following supporting information can be downloaded at www.mdpi.com/xxx/s1: Figure S1. Effect of extract of *Eugenia punicifolia* leaves on viability of Vero E6 cells. Vero E6 cells were treated with each compound at the highest non-cytotoxic concentration. After 72 h, cell viability was measured via the MTT assay. Viability was measured by absorbance (560 ηM). DMSO was used as the untreated control. Mean values of two independent experiments, each measured in triplicate including the standard error of the mean, are shown. *P* values < 0.05 were considered significant. (**) $p < 0.01$, (***) $p < 0.001$, and (****) $p < 0.0001$, Figure S2. ^{1}H NMR spectrum (500 MHz, DMSO-d_6) of MEW extract of *Eugenia punicifolia* leaves collected during the dry season (−1.00 to 10.00 ppm), Figure S3. HSQC spectrum (500 MHz, DMSO-d_6) of MEW extract of *Eugenia punicifolia* leaves collected during the dry season (range magnification of ^{1}H: −0.50 to 8.30 ppm—13C: −3.0 to 158.0 ppm), Figure S4. HSQC spectrum (^{1}H: 500 MHz, ^{13}C: 125 MHz DMSO-d_6) of MEW extract of *Eugenia punicifolia* leaves collected during the dry season (range magnification of ^{1}H: 5.50 to 7.80 ppm—^{13}C: 96.0 to 128.0 ppm). Signals corresponding to gallic acid (**1**: δ 6.95—δ 108.6), quercetin (**2**: δ 7.30—δ 115.5), myricetin (**3**: δ 7.01—δ 108.7), catechin (**4**: δ 5.93—δ 95.4) and epigallocatechin (**5**: δ 5.89—δ 95.1)], Figure S5. HMBC spectrum (^{1}H: 500 MHz, ^{13}C: 125 MHz DMSO-d_6) of MEW extract of *Eugenia punicifolia* leaves collected during the dry season (range magnification of ^{1}H: −0.50 to 8.50 ppm—13C: −4.7 to 193.3 ppm), Figure S6. HMBC spectrum (^{1}H: 500 MHz, ^{13}C: 125 MHz DMSO-d_6) of MEW extract of *Eugenia punicifolia* leaves collected during the dry season (range magnification of ^{1}H: 5.55 to 7.40 ppm—^{13}C: 50.7 to 180.2 ppm), Figure S7. ^{1}H NMR spectrum (500 MHz, DMSO-d_6) of extracts of *Eugenia punicifolia* leaves collected during the dry season (−1.00 to 10.00 ppm), Figure S8. ^{1}H NMR spectrum (500 MHz, DMSO-d_6—range magnification from 8.00 to 5.50 ppm) of extracts of *Eugenia punicifolia* leaves collected during the dry season. Signals corresponding to gallic acid (**1**: δ 6.95), quercetin (**2**: δ 7.30), myricetin (**3**: δ 7.01), catechin (**4**: δ 5.93) and epigallocatechin (**5**: δ 5.89)]. Extract acronyms: MEW—methanol/ethanol/water; M—methanol; EM—ethanol/methanol; and E—ethanol, Figure S9. ^{1}H NMR spectrum (500 MHz, DMSO-d_6) of extracts of *Eugenia punicifolia* leaves collected during the transition season (−1.00 to 10.00 ppm region), Figure S10. ^{1}H NMR spectrum (500 MHz, DMSO-d_6—range magnification from 8.00 to 5.50 ppm) of extracts of *Eugenia punicifolia* leaves collected during the transition season. Signals corresponding to gallic acid (**1**: δ 6.95), quercetin (**2**: δ 7.30), myricetin (**3**: δ 7.01), catechin (**4**: δ 5.93) and epigallocatechin (**5**: δ 5.89)]. Extract acronyms: MEW—methanol/ethanol/water; M—methanol; EM—ethanol/methanol; and E—ethanol, Figure S11**.** ^{1}H NMR spectrum (500 MHz, DMSO-d_6) of extracts of *Eugenia punicifolia* leaves collected during the rainy season (−1.00 to 10.00 ppm), Figure S12. ^{1}H NMR spectrum (500 MHz, DMSO-d_6—range magnification from 8.00 to 5.50 ppm) of extracts of *Eugenia punicifolia* collected during the transition season. Signals corresponding to gallic acid (**1**: δ 6.95), quercetin (**2**: δ 7.30), myricetin (**3**: δ 7.01), catechin (**4**: δ 5.93) and epigallocatechin (**5**: δ 5.89). Extract acronyms: MEW—methanol/ethanol/water; M—methanol; EM—ethanol/methanol; and E—ethanol, Table S1**.** Pearson correlation coefficient between the concentration determined by ^{1}H NMR and

the scavenging capacity of the DPPH radical, the ABTS radical cation and inhibition of AGE formation. **1**—gallic acid, **2**—epigallocatechin, **3**—catechin, **4**—quercetin and **5**—myricetin.

Author Contributions: Conceptualization: K.O.G.N., A.D.C.S., and M.B.M.; methodology, identification and collection of botanical material: F.C.M.C.; NMR analysis: K.O.G.N., S.O.S., and M.S.C.; antiglycation activity: L.D.R.A. and E.S.L.; antioxidant potential: J.M.M., J.A.B., and E.A.S.; cell viability assay and antiviral assay: N.M.C., G.A.A., and A.C.G.J.; statistical analysis: K.O.G.N.; writing—review and editing: K.O.G.N., A.D.C.S., and M.B.M. All authors have read and agreed to the published version of the manuscript.

Funding: This research has also provided by FAPEMIG (Fundação de Pesquisa do Estado de Minas Gerais, APQ-01487-22, APQ-04686-22), CAPES Prevention and Combat of Outbreaks, Endemics, Epidemics and Pandemics (88887.506792/2020-00) under Finance Code 001, CNPq (Conselho Nacional de Ciência e Tecnologia, 409187/2023-2 and 421935/2023-5), and Fundação de Amparo à Pesquisa do Estado do Amazonas—FAPEAM (Edital number 010/2021—CT&I Áreas Prioritárias).

Institutional Review Board Statement: Not applicable.

Informed Consent Statement: Not applicable.

Data Availability Statement: The primary data and contributions of this study are provided within the article and supplementary materials. For additional information, please contact the corresponding author(s).

Acknowledgments: The authors would like to thank CAPES, Financiadora de Estudos de Projetos e Programa—FINEP, FAPEMIG, and FAPEAM. A.C.G.J. received a CNPq productivity fellowship.

Conflicts of Interest: The authors declare that there are no conflicts of interest.

References

1. Jorge, U.; Aguiar, J.; Silva, M. Anatomia foliar de pedra-hume-caá (*Myrcia sphaerocarpa*, *Myrcia guianensis*, *Eugenia punicifolia*—Myrtaceae). *Acta Amaz.* **2000**, *30*, 49.
2. Oliveira, E.S.C.; Pontes, F.L.D.; Acho, L.D.R.; Silva, B.J.P.; Rosário, A.S.; Chaves, F.C.M.; Campos, F.R.; Bezerra, J.A.; Lima, E.S.; Machado, M.B. NMR and multivariate methods: Identification of chemical markers in extracts of pedra-ume-caá and their antiglycation, antioxidant, and enzymatic inhibition activities. *Phytochem. Anal.* **2024**, *35*, 552–566.
3. Amorim, M.; Verdan, M.; Oliveira, C.; Santos, A.D.C. Essential Oils of Neotropical Myrtaceae Species from 2011 until 2023: An Update. *Chem. Biodivers.* **2024**, 10.1002/cbdv.202401503.
4. Teixeira, R.G.S.; Pascual, R.; Araújo, K.G.L.; Brito, M.A.; Rios, C.L.; Carmo, A.F.; Gandía, L.; Silva, C.L.M.; Machado, T.B.; Santos, W.C. In vitro and in silico studies for barbinervic acid, a triterpene isolated from *Eugenia punicifolia* that inhibits vasopressor tone. *Nat. Prod. Res.* **2021**, *35*, 4870–4875.
5. Basting, R.T.; Nishijima, C.M.; Lopes, J.A.; Santos, R.C.; Lucena Périco, L.; Laufer, S.; Bauer, S.; Costa, M.F.; Santos, L.C.; Rocha, L.R.M.; et al. Antinociceptive, anti-inflammatory and gastroprotective effects of a hydroalcoholic extract from the leaves of *Eugenia punicifolia* (Kunth) DC. in rodents. *J. Ethnopharmacol.* **2014**, *157*, 257–267.
6. Sales, D.S.; Carmona, F.; Azevedo, B.C.; Taleb-Contini, S.H.; Bartolomeu, A.C.D.; Honorato, F.B.; Martinez, E.Z.; Pereira, A.M.S. *Eugenia punicifolia* (Kunth) DC. as an Adjuvant Treatment for Type-2 Diabetes Mellitus: A non-Controlled, Pilot Study. *Phytother. Res.* **2014**, *28*, 1816–1821.
7. Ramos, A.; Mar, J.; Silva, L.; Acho, L.D.; Silva, B.; Lima, E.; Campelo, P.; Sanches, E.; Bezerra, A.J.; Chaves, F.; et al. Pedra-ume caá fruit: An Amazon cherry rich in phenolic compounds with antiglycant and antioxidant properties. *Food Res. Int.* **2019**, *123*, 674–683.
8. Souza, A.; Oliveira, C.; Oliveira, V.; Betim, F.; Miguel, M. Traditional Uses, Phytochemistry, and Antimicrobial Activities of *Eugenia* Species—A Review. *Planta Med.* **2018**, *84*, 1232–1248.
9. Santos, C.; Mizobucchi, A.L.; Escaramboni, B.; Lopes, B.P.; Angolini, C.F.F.; Eberlin, M.N.; de Toledo, K.A.; Núñez, E.G.F. Optimization of *Eugenia punicifolia* (Kunth) DC. leaf extraction using a simplex centroid design focused on extracting phenolics with antioxidant and antiproliferative activities. *BMC Chem.* **2020**, *14*, 34.

10. Zhang, Q.W.; Lin, L.G.; Ye, W.C. Techniques for extraction and isolation of natural products: A comprehensive review. *Chin. Med.* **2018**, *13*, 20.
11. Neves, K.O.G.; Santos, M.F.C.; Mar, J.M.; Pontes, F.L.D.; Tormena, C.F.; Chaves, F.C.M.; Campos, F.R.; Sanches, E.A.; Bezerra, J.A.; Machado, M.B.; et al. ^{1}H NMR Chemical Profile and Antioxidant Activity of *Eugenia punicifolia* Extracts Over Seasons: A Metabolomic Pilot Study. *J. Braz. Chem. Soc.* **2024**, *35*, e20240010.
12. Brunetti, I.L.; Vendramini, R.C.; Januário, A.H.; França, S.C.; Pepato, M.T. Effects and Toxicity of *Eugenia punicifolia*. Extracts in Streptozotocin-Diabetic Rats. *Pharm. Biol.* **2006**, *44*, 35.
13. Dogara, A.M.; Ibrahim, M.T.; Mahmud, A.A.; Danladi, M.D.; Lema, A.A.; Usman, M.; Tahir, A.S.; Tabti, K. Biological activity, chemical composition, and molecular docking of *Eugenia punicifolia* (Kunth) DC. *J. Umm Al-Qura Univ. Appll. Sci.* **2024**. 10.1007/s43994-024-00160-y
14. Sehlakgwe, P.F.; Lall, N.; Prinsloo, G. ^{1}H-NMR Metabolomics and LC-MS Analysis to Determine Seasonal Variation in a Cosmeceutical Plant *Leucosidea sericea*. *Front. Pharmacol.* **2020**, *11*, 219.
15. Ravaglia, L.M.; Oliveira, P.D.; Holzgrabe, U.; Alcantara, G.B. qNMR in natural products: Practical approaches. What nobody tells you before starting your qNMR study! *Front. Nat. Prod.* **2024**, *3*, 1416195.
16. Fátima, C.S.M.; Rech, K.S.; Dutra, L.M.; Menezes, L.R.A.; Santos, A.D.C.; Nagata, N.; Stefanello, M.É.A.; Barison, A. ^{1}H HR-MAS NMR chemical profile and chemometric analysis as a tool for quality control of different cultivars of green tea (*Camellia sinensis*). *Food Chem.* **2023**, *408*, 135016.
17. Delgado-Altamirano, R.; García-Aguilera, M.E.; Delgado-Domínguez, J.; Becker, I.; Rodríguez de San Miguel, E.; Rojas-Molina, A.; Esturau-Escofet, N. ^{1}H NMR profiling and chemometric analysis as an approach to predict the leishmanicidal activity of dichloromethane extracts from *Lantana camara* (L.). *J. Pharm. Biomed. Anal.* **2021**, *199*, 114060.
18. Bailey, N.J.; Wang, Y.; Sampson, J.; Davis, W.; Whitcombe, I.; Hylands, P.J.; Croft, S.L.; Holmes, E. Prediction of anti-plasmodial activity of Artemisia annua extracts: Application of ^{1}H NMR spectroscopy and chemometrics. *J. Pharm. Biomed. Anal.* **2004**, *35*, 117–126.
19. Souza, C.A.; Oliveira, A.P.; Santos, A.D.C.; Guimarães, A.L.; Silva, N.D.S.; Queiroz, M.A.Á.; Araújo, E.C.C.; Almeida, J.R.G.S. Total content of kaurene diterpenes in Annona vepretorum stems via ^{1}H qNMR: A method for speeding the identification of bioactive extracts. *Phytochem. Anal.* **2019**, *30*, 83–88.
20. Khalef, L.; Lydia, R.; Filicia, K.; Moussa, B. Cell viability and cytotoxicity assays: Biochemical elements and cellular compartments. *Cell Biochem. Funct.* **2024**, *42*, e4007.
21. Huang, D.J.; Ou, B.X.; Prior, R.L. The chemistry behind antioxidant capacity assays. *J. Agric. Food Chem.* **2005**, *53*, 1841–1856.
22. Dudonne, S.; Vitrac, X.; Coutiere, P.; Woillez, M.; Merillon, J.M. Comparative Study of Antioxidant Properties and Total Phenolic Content of 30 Plant Extracts of Industrial Interest Using DPPH, ABTS, FRAP, SOD, and ORAC Assays. *J. Agric. Food Chem.* **2009**, *57*, 1768–1774.
23. Zargoosh, Z.; Ghavam, M.; Bacchetta, G.; Tavili, A. Effects of ecological factors on the antioxidant potential and total phenol content of Scrophularia striata Boiss. *Sci. Rep.* **2019**, *9*, 16021.
24. Li, H.; Tsao, R.; Deng, Z. Factors affecting the antioxidant potential and health benefits of plant foods. *Can. J. Plant. Sci.* **2012**, *92*, 1101–1111.
25. Khalid, M.; Petroianu, G.; Adem, A. Advanced Glycation End Products and Diabetes Mellitus: Mechanisms and Perspectives. *Biomolecules* **2022**, *12*, 542.
26. López-Martínez, L.M.; Santacruz-Ortega, H.; Navarro, R.E.; Sotelo-Mundo, R.R.; González-Aguilar, G.A. A ^{1}H NMR Investigation of the Interaction between Phenolic Acids Found in Mango (*Manguifera indica* cv *Ataulfo*) and Papaya (*Carica papaya* cv *Maradol*) and 1,1-diphenyl-2-picrylhydrazyl (DPPH) Free Radicals. *PLoS ONE* **2015**, *10*, e0140242.
27. Napolitano, J.; Gödecke, T.; Lankin, D.; Jaki, B.; McAlpine, J.; Chen, S.N.; Pauli, G. Orthogonal analytical methods for botanical standardization: Determination of green tea catechins by qNMR and LC–MS/MS. *J. Pharm. Biomed. Anal.* **2013**, *93*, 59–67.
28. Oliveira, E.S.C.; Acho, L.D.R.; Silva, B.J.P.; Morales-Gamba, R.D.; Pontes, F.L.D.; Rosário, A.S.; Bezerra, J.A.; Campos, F.R.; Barcellos, J.F.M.; et al. Hypoglycemic effect and toxicity of the dry extract of *Eugenia biflora* (L.) DC. leaves. *J. Ethnopharmacol.* **2022**, *293*, 115276.
29. Oliveira, E.S.C.; Pontes, F.L.D.; Acho, L.D.R.; Rosário, A.S.; Silva, B.J.P.; Araújo, B.J.; Campos, F.R.; Lima, E.S.; Machado, M.B. qNMR quantification of phenolic compounds in dry extract of *Myrcia multiflora* leaves and its antioxidant, anti-AGE, and enzymatic inhibition activities. *J. Pharm. Biomed. Anal.* **2021**, *201*, 114109.
30. Truzzi, E.; Marchetti, L.; Benvenuti, S.; Righi, V.; Rossi, M.C.; Gallo, V.; Bertelli, D. A Novel qNMR Application for the Quantification of Vegetable Oils Used as Adulterants in Essential Oils. *Molecules* **2021**, *26*, 5439.

31. Mak, J.Y.W. Determination of Sample Concentrations by PULCON NMR Spectroscopy. *Aust. J. Chem.* **2022**, *75*, 160–164.
32. Watanabe, R.; Sugai, C.; Yamazaki, T.; Matsushima, R.; Uchida, H.; Matsumiya, M.; Takatsu, A.; Suzuki, T. Quantitative Nuclear Magnetic Resonance Spectroscopy Based on PULCON Methodology: Application to Quantification of Invaluable Marine Toxin, Okadaic Acid. *Toxins* **2016**, *8*, 294.
33. Yang, X.; Liu, W.; Tao, D. A Survey on Canonical Correlation Analysis. *IEEE Trans. Knowl. Data Eng.* **2021**, *33*, 2349–2368.
34. Zhou, X.; Liu, H.; Zhang, M.; Li, C.; Li, G. Spectrum-effect relationship between UPLC fingerprints and anti-lung cancer effect of Panax ginseng. *Phytochem. Anal.* **2021**, *32*, 339–346.
35. Chen, Y.; Pan, G.; Xu, W.; Sun, Q.; Wang, B.; Zhang, Y.; Yang, T. Spectrum-effect relationship study between HPLC fingerprints and antioxidant activity of *Sabia parviflora*. *J. Chromatogr. B* **2020**, *1140*, 121970.
36. Ugur, S.; Kılınc, O.; Selamoglu, Z. Antioxidant Activity of Quercetin: A Mechanistic Review. *Turk. J. Agric. For.* **2016**, *4*, 1134–1138.
37. Hassanpour, S.H.; Doroudi, A. Review of the antioxidant potential of flavonoids as a subgroup of polyphenols and partial substitute for synthetic antioxidants. *Avicenna J. Phytomed.* **2023**, *13*, 354–376.
38. Figueiroa, E.O.; Silva, L.C.N.; Melo, C.M.L.; Neves, J.K.A.L.; Silva, N.H.; Pereira, V.R.A.; Correia, M.T.S. Evaluation of Antioxidant, Immunomodulatory, and Cytotoxic Action of Fractions from *Eugenia uniflora* L. and *Eugenia malaccensis* L.: Correlation with Polyphenol and Flavanoid Content. *Sci. World J.* **2013**, *2013*, 1-7.
39. Yeh, W.J.; Hsia, S.M.; Lee, W.H.; Wu, C.H. Polyphenols with antiglycation activity and mechanisms of action: A review of recent findings. *J. Food Drug Anal.* **2017**, *25*, 84–92.
40. Wang, Y.; Li, S.; Zhang, T.; Wang, J.; Zhang, X.; Li, M.; Gao, Y.; Zhang, M.; Chen, H. Effects of myricetin and its derivatives on nonenzymatic glycation: A mechanism study based on proteomic modification and fluorescence spectroscopy analysis. *Food Chem.* **2024**, *455*, 139880.
41. Cataneo, A.H.D.; Ávila, E.P.; Mendes, L.A. d. O.; de Oliveira, V.G.; Ferraz, C.R.; Almeida, M.V.; Frabasile, S.; Santos, C.N.D.; Verri, W.A.; Bordignon, J.; et al. Flavonoids as Molecules With Anti-Zika virus Activity. *Front. Microbiol.* **2021**, *12*, 710359.
42. Pereira, R.S.; Santos, F.C.; Campana, P.R.; Costa, V.V.; de Pádua, R.M.; Souza, D.G.; Teixeira, M.M.; Braga, F.C. Natural Products and Derivatives as Potential Zika virus Inhibitors: A Comprehensive Review. *Viruses* **2023**, *15*, 1211.
43. Liga, S.; Paul, C.; Péter, F. Flavonoids: Overview of Biosynthesis, Biological Activity, and Current Extraction Techniques. *Plants* **2023**, *12*, 2732.
44. Rahmani, A.H.; Almatroudi, A.; Allemailem, K.S.; Alwanian, W.M.; Alharbi, B.F.; Alrumaihi, F.; Khan, A.A.; Almatroodi, S.A. Myricetin: A Significant Emphasis on Its Anticancer Potential via the Modulation of Inflammation and Signal Transduction Pathways. *Int. J. Mol. Sci.* **2023**, *24*, 9665.
45. Oliveira, M.R.; Nabavi, S.M.; Braidy, N.; Setzer, W.N.; Ahmed, T.; Nabavi, S.F. Quercetin and the mitochondria: A mechanistic view. *Biotechnol. Adv.* **2016**, *34*, 532–549.
46. Lim, H.J.; Nguyen, T.T.H.; Kim, N.M.; Park, J.S.; Jang, T.S.; Kim, D. Inhibitory effect of flavonoids against NS2B-NS3 protease of ZIKA virus and their structure activity relationship. *Biotechnol. Lett.* **2017**, *39*, 415–421.
47. Ramos, P.R.; Mottin, M.; Lima, C.S.; Assis, L.R.; de Oliveira, K.Z.; Mesquita, N.C.; Cassani, N.M.; Santos, I.A.; Borba, J.V.; Fiaia Costa, V.A.; et al. Natural Compounds as Non-Nucleoside Inhibitors of Zika Virus Polymerase through Integration of In Silico and In Vitro Approaches. *Pharmaceuticals* **2022**, *15*, 1493.
48. Zou, M.; Liu, H.; Li, J.; Yao, X.; Chen, Y.; Ke, C.; Liu, S. Structure-activity relationship of flavonoid bifunctional inhibitors against Zika virus infection. *Biochem. Pharmacol.* **2020**, *177*, 113962.
49. Lum, F.M.; Lin, C.; Susova, O.Y.; Teo, T.H.; Fong, S.W.; Mak, T.M.; Lee, L.K.; Chong, C.Y.; Lye, D.C.B.; Lin, R.T.P.; et al. A Sensitive Method for Detecting Zika Virus Antigen in Patients' Whole-Blood Specimens as an Alternative Diagnostic Approach. *J. Infect. Dis.* **2017**, *216*, 182–190.
50. Minitab Inc. *Minitab® 18.1*; Minitab Inc.: State College, PA, USA, 2017.
51. Bruker BioSpin LGmbH & Co. KG *TopSpin 3.6.3*; Academia License,: Ettlingen, Germany, 2021.
52. Hong, R.; Hwang, K.; Kim, S.; Cho, H.; Lee, H.; Hong, J.; Moon, D.C. Survey of ERETIC2 NMR for quantification. *J. Korean Soc. Magn. Reson. Med.* **2013**, *17*, 98–104.
53. Donald, C.L.; Brennan, B.; Cumberworth, S.L.; Rezelj, V.V.; Clark, J.J.; Cordeiro, M.T.; França, R.F.O.; Pena, L.J.; Wilkie, G.S.; Silva, F.A.; et al. Full Genome Sequence and sfRNA Interferon Antagonist Activity of Zika Virus from Recife, Brazil. *PLoS Negl. Trop. Dis.* **2016**, *10*, e0005048.

54. Cassani, N.M.; Santos, I.A.; Grosche, V.R.; Ferreira, G.M.; Guevara-Vega, M.; Rosa, R.B.; Pena, L.J.; Nicolau-Junior, N.; Cintra, A.C.O.; Mineo, T.P. Roles of Bothrops jararacussu toxins I and II: Antiviral findings against Zika virus. *Int. J. Biol. Macromol.* **2023**, *227*, 630–640.
55. GraphPad Software, LLC. *One-Way ANOVA Followed by Dunnett's Multiple Comparisons Test Was Performed Using GraphPad Prism Version 10.3.0 for Windows*; GraphPad Software: Boston, MA, USA, 2024.
56. Samaniego-Sanchez, C.; Inurreta-Salinas, Y.; Quesada-Granados, J.J.; Blanca-Herrera, R.; Villalon-Mir, M.; Lopez-Garcia de la Serrana, H.; Lopez Martınez, M.C. The influence of domestic culinary processes on the Trolox Equivalent Antioxidant Capacity of green tea infusions. *J. Food Compos. Anal.* **2011**, *24*, 79–86.
57. Mar, J.M.; Silva, L.S.; Moreira, W.P.; Biondo, M.M.; Pontes, F.L.D.; Campos, F.R.; Kinupp, V.F.; Campelo, P.H.; Sanches, E.A.; Bezerra, J.A. Edible flowers from Theobroma speciosum: Aqueous extract rich in antioxidant compounds. *Food Chem.* **2021**, *356*, 129723.
58. Kiho, T.; Usui, S.; Hirano, K.; Aizawa, K.; Inakuma, T. Tomato paste fraction inhibiting the formation of advanced glycation end-products. *Biosci. Biotechnol. Biochem.* **2004**, *68*, 200–205.

4.3. Como a sazonalidade molda os principais compostos fenólicos de *Eugenia punicifolia*: uma abordagem metabolômica para o estresse abiótico

A metodologia deste estudo investigou a influência da sazonalidade no perfil metabolômico das folhas de *Eugenia punicifolia* por meio da combinação da espectroscopia de ressonância magnética nuclear de hidrogênio (RMN de ^{1}H) com análises multivariadas. As folhas foram coletadas mensalmente ao longo de um ano e submetidas a um protocolo de extração utilizando um sistema solvente composto por metanol, etanol e água, em proporções otimizadas (3:1:1, MEW). Os dados espectroscópicos obtidos por RMN de ^{1}H foram submetidos a pré-processamento e utilizados para análises exploratórias, por meio da análise de componentes principais (PCA), a qual identificou padrões de agrupamento relacionados aos períodos chuvoso, seco e de transição. Para validar essas diferenças e identificar os compostos químicos responsáveis pelas variações sazonais, foi realizada a análise discriminante de mínimos quadrados parciais (PLS-DA), seguido da validação do modelo. Os compostos quercetina, miricetina, ácido gálico, catequina e epigalocatequina foram identificados como marcadores químicos associados às respostas metabólicas da planta ao estresse abiótico. Adicionalmente, foram calculados coeficientes de correlação de Pearson entre os metabólitos identificados e parâmetros climáticos, como temperatura média, umidade relativa, precipitação e exposição solar. Essas análises revelaram relações significativas entre as condições ambientais e a biossíntese de compostos fenólicos, evidenciando mecanismos adaptativos da planta. A combinação dessas abordagens proporcionou um modelo robusto para compreender o impacto da sazonalidade no metabolismo secundário de *E. punicifolia*, oferecendo base científica para a otimização de sua exploração em aplicações farmacológicas e fitoterápicas.

Situação: Artigo em processo de submissão para o *Journal of Agricultural and Food Chemistry*.

How seasonality shapes key phenolic compounds of *Eugenia punicifolia*: a metabolomic approach to abiotic stress

Kidney O. G. Neves [1], Samuel O. Silva [1], Marinildo S. Cruz [1], Francisco C. M. Chaves[2], Marcos B. Machado [1,*] and Alan D. C. Santos [1,3,#]

[1]Núcleo de Estudos Químicos de Micromoléculas da Amazônia - NEQUIMA, Universidade Federal do Amazonas, 69067-005, Manaus, AM, Brazil

[2]Empresa Brasileira de Pesquisa Agropecuária - Embrapa Amazônia Ocidental, 69010-970, Manaus, AM, Brazil

[3]Núcleo de Pesquisa de Produtos Naturais, Universidade Federal de Santa Maria, Santa Maria, RS, 97105-900, Brazil

Correspondence: #alandiegormn@gmail.com.br, marcosmachado@ufam.edu.br,

Alan D. C. Santos: https://orcid.org/0000-0002-3877-0313

Marcos B. Machado: https://orcid.org/0000-0002-8791-4803

ABSTRACT

Eugenia punicifolia DC. is a medicinal plant with a chemical profile rich in bioactive phenolic compounds, widely recognized for its association with the prevention of type 2 diabetes mellitus. This study aimed to investigate the seasonal influence on the chemical profiles of methanol:ethanol:water extracts (3:1:1, MEW) from *E. punicifolia* leaves using ^{1}H NMR spectroscopy combined with multivariate statistical analyses. Principal Component Analysis (PCA) and Partial Least Squares Discriminant Analysis (PLS-DA) revealed distinct sample groupings corresponding to rainy, dry, and transitional periods. The PLS-DA model demonstrated high predictive accuracy ($R^2 > 0.85$, $Q^2 > 0.85$), validating the influence of climatic conditions on predefined classes and identifying quercetin, myricetin, gallic acid, catechin, and epigallocatechin as chemical markers of abiotic stress responses. Pearson correlation coefficients highlighted significant relationships, such as increased catechin production at higher temperatures ($r = 0.60$) and quercetin production under greater sunlight exposure ($r = 0.60$), as well as the increase in gallic acid production in response to rainfall ($r = 0.62$) and the number of rainy days ($r = 0.74$). Therefore, this study demonstrates that environmental factors play a crucial role in regulating the biosynthesis of phenolic compounds, reflecting the plant's adaptive response to abiotic stress. These findings provide insights into the ecological and pharmacological potential of *E. punicifolia*, while offering a framework to optimize harvesting periods for higher yields of bioactive compounds.

Keywords: *Eugenia punicifolia* DC., medicinal plant, seasonality, NMR, Principal Component Analysis, Partial Least Squares Discriminant Analysis, chemical markers.

1. Introduction

Eugenia punicifolia DC., a species belonging to the Myrtaceae family, is widely used in traditional medicine in the form of tea made from its leaves. Its consumption is mainly due to its antiglycant properties, which are associated with the prevention of damage caused by oxidative stress and the accumulation of advanced glycation end products (AGEs).[1, 2] In addition to this action, several studies have highlighted the therapeutic potential of this species, attributed to its phytochemical composition rich in phenolic compounds, such as flavonoids and organic acids.[2-4] These secondary metabolites not only play essential roles in the plant's ecological interactions but are also responsible for its pharmacological activities of medicinal interest.

The chemical composition of *E. punicifolia*, however, can be significantly influenced by seasonality. Environmental factors such as temperature, humidity, precipitation, and solar incidence modulate the production and concentration of these bioactive compounds.[5, 6] This seasonal variation can directly impact both the species' pharmacological potential and its adaptability to the environment, making *E. punicifolia* a promising plant matrix for investigating how climate changes affect the biosynthesis of secondary metabolites throughout the year.

To understand these chemical variations, spectroscopic techniques are frequently employed, with Nuclear Magnetic Resonance (NMR) being one of the most effective.[7, 8] NMR enables the identification and quantification of organic compounds in a fast and non-destructive manner, providing a comprehensive view of the sample's chemical composition.[9] However, for the generated data to be interpreted more robustly, it is essential to associate them with multivariate methods. This integration allows the construction of predictive models that help classify samples according to seasonality and identify the chemical compounds most influenced by climatic factors.[7, 10, 11]

In this context, multivariate analyses, such as Principal Component Analysis (PCA) and Partial Least Squares Discriminant Analysis (PLS-DA), play a fundamental role. PCA is widely used to explore data patterns, reducing complexity and facilitating the interpretation of variations in the chemical profile of samples.[12] On the other hand, PLS-DA enables the discrimination of different seasonal groups and the identification of metabolites that most contribute to these differences.[13] To ensure the robustness of the generated models, metrics such as Root Mean Square Error of Calibration (RMSEC), Root Mean Square Error

of Cross-Validation (RMSECV), Coefficient of Determination (R^2), and Cross-Validated Coefficient of Determination (Q^2) are evaluated, ensuring the reliability of the results.[13-15]

Recent studies by Neves et al. (2024 and 2025) have demonstrated, through NMR combined with multivariate analyses, that seasonality directly influences the production of primary and secondary metabolites in *E. punicifolia*, with variations depending on the extraction system used.[2, 16] However, there is still a gap in the literature regarding the specific impact of climatic parameters such as average temperature, precipitation, and relative humidity on the composition of phenolic compounds in the leaves of this species.

Thus, this study aims to develop a model based on ^{1}H NMR data combined with multivariate methods to evaluate how variations in climatic parameters affect the metabolomic profile of the Methanol:Water:Ethanol (3:1:1, MEW) extract from *E. punicifolia* leaves collected at different times of the year. Through these results, we hope not only to better understand the factors regulating the production of bioactive metabolites but also to identify potential chemical markers that play an essential role in the plant's defense mechanisms against environmental variations.

2. Experimental

2.1.Chemicals

Methanol (HPLC) and absolute ethanol (99.5 % PA) used for plant material extraction were purchased from Sigma-Aldrich (St. Louis, MO, USA). Deuterated dimethyl sulfoxide (DMSO-*d*6, 99.9 %) with tetramethylsilane (TMS, 0.05 % V/V) for NMR analyses, was obtained from Cambridge Isotope Laboratories Inc. (Andover, Massachusetts, USA).

2.2.Plant Material

Leaves of *E. punicifolia* were collected monthly throughout the year 2023 at the Brazilian Agricultural Research Corporation (Embrapa Amazônia Ocidental), located along Rodovia AM-010, Km 29 (2° 53' 23" S 59° 58' 26" W). Access to genetic heritage was registered (A82BD35) in the National System of Management of Genetic Heritage and Associated Traditional Knowledge (SisGen). From a plantation of 150 individuals, three trees were randomly selected each month, and leaves were gathered from various heights to

ensure a representative sampling (15 leaves each from the lower, middle and upper parts of the trees). The collected plant material was dried at room temperature for 24 h. After drying, each sample was subjected to cold maceration with liquid nitrogen, weighed, and then stored in a freezer at – 80 °C until the extraction procedure.

2.3.Environmental data

The climate data for the 12 months of the study were obtained from the Agroclimatology Laboratory of Embrapa Amazônia Ocidental and are detailed in the Supplementary Information (**Table S1**).

2.4.Extraction procedure

The extraction system was selected based on the methodology described by Neves et al. (2025).[2] For the extractions, 1.0 g of each sample was subjected, in triplicate, to extraction with the solvent system consisting of methanol (60%) - ethanol (20%) - water (20%), called MEW system. Each extraction was performed four times and sonicated in an ultrasonic bath for 15 min, followed by centrifugation at 4,000 rpm for 10 min (4226 *g*). The supernatant was then separated and dried using nitrogen gas.

2.5.Acquisition NMR spectroscopy data

Twenty milligrams of *E. punicifolia* leaf extracts were solubilized in 520 μL of deuterated dimethyl sulfoxide (DMSO-d_6) and transferred to a 5 mm NMR tube. The NMR analyses were performed using a Bruker Avance III HD NMR spectrometer (Bruker, Billerica, Massachusetts, USA), operating at 11.7 T (500 MHz for ^{1}H) and equipped with a 5 mm BBFO Plus SmartProbe™ with a Z-axis gradient. ^{1}H NMR spectra were obtained at 25 °C using the *zgpr* pulse sequence. The 90º pulse duration was calculated individually for sample each. A total of 2 dummy scans and 32 scans were acquired with 32k data points using a spectral width of 10 kHz, a relaxation time of 15.0 s, and an acquisition time of 1.64 s. The residual water signal of DMSO-d_6 (δ_H 3.36, s) was suppressed using a power of 8.13 e^{-5} W, and the receiver gain was set to 64. Phase and baseline corrections of the spectra were

performed manually using TopSpin 3.6.3 software.[17] The chemical shift (in ppm) of ^{1}H NMR spectra was referenced to the methyl signal of tetramethylsilane at δ_H 0.0. ^{1}H–^{13}C correlations from HSQC and HMBC NMR experiments were acquired using the coupling constants *J* (H,C - one-bond) and *J* (H,C - long-range) of 145 and 8 Hz, respectively.

2.6.Multivariate Analysis

2.6.1. PCA

^{1}H NMR spectra of the 36 samples were acquired in triplicate, exported from TopSpin 3.6.3 software in .csv format, and transferred to OriginPro 2018 software to build the data matrix.[17, 18] Chemometric analysis was carried out using the ^{1}H NMR spectral region between 5.60 to 8.10 ppm, resulting in a matrix of 108 samples x 2048 variables. Principal Component Analysis (PCA) was performed using the PLS-Toolbox Solo 9.0 software.[19] Spectra preprocessing involved baseline correction using Automatic Whittaker Filter (asymmetry = 0.001, lambda = 100) and variable alignment with Correlation Optimized Warping (Slack 2, Segment Length 87). The data were normalized to the area and mean-centered. Scores and loadings graphs were plotted using the Singular Value Decomposition (SVD) algorithm.

2.6.2. Construction of the PLS-DA calibration model

To perform the Partial Least Squares-Discriminant Analysis (PLS-DA), the same data matrix used for PCA analysis was employed. The samples were classified into three groups: Group 1 (Rainy period) included February, March, April, and May; Group 2 (Dry period) included August, September, October, and November; and Group 3 (Transition period) included January, June, July, and December . In the PLS-Toolbox Solo 9.0 software, the spectra were processed using baseline correction (Automatic Whittaker Filter with asymmetry = 0.001 and lambda = 100), variable alignment (Correlation Optimized Warping: Slack = 2, Segment Length = 87), and normalization to the area and mean-centering.[19] The processed data were then used to construct the PLS-DA calibration model. The cross-validation was performed using the Venetian Blinds method, with 10 splits and a blind thickness of 1. Statistical parameters, including the root mean square error of calibration

(RMSEC), root mean square error of cross-validation (RMSECV), Q^2, and R^2, was analyzed using OriginPro 2018.[18] A validação cruzada foi realizada utilizando o modelo venetian blinds w/ 10 splits and blind thickness = 1.

2.7.Pearson correlation coefficient analysis

For this analysis, the ^{1}H NMR spectra of the 108 *E. punicifolia* samples were initially exported to R-Studio software (version 2022.07.2).[20] Subsequently, the spectral region from 5.60 to 8.10 ppm was aligned and divided into 0.03 ppm buckets with a 50% degree of freedom, resulting in a table containing 108 samples and 101 variables. The areas of the buckets corresponding to the compounds quercetin (δ_H 7.30, d), myricetin (δ_H 7.01, s), gallic acid (δ_H 6.96, s), catechin (δ_H 5.93, d), and epigallocatechin (δ_H 5.89, d) were then normalized relative to the total area. Pearson's correlation coefficients were calculated using Minitab™ 18.1 software by correlating the normalized bucket areas with the climatic parameter values [mean temperature (ºC), relative humidity (%), precipitation (mm), evaporation (mm), number of rainy days, and sunshine duration (hours)].[21] Statistical significance was set at p-values < 0.05. Furthermore, the Pearson correlation coefficients were exported to OriginPro 2018 software and used to construct the heatmap.[18]

3. Results

3.1.Chemical profile of *E. punicifolia* leaves extract via NMR spectroscopy

Aromatic compounds in *Eugenia punicifolia* leaf extracts were identified through the analysis of ^{1}H NMR, ^{1}H-^{13}C HSQC, and ^{1}H-^{13}C HMBC data. The ^{1}H NMR spectra revealed two singlets at δ_H 6.96 and δ_H 7.42, corresponding to the structures of gallic acid (**1**) and ellagic acid (**2**), respectively (**Figure S1**).[22] Additionally, characteristic signals of flavonoids from the flavanols (catechin and epigallocatechin) and flavonols (kaempferol, quercetin and myricetin) classes were observed.[23] Within the flavanols class, two distinct sets of signals were identified. The first set included δ_H 5.83 (d, 2.3 Hz), δ_H 5.93 (d, 2.3 Hz), δ_H 6.86 (d, 1.9 Hz), δ_H 6.66 (d, 8.1 Hz), and δ_H 6.74 (dd, 1.9 Hz, 8.1 Hz), corresponding to positions 6, 8, 2', 5', and 6' of rings A and B in catechin (**3**).[24] The second set included signals at δ_H 5.89 (d, 2.1 Hz), δ_H 5.74 (d, 2.1 Hz), and δ_H 6.40 (s), attributed to positions 6, 8, 2', and 5' of rings A

and B in epigallocatechin (**4**).[25] For the flavonols class, characteristic signals from ring B were observed for kaempferol (**5**; H2', H5' - δ_H 7.75, d, 8.7 Hz; H3', H4' - δ_H 6.91, d, 8.7 Hz), quercetin (**6**; H1' - δ_H 7.30, d, 2.1 Hz; H4' - δ_H 6.87, d, 8.3 Hz; H5' - δ_H 7.25, dd, 8.3 Hz, 2.1 Hz), and myricetin (**7**, H2', H5' - δ_H 7.01, s) were identified.[24, 26] In addition, signals at δ_H 6.40 and δ_H 6.21, corresponding to ring A of flavonols identified. The ^{1}H-^{13}C HMBC spectrum revealed correlations between rings B and C, confirming the structures of the flavonoids identified by ^{1}H NMR (**Figures S1**-**S8**).

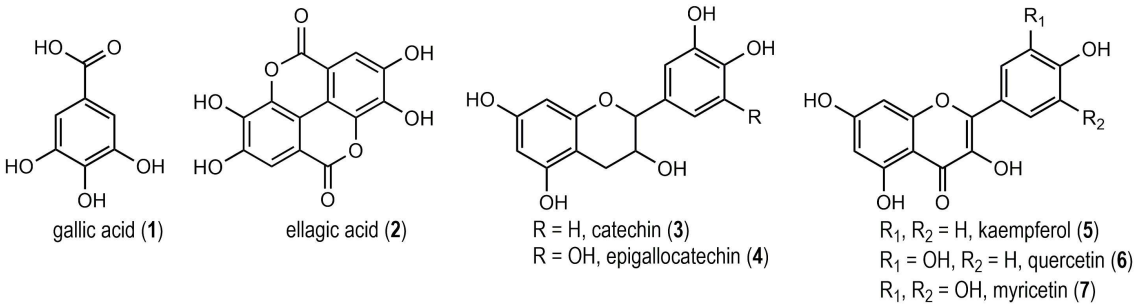

Figure 1. Compounds identified by 1D and 2D NMR analysis of MEW extracts from *E. punicifolia* leaves.

3.2. Principal Component Analysis

^{1}H NMR spectra of extracts from *E. punicifolia* leaves collected over 12 months were analyzed using PCA to identify clustering patterns and key compounds. The score plot in **Figure 2** indicates that PC1 and PC2 account for 38.21% of the explained variance. The analysis suggests the presence of three groups: **Group 1**, consists primarily of samples collected in February, March, April, May, and August; **Group 2,** includes samples collected in September, October, and November; and **Group 3,** comprises samples collected in January, June, July, and December.

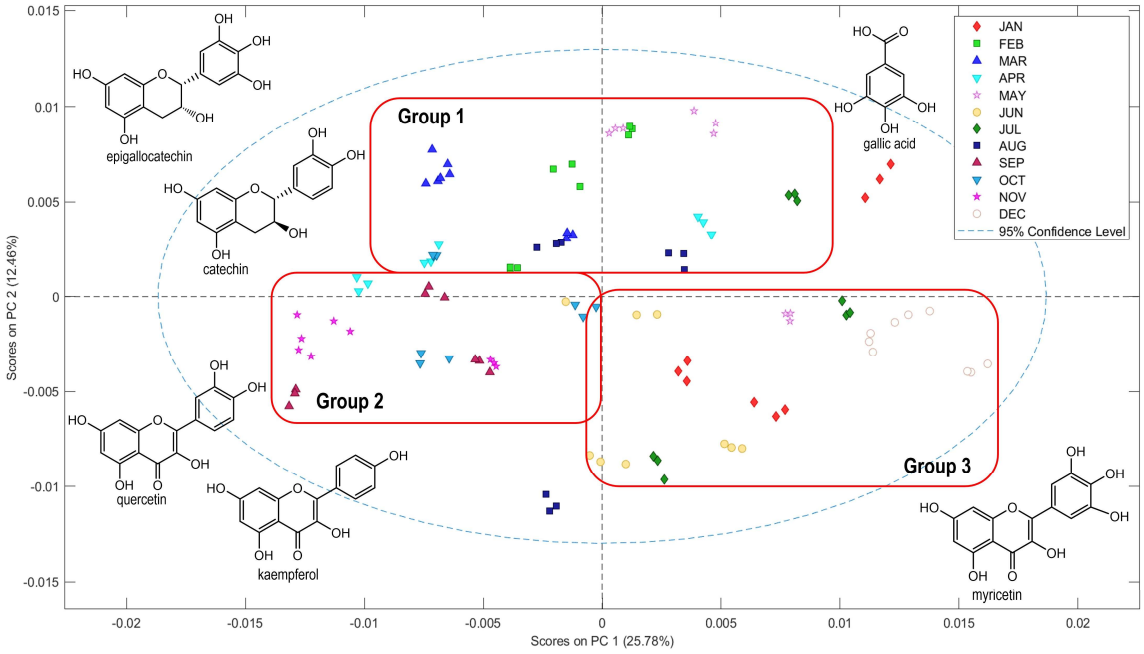

Figure 2. Principal components analysis (PCA) of extracts of *E. punicifolia* leaves. Scores plot of PC1 (25.78 %) versus PC2 (12.46 %). The structures of gallic acid, catechin, epigallocatechin, kaempferol, quercetin, and myricetin were identified from the loading plots of PC1 and PC2.

The analysis of PCA data together with meteorological data indicates that, except for August, the samples corresponding to the months that make up Groups 1 and 2 were directly influenced by similar climatic factors, such as the number of rainy days, precipitation, relative humidity, temperature, and solar radiation. (**Table S1**). Studies suggest that these parameters can be used to define dry and rainy periods.[27-29] However, unlike the other groups, **Group 3** showed no well-defined climatic patterns, as an analysis of the solar radiation parameter indicates that this group includes months (June and July) that are more similar to **Group 2** (rainy), while January and December resemble the months that make up **Group 1** (dry). This variability makes it impossible to classify its samples strictly into dry or rainy periods.

Regarding the chemical profile, the analysis of the loading plot allowed us to establish associations between specific compounds and the observed clustering patterns (**Figure S9**). Gallic acid (δ_H 6.96, s), catechin (δ_H 5.93, d), and epigallocatechin (δ_H 5.89, d) were linked to samples in **Group 1**, while quercetin (δ_H 7.30, d) and kaempferol (δ_H 7.75, d) were associated with **Group 2**, and myricetin (δ_H 7.01, s) was linked to **Group 3** (**Figure**

2). When comparing samples from the rainy (**Group 1**) and dry (**Group 2**) periods, the analysis suggests that climatic parameters play a significant role in shaping the biosynthesis of flavonoids, particularly flavanols and flavonols - two distinct classes known for their strong association with the bioactivity of *E. punicifolia* leaves.

These findings align with a growing body of research demonstrating that flavonoid production in plants is directly influenced by climatic conditions. For instance, Lu et al. (2021) reported that seasonal climatic variations significantly impact flavonoid concentrations in *Vitis vinifera* cultivars. Their study found that, in 2015, anthocyanin levels in winter samples were approximately 10 times higher than those in summer, while in 2014, the variation was about sevenfold.[30] Similarly, Zheng et al. (2022) applied Pearson's correlation coefficient to investigate the relationship between flavonoid concentrations and climatic factors in Chinese prickly ash bark. Their results indicated a moderate correlation between the flavonoid content (mg g^{-1}), measured by HPLC-MS, and environmental variables such as average temperature (°C) and annual precipitation (mm).[31] Further supporting this trend, Shi et al. (2022) examined the seasonal influence on flavonoid biosynthesis in *Tetrastigma hemsleyanum* using UPLC to track fluctuations in the concentrations of nine distinct flavonoids over a one-year period. Their study revealed that the selectivity of flavonoid biosynthesis is influenced by its synthetic pathway, enzymatic activity, and environmental factors, highlighting the complex interplay between seasonal changes and metabolite production.[32]

3.3. Classification by PLS-DA

To conduct a more detailed assessment of the effects of different climatic parameters on the clustering trends observed in the PCA analysis, the ^{1}H NMR spectra of the samples corresponding to **Groups 1**, **2**, and **3** were subjected to PLS-DA analysis. In addition to validating the results observed in the PCA, the PLS-DA analysis provides loading plots and VIP scores that, when analyzed together, aid in identifying the chemical markers responsible for the observed groupings.

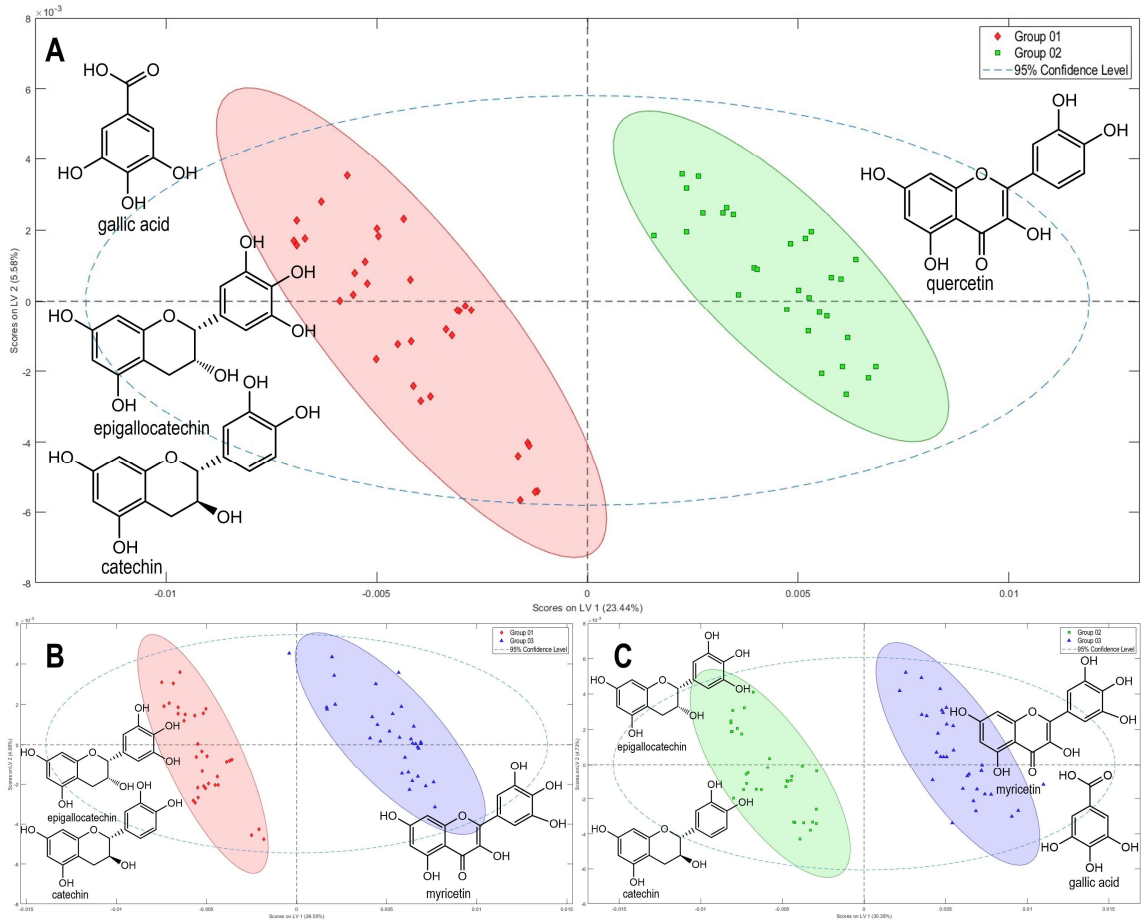

Figure 3. PLS-DA score plot illustrating the separation of samples based on the following models: **A** - **Group 1** vs. **Group 2**, **B** - **Group 1** vs. **Group 3**, and **C** - **Group 2** vs. **Group 3**. The structures of gallic acid, catechin, epigallocatechin, kaempferol, quercetin, and myricetin were identified from the loading plots of LV1 and LV2.

The analysis of the PLS-DA score plot reveals that first latent variable is responsible for classifying the samples according to the clusters observed in the PCA. Additionally, the clustering of the samples is indeed associated with the period in which the collections were performed. Samples from **Group 1** were collected during the months characteristic of the Amazonian winter, defined by average temperature below 28°C, relative humidity above 85%, total precipitation exceeding 180 mm, more than 18 rainy days, and sunshine duration below 123 hours (**Table S1**). In contrast, samples from **Group 2** correspond to months of the Amazonian summer, characterized by average temperature above 28°C, relative humidity below 80%, total precipitation under 115 mm, fewer than 10 rainy days, and sunshine duration above 134 hours (**Table S1**). Samples from **Group 3**, on the other hand,

were collected during a transitional period between summer and winter. This period is marked by significant variations in climatic parameters, with some months exhibiting characteristics of the rainy season and others resembling the dry season.

The quality of the PLS-DA model was assessed through the root mean square error of calibration (RMSEC), root mean square error of cross-validation (RMSECV), Q^2, and R^2. These diagnostics provide a statistically significant measures of the model's ability to discriminate between two classes of subjects.[13, 14] Among the analyzed parameters, RMSEC indicates how well the model fits the calibration data, while RMSECV evaluates the model's performance on new data, thereby verifying its robustness.[33] R^2 and Q^2 represent the explanatory and predictive capabilities in the model, respectively.[14, 34, 35]

Table 1. RMSECV, RMSEC, R^2, and Q^2 values obtained in the cross-validation of the PLS-DA model to latent variable.

Model	LV	X VC (%)	Y VC (%)	RMSECV	RMSEC	Q^2	R^2
A	1	23.43	87.86	0.20	0.17	0.84	0.88
B	1	26.55	90.30	0.18	0.15	0.88	0.90
C	1	30.38	90.41	0.18	0.15	0.87	0.90

Models **A**, **B**, and **C** in the first latent variable showed low RMSEC and RMSECV values (≤ 0.20) with minimal differences between calibration and cross-validation errors. The results indicate that the models fit the calibration data well and possess satisfactory generalization capability for new data. An R^2 value greater than 0.85 indicates that the models effectively explain the total variance of the calibration data, demonstrating its robustness in describing the intrinsic variability of the analyzed variables. Similarly, the high Q^2 value (> 0.85) reflect strong predictive capacity, consistent with the R^2.[34, 36, 37] The small difference between R^2 and Q^2 further reinforces the absence of overfitting, indicating that the models possess reliable discriminatory and predictive capabilities for the studied classes. To confirm these findings, RMSEC, RMSECV, R^2, and Q^2 values were analyzed for additional latent variables, showing that the models do not exhibit overfitting, as illustrated in **Figure 4**.[15, 37]

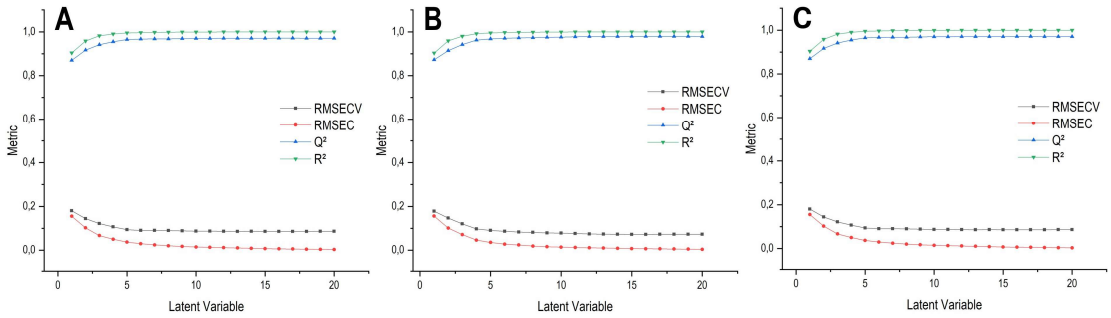

Figure 4. Evolution of RMSECV (black squares), RMSEC (red circles), Q^2 (blue triangles), and R^2 (green triangles) is presented as a function of the number of latent variables used in constructing the prediction model. The graphs were generated in OriginPro 2018 using data extracted from the PLSToolbox Solo 9.2 software. Metric values were derived from PLS-DA models constructed for comparisons between **Groups 1** vs **2** (**A**), **Groups 1** vs **3** (**B**), and **Groups 2** vs **3** (**C**).

After model validation, the variable importance projection (VIP) scores was used to evaluate the contribution of each compound to explaining chemical variation across seasons (**Figures S10-S15**). For the analysis of the VIP scores graph, only signals (δH) with a value greater than 1 were considered statistically significant for the model. Based on the combined analysis of the loadings graph and VIP scores, the compounds identified as statistically significant for the model were quercetin (δ_H 7.30, d), myricetin (δ_H 7.01, s), gallic acid (δ_H 6.96, s), catechin (δ_H 5.93, d), and epigallocatechin (δ_H 5.89, d).

The metabolites responsible for the patterns observed in models A, B, and C are highlighted in **Figure 3**. Similar to the PCA results, flavonoids from the flavanol (catechin and epigallocatechin) and flavonol (quercetin and myricetin) classes remain key compounds. In model A, catechin, epigallocatechin, and quercetin were responsible for differentiation of samples from rainy (**Group 1**) and dry (**Group 2**), consistent with the observations from PCA. In model B, catechin and epigallocatechin continued to be the main contributors to the distinction of samples from the rainy period, while myricetin emerged as the key compound differentiating the transition samples (**Group 3**). In model C, flavanols became the primary contributors to distinguishing samples from the dry period, whereas myricetin and gallic acid were prominent during the transition period. These findings underscore that the biosynthesis of flavonoids in *Eugenia punicifolia* leaves is directly influenced by seasonality.

3.4.Correlation between NMR and climate data

To verify the correlation between chemical composition and climatic parameters (Table S1), the principle that the signal area in a properly calibrated ^{1}H NMR spectrum is proportional to the quantity of active nuclei present was applied.[38, 39] The aromatic region of the spectrum was carefully aligned and divided into buckets, with each bucket representing a specific range of chemical shifts. This alignment and bucketing process is essential to minimize spectral variations resulting from different chemical profiles and the experimental acquisition process. By ensuring greater consistency in the data, this approach facilitates reliable comparative analysis between samples.[40-42]

The bucket areas corresponding to the signals of quercetin (δ_H 7.30, d), myricetin (δ_H 7.01, s), gallic acid (δ_H 6.96, s), catechin (δ_H 5.93, d), and epigallocatechin (δ_H 5.89, d) were normalized to the total area and selected to evaluate variations across collection periods (**Figure 5A**). Furthermore, Pearson's correlation coefficient was employed to quantify the strength of the correlations between the chemical profile and climatic parameters (**Figure 5B**).

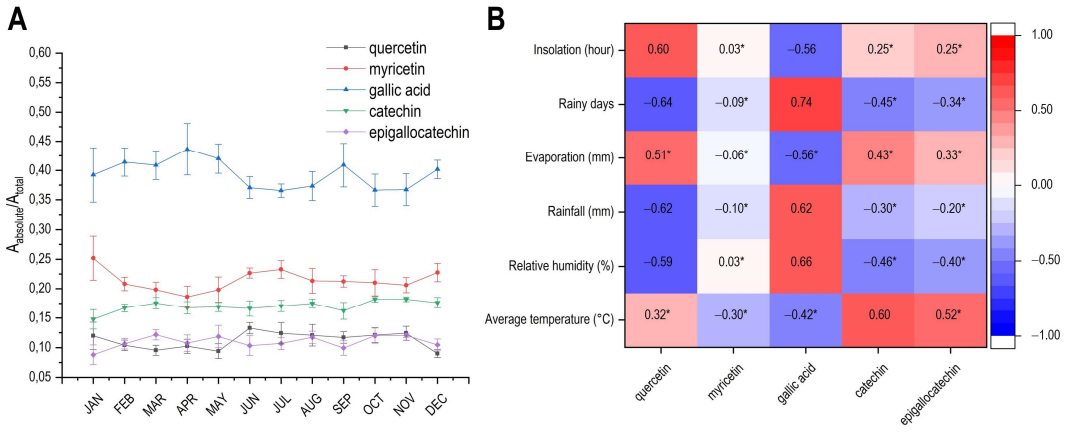

Figure 5. Variation in the absolute area of the ^{1}H NMR signal as a function of the collection month (**A**), and heatmap of Pearson correlation coefficients between chemical composition and climatic parameters (**B**). *p-values > 0.05 were considered not significant.

Figure 5A shows that the concentration of quercetin increases between June and November, suggesting an increase in its production during this period. Myricetin exhibits a similar trend, though with less pronounced monthly variations and a slight decline over time. Gallic acid, on the other hand, shows higher and more stable values between January and

May, with a reduction starting in June. As for catechin and epigallocatechin, both display monthly fluctuations; however, like gallic acid, their concentrations are slightly higher at the beginning of the analyzed period, decreasing in subsequent months.

In **Figure 5B**, catechin production is positively correlated with rising temperatures (r = 0.60), while quercetin production is favored by greater sunlight exposure (r = 0.60). In contrast, higher levels of relative humidity (r = –0.59), precipitation (r = –0.62), and the number of rainy days (r = –0.64) are associated with a decrease in quercetin production by the leaves of *E. punicifolia*. On the other hand, gallic acid production exhibits the opposite trend, being stimulated under conditions of high relative humidity (r = 0.66), increased precipitation (r = 0.62), and a greater number of rainy days (r = 0.74). Conversely, periods of higher sunlight incidence are correlated with a reduction in gallic acid production (r = –0.56).

The statistical analysis of ^{1}H NMR data combined with climatic parameters seemed to be an effective strategy for assessing how the chemical composition of MEW extracts from *Eugenia punicifolia* leaves is influenced by seasonality.

3.5.Biosynthetic considerations

From the biosynthetic perspective, when a plant is subjected to different types of abiotic stress, it tends to produce metabolites that play a role in its defense mechanisms. Among these metabolites, phenolic compounds play a fundamental role in the plant's resistance to extreme conditions.[43-45] Flavonoids, especially known for their diverse pharmacological activities, play a crucial role in mitigating oxidative stress caused by environmental factors, helping to protect plant cells.[46, 47] Their ability to scavenge free radicals, stabilize cell membranes, and modulate stress response pathways makes them essential in reducing damage caused by excessive solar radiation, water stress, and other abiotic factors.[6, 48, 49] Under drought conditions with high levels of sunlight, the synthesis of flavonols, a subclass of flavonoids, is intensified, with compounds such as quercetin, kaempferol, and myricetin standing out for their capacity to protect plant cells against damage from excessive solar radiation.[5, 50-53]

Quercetin, which contains a catechol group on the B ring, enhances its antioxidant activity and is a key factor in the plant's response to excess light and drought stress. Its concentration increases significantly under these conditions, highlighting its importance as a defense molecule.[54, 55] Moreover, during periods of low water availability, plants close their stomata and release abscisic acid (ABA), which interacts with flavonoids like quercetin and kaempferol, aiding in water loss control.[56]

Evaluating the influence of temperature on catechin production becomes a more complex task, as various studies report significant responses under both low and high temperatures.[57, 58] However, Xiang et al. (2020) demonstrated that, under specific environmental conditions, higher temperatures accelerated the growth of young shoots of *Camellia sinensis L.* and induced the expression of genes related to catechin biosynthesis.[59] Examining other climatic parameters, Wang et al. (2011) reported a significant increase in catechin production in *Camellia sinensis L.* teas collected during the rainy season .[60] Similarly, Yao et al. (2005) observed higher catechin and epigallocatechin production during colder months, further supporting the idea that climatic factors significantly influence catechin synthesis.[61]

Additionally, periods of high precipitation directly influence the virulence of pathogens that infect aerial tissues, which is intensified by rain and high humidity.[62] In response to these pathogens, plants produce stress hormones such as jasmonic acid and ethylene, which regulate biotic responses and interact in a complex manner to control plant growth, development, and defense. [63] Zhao et al. (2020) reported a direct relationship between jasmonic acid and the accumulation of catechin gallate, as well as its ability to regulate catechin content.[64] Jasmonic acid, particularly associated with insect-induced stress, induces the expression of genes involved in catechin production, which may contribute to the increase in this flavonoid during periods of high humidity and precipitation.[65]

In the biosynthesis of catechin and quercetin, the enzymes Phenylalanine Ammonia-Lyase (PAL), Chalcone Synthase (CHS), Chalcone Isomerase (CHI), and Flavanone 3-Hydroxylase (F3H) play pivotal roles in the early stages, transforming phenylalanine into dihydrokaempferol. Subsequently, Flavonoid 3'-Hydroxylase (F3'H) catalyzes the hydroxylation at the 3' position of the B-ring, leading to the production of dihydroquercetin, a key substrate for the synthesis of quercetin and catechin.[66]

If the subsequent step involves the action of the enzyme Flavonol Synthase (FLS), the resulting product will be quercetin. Conversely, if dihydroquercetin undergoes the action of Dihydroflavonol Reductase (DFR), followed by Leucoanthocyanidin Reductase (LAR), catechin is produced, as illustrated in **Figure 6**.

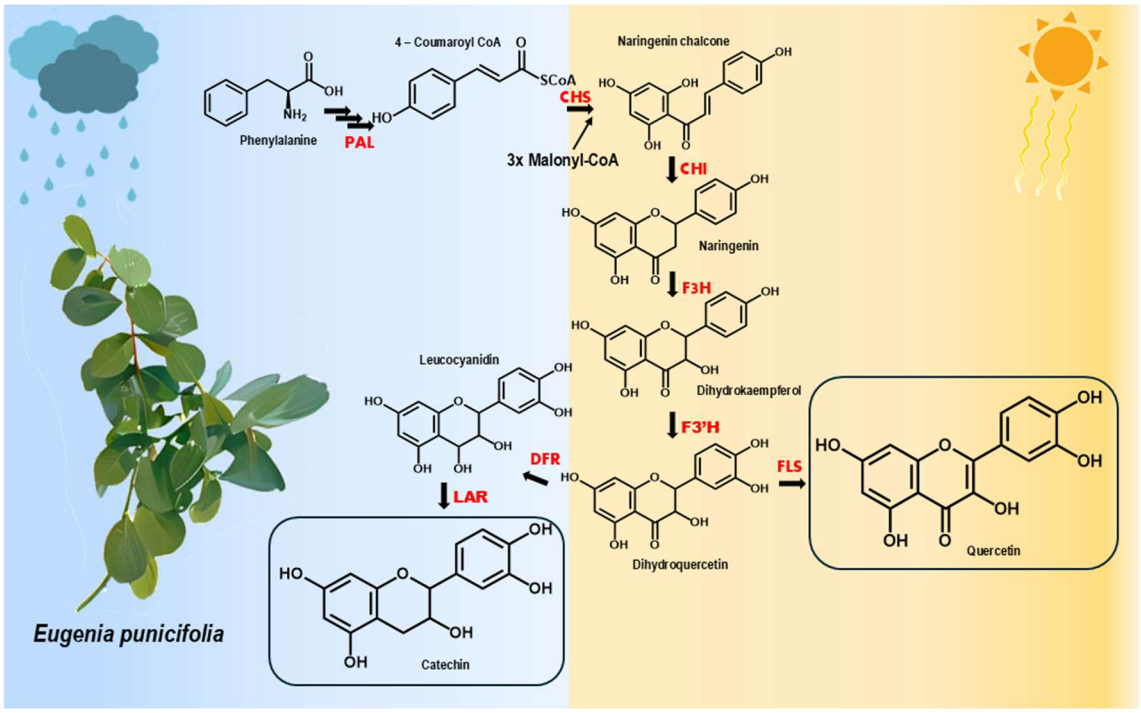

Figure 6. Schematic representation of the biosynthetic pathway for quercetin and catechin production as influenced by seasonality. Enzyme abbreviation: Ammonia-Lyase (PAL), Chalcone Synthase (CHS), Chalcone Isomerase (CHI), and Flavanone 3-Hydroxylase (F3H), Flavonoid 3'-Hydroxylase (F3'H), Flavonol Synthase (FLS), Dihydroflavonol Reductase (DFR) and Leucoanthocyanidin Reductase (LAR).

Temperature variations affect the production of both enzymes, FLS and LAR. Under moderate temperatures and high UV light exposure, plants tend to express higher levels of (FLS, favoring the production of flavonols, which play vital roles in UV radiation protection and oxidative stress mitigation. However, elevated temperatures can damage cells, impairing FLS expression.[66, 67] Conversely, the transformation of leucoanthocyanidin into catechin via LAR is amplified under low light conditions.[68] Additionally, higher temperatures tend to favor LAR expression, as catechins are often associated with protection against thermal stress and defense against pathogens.[69, 70]

Therefore, catechin and quercetin can be considered potential chemical markers for the species *E. punicifolia*, as they play essential roles in the plant's defense mechanisms and show a strong correlation with specific environmental conditions and stress responses. These compounds are biosynthesized through well-characterized enzymatic pathways influenced by abiotic factors such as temperature, UV light, and humidity. Variations in their concentrations are a direct result of the plant's adaptive responses, with quercetin being associated with UV protection and oxidative stress mitigation, and catechin with thermal stress protection and pathogen defense. The environmental and enzymatic regulation of these metabolites provides reliable indicators of the physiological state of plants, making them effective markers for ecological studies, agricultural monitoring, and quality assessment of *E.punicifolia* leaves-derived products.

4. Conclusion

This study highlights the significant influence of seasonality on the chemical profiles of *E. punicifolia* leaves. Quercetin, myricetin, gallic acid, catechin, and epigallocatechin were employed as probes (chemical markers) to assess how *E. punicifolia* leaves respond to abiotic stress resulting from seasonal variations. Distinct sample groupings based on the rainy, dry, and transitional periods were evident through PCA and validated using various metrics of the PLS-DA model. Correlation analysis demonstrated that the biosynthesis of gallic acid, quercetine, and catechine in *E. punicifolia* was highly responsive to environmental factors such as average temperature, relative humidity, rainfall, rainy days, and sunlight exposure. Overall, the study provides a valuable scientific basis for understanding how seasonality impacts the chemical composition of medicinal plants, laying the groundwork for future ecological studies.

5. References

1. Oliveira, E. S. C.; Pontes, F. L. D.; Acho, L. D. R.; da Silva, B. J. P.; do Rosário, A. S.; Chaves, F. C. M.; Campos, F. R.; Bezerra, J. d. A.; Lima, E. S.; Machado, M. B. NMR and multivariate methods: Identification of chemical markers in extracts of pedra-ume-caá and their antiglycation, antioxidant, and enzymatic inhibition activities. *Phytochem. Anal.* **2024**, *35*, 552-566.

2. Neves, K. O. G.; Silva, S. O.; Cruz, M. S.; Mar, J. M.; Bezerra, J. A.; Sanches, E. A.; Cassani, N. M.; Antoniucci, G. A.; Jardim, A. C.; Chaves, F. C. M.; et al. Investigation of the Influence of the Extraction System and Seasonality on the Pharmacological Potential of *Eugenia punicifolia* Leaves. *Molecules*, **2025**; *30*, 713.

3. Dos Santos, C.; Mizobucchi, A. L.; Escaramboni, B.; Lopes, B. P.; Angolini, C. F. F.; Eberlin, M. N.; de Toledo, K. A.; Núñez, E. G. F. Optimization of Eugenia punicifolia (Kunth) D. C. leaf extraction using a simplex centroid design focused on extracting phenolics with antioxidant and antiproliferative activities. *BMC Chem.* **2020**, *14*, 34.

4. Basting, R. T.; Nishijima, C. M.; Lopes, J. A.; Santos, R. C.; Lucena Périco, L.; Laufer, S.; Bauer, S.; Costa, M. F.; Santos, L. C.; Rocha, L. R. M.; et al. Antinociceptive, anti-inflammatory and gastroprotective effects of a hydroalcoholic extract from the leaves of *Eugenia punicifolia* (Kunth) DC. in rodents. *J. Ethnopharmacol.* **2014**, *157*, 257-267.

5. Zagoskina, N. V.; Zubova, M. Y.; Nechaeva, T. L.; Kazantseva, V. V.; Goncharuk, E. A.; Katanskaya, V. M.; Baranova, E. N.; Aksenova, M. A. Polyphenols in Plants: Structure, Biosynthesis, Abiotic Stress Regulation, and Practical Applications (Review). *Int. J. Mol. Sci.* **2023,** *24*, 13874.

6. Patil, J. R.; Mhatre, K. J.; Yadav, K.; Yadav, L. S.; Srivastava, S.; Nikalje, G. C. Flavonoids in plant-environment interactions and stress responses. *Discover Plants* **2024**, *1*, 68.

7. Scognamiglio, M.; D'Abrosca, B.; Esposito, A.; Fiorentino, A. Chemical Composition and Seasonality of Aromatic Mediterranean Plant Species by NMR-Based Metabolomics. *J. Anal. Methods Chem.* **2015**, *2015*, 258570.

8. Aru, V.; Engelsen, S.; Savorani, F.; Culurgioni, J.; Sarais, G.; Atzori, G.; Cabiddu, s.; Marincola, F. The Effect of Season on the Metabolic Profile of the European Clam Ruditapes decussatus as Studied by ^{1}H-NMR Spectroscopy. *Metabolites* **2017**, *7*, 36.

9. Ravaglia, L. M.; de Oliveira, P. D.; Holzgrabe, U.; Alcantara, G. B. qNMR in natural products: practical approaches. What nobody tells you before starting your qNMR study! *Front. Nat. Prod.* **2024**, *3*, 1416195 .

10. Alves Filho, E.; Silva, L. M.; Riceli, P.; Brito, E.; Zocolo, G.; Leão, P.; Marques, A.; Quintela, A.; Larsen, F.; Canuto, K. ^{1}H NMR and LC-MS-based metabolomic approach for evaluation of the seasonality and viticultural practices in wines from São Francisco River Valley, a Brazilian semi-arid region. *Food Chem.* **2019**, *289*, 558-567.

11. van Wyk, A. S.; Prinsloo, G. NMR-based metabolomic analysis of the seasonal and regional variability of phytochemical compounds in Curtisia dentata stem bark. *Biochem. Syst. Ecol.* **2021**, *94*, 104197.

12. Jolliffe, I. T.; Cadima, J. Principal component analysis: a review and recent developments. *Philos. Transact. A Math. Phys. Eng. Sci.* **2016**, *374*, 20150202.

13. Lee, L. C.; Liong, C. Y.; Jemain, A. A. Partial least squares-discriminant analysis (PLS-DA) for classification of high-dimensional (HD) data: a review of contemporary practice strategies and knowledge gaps. *Analyst* **2018**, *143*, 3526-3539.

14. Szymańska, E.; Saccenti, E.; Smilde, A. K.; Westerhuis, J. A. Double-check: validation of diagnostic statistics for PLS-DA models in metabolomics studies. *Metabolomics* **2012**, *8*, 3-16.

15. Faber, N. M.; Rajkó, R. How to avoid over-fitting in multivariate calibration—The conventional validation approach and an alternative. *Anal. Chim. Acta.* **2007**, *595*, 98-106.

16. Neves, K. O. G.; Santos, M. F. C.; Mar, J. M.; Pontes, F. L. D.; Tormena, C. F.; Chaves, F. C. M.; Campos, F. R.; Sanches, E. A.; Bezerra, J. A.; Machado, M. B.; et al. ^{1}H NMR Chemical Profile and Antioxidant Activity of *Eugenia punicifolia* Extracts Over Seasons: A Metabolomic Pilot Study. *J. Braz. Chem. Soc.* **2024**, *35*, e20240010.

17. *TopSpin 3.6.3*; Academia License, Bruker Optics GmbH & Co. KG: Ettlingen, Germany, 2021.

18. *OriginPro 2018*; OriginLab Corporation: Northampton, MA, USA, 2018.

19. *PLS-Toolbox Solo 9.0*; Eigenvector Research Inc.: Wenatchee, WA, USA, 2021.

20. *RStudio: Integrated Development Environment for R*; RStudio, PBC.: Boston, MA, USA 2020.

21. *Minitab® 18.1*; Minitab Inc., State College: PA, USA, 2017.

22. López-Martínez, L. M.; Santacruz-Ortega, H.; Navarro, R. E.; Sotelo-Mundo, R. R.; González-Aguilar, G. A. A. ^{1}H NMR Investigation of the Interaction between Phenolic Acids Found in Mango (*Manguifera indica* cv Ataulfo) and Papaya (*Carica papaya* cv Maradol) and 1,1-diphenyl-2-picrylhydrazyl (DPPH) Free Radicals. *PLoS One* **2015**, *10*, e0140242.

23. Chen, S.; Wang, X.; Cheng, Y.; Gao, H.; Chen, X. A Review of Classification, Biosynthesis, Biological Activities and Potential Applications of Flavonoids. *Molecules* **2023**, *28*, 4982.

24. Oliveira, E. S. C.; Pontes, F. L. D.; Acho, L. D. R.; do Rosário, A. S.; da Silva, B. J. P.; de, A. B. J.; Campos, F. R.; Lima, E. S.; Machado, M. B. qNMR quantification of phenolic compounds in dry extract of *Myrcia multiflora* leaves and its antioxidant, anti-AGE, and enzymatic inhibition activities. *J. Pharm. Biomed. Anal.* **2021**, *201*, 114109.

25. Napolitano, J.; Gödecke, T.; Lankin, D.; Jaki, B.; McAlpine, J.; Chen, S.-N.; Pauli, G. Orthogonal analytical methods for botanical standardization: Determination of green tea catechins by qNMR and LC–MS/MS. *J. Pharm. Biomed. Anal.* **2013**, *93*, 59-67.

26. Choi, J.; Lee, H.-D.; Cho, H.; Lee, C.-D.; Tran, G. H.; Kim, H.; Moon, S.-K.; Lee, S. Antioxidative phenolic compounds from the aerial parts of Cyperus exaltatus var. iwasakii and their HPLC analysis. *Appl. Biol. Chem.* **2023**, *66*, 61.

27. Caloiero, T.; Sirangelo, B.; Coscarelli, R.; Ferrari, E. An Analysis of the Occurrence Probabilities of Wet and Dry Periods through a Stochastic Monthly Rainfall Model. *Water*, **2016**, *8*, 39.

28. Lai, H.; Chen, B.; Yin, X.; Wang, G.; Wang, X.; Yun, T.; Lan, G.; Wu, Z.; Yang, C.; Kou, W. Dry season temperature and rainy season precipitation significantly affect the spatio-temporal pattern of rubber plantation phenology in Yunnan province. *Front. Plant. Sci.* **2023**, *14*, 1283315.

29. Fattah, M. A.; Gupta, S. D.; Farouque, M. Z.; Ghosh, B.; Morshed, S. R.; Chakraborty, T.; Kafy, A. A.; Rahman, M. T. Spatiotemporal characterization of relative humidity trends and influence of climatic factors in Bangladesh. *Heliyon* **2023**, *9*, e19991.

30. Lu, H. C.; Chen, W. K.; Wang, Y.; Bai, X. J.; Cheng, G.; Duan, C. Q.; Wang, J.; He, F. Effect of the Seasonal Climatic Variations on the Flavonoid Accumulation in Vitis vinifera cvs. 'Muscat Hamburg' and 'Victoria' Grapes under the Double Cropping System. *Foods* **2022**, *11*, 48.

31. Zheng, T.; Zhang, D.-L.; Sun, B.-Y.; Liu, S.-M. Evaluating the Impacts of Climate Factors and Flavonoids Content on Chinese Prickly Ash Peel Color Based on HPLC-MS and Structural Equation Model. *Foods* **2022**, *11*, 2539.

32. Shi, Y.; Yang, L.; Yu, M.; Li, Z.; Ke, Z.; Qian, X.; Ruan, X.; He, L.; Wei, F.; Zhao, Y.; et al. Seasonal variation influences flavonoid biosynthesis path and content, and antioxidant activity of metabolites in *Tetrastigma hemsleyanum* Diels & Gilg. *PLoS One* **2022**, *17*, e0265954.

33. Rutledge, D.; Roger, J.-M.; Lesnoff, M. Different Methods for Determining the Dimensionality of Multivariate Models. *Front. Anal. Sci.* **2021**, *1*, 754447.

34. Westerhuis, J. A.; van Velzen, E. J. J.; Hoefsloot, H. C. J.; Smilde, A. K. Discriminant Q^2 (DQ^2) for improved discrimination in PLSDA models. *Metabolomics* **2008**, *4*, 293-296.

35. Wang, Z.; Chen, Z.; Yang, S.; Wang, Y.; Yu, L.; Zhang, B.; Rao, Z.; Gao, J.; Tu, S. 1H NMR-based metabolomic analysis for identifying serum biomarkers to evaluate methotrexate treatment in patients with early rheumatoid arthritis. *Exp. Ther. Med.* **2012**, *4*, 165-171.

36. Kong, X.; Yang, X.; Zhou, J.; Chen, S.; Li, X.; Jian, F.; Deng, P.; Li, W. Analysis of plasma metabolic biomarkers in the development of 4-nitroquinoline-1-oxide-induced oral carcinogenesis in rats. *Oncol. Lett.* **2015**, *9*, 283-289.

37. Westerhuis, J. A.; Hoefsloot, H. C. J.; Smit, S.; Vis, D. J.; Smilde, A. K.; van Velzen, E. J. J.; van Duijnhoven, J. P. M.; van Dorsten, F. A. Assessment of PLSDA cross validation. *Metabolomics* **2008**, *4*, 81-89.

38. Bharti, S. K.; Roy, R. Quantitative ^{1}H NMR spectroscopy. *TrAC, Trends Anal. Chem.* **2012**, *35*, 5-26.

39. Khalil, A.; Kashif, M. Nuclear Magnetic Resonance Spectroscopy for Quantitative Analysis: A Review for Its Application in the Chemical, Pharmaceutical and Medicinal Domains. *Critical Reviews in Analytical Chemistry* **2023**, *53*, 997-1011.

40. Wang, B.; Goodpaster, A.; Kennedy, M. Coefficient of Variation, Signal-to-Noise Ratio, and Effects of Normalization in Validation of Biomarkers from NMR-based Metabonomics Studies. *Chemom. Intell. Lab. Syst.* **2013**, *128*, 9-16.

41. Sousa, S. A. A.; Magalhães, A.; Ferreira, M. M. C. Optimized bucketing for NMR spectra: Three case studies. *Chemom. Intell. Lab. Syst.* **2013**, *122*, 93-102.

42. Chai, X.; Liu, C.; Fan, X.; Huang, T.; Zhang, X.; Jiang, B.; Liu, M. Combination of peak-picking and binning for NMR-based untargeted metabonomics study. *J. Magn. Reson.* **2023**, *351*, 107429.

43. Parvaiz, A.; Satyawati, S. Salt stress and phyto-biochemical responses of plants - a review. *Plant Soil Environ.* **2008**, *54*, 89-99.

44. Akula, R.; Ravishankar, G. A. Influence of abiotic stress signals on secondary metabolites in plants. *Plant Signal Behav.* **2011**, *6*, 1720-1731.

45. Sharma, A.; Shahzad, B.; Rehman, A.; Bhardwaj, R.; Landi, M.; Zheng, B. Response of Phenylpropanoid Pathway and the Role of Polyphenols in Plants under Abiotic Stress. *Molecules*, **2019**, *24*, 2452.

46. Zahra, M.; Abrahamse, H.; George, B. P. Flavonoids: Antioxidant Powerhouses and Their Role in Nanomedicine. *Antioxidants (Basel)* **2024**, *13*, 922.

47. Agati, G.; Brunetti, C.; Fini, A.; Gori, A.; Guidi, L.; Landi, M.; Sebastiani, F.; Tattini, M. Are Flavonoids Effective Antioxidants in Plants? Twenty Years of Our Investigation. *Antioxidants (Basel)* **2020**, *9*, 1098.

48. Mirás-Avalos, J. M.; Intrigliolo, D. S. Grape Composition under Abiotic Constrains: Water Stress and Salinity. *Front. Plant Sci.* **2017**, *8*, 851.

49. González-Chavira, M. M.; Herrera-Hernández, M. G.; Guzmán-Maldonado, H.; Pons-Hernández, J. L. Controlled water deficit as abiotic stress factor for enhancing the phytochemical content and adding-value of crops. *Sci. Hortic.* **2018**, *234*, 354-360.

50. Cao, Y.; Mei, Y.; Zhang, R.; Zhong, Z.; Yang, X.; Xu, C.; Chen, K.; Li, X. Transcriptional regulation of flavonol biosynthesis in plants. *Hortic. Res.* **2024**, *11*, 257.

51. Pollastri, S.; Tattini, M. Flavonols: old compounds for old roles. *Ann. Bot.* **2011**, *108*, 1225-1233.

52. Gori, A.; Nascimento, L. B.; Ferrini, F.; Centritto, M.; Brunetti, C. Seasonal and Diurnal Variation in Leaf Phenolics of Three Medicinal Mediterranean Wild Species: What Is the Best Harvesting Moment to Obtain the Richest and the Most Antioxidant Extracts? *Molecules*, **2020**, *25*, 956.

53. Laoué, J.; Fernandez, C.; Ormeño, E. Plant Flavonoids in Mediterranean Species: A Focus on Flavonols as Protective Metabolites under Climate Stress. *Plants*, **2022**, *11*, 172.

54. Tattini, M.; Galardi, C.; Pinelli, P.; Massai, R.; Remorini, D.; Agati, G. Differential accumulation of flavonoids and hydroxycinnamates in leaves of *Ligustrum vulgare* under excess light and drought stress. *New Phytol.* **2004**, *163*, 547-561.

55. Peña Barrena, L. E.; Mats, L.; Earl, H. J.; Bozzo, G. G. Phenylpropanoid Metabolism in *Phaseolus vulgaris* during Growth under Severe Drought. *Metabolites*, **2024**; *14*, 319.

56. Jan, R.; Khan, M.; Asaf, S.; Lubna; Asif, S.; Kim, K.-M. Bioactivity and Therapeutic Potential of Kaempferol and Quercetin: New Insights for Plant and Human Health. *Plants* **2022**, *11*, 2623.

57. Li, X.; Li, M.-H.; Deng, W.-W.; Ahammed, G. J.; Wei, J.-P.; Yan, P.; Zhang, L.-P.; Fu, J.-Y.; Han, W.-Y. Exogenous melatonin improves tea quality under moderate high temperatures by increasing epigallocatechin-3-gallate and theanine biosynthesis in *Camellia sinensis* L. *J. Plant Physiol.* **2020**, *253*, 153273.

58. Yu, J.; Wang, Q.; Wang, W.; Ma, R.; Ding, C.; Wei, K.; Wang, L.; Ge, S.; Shi, Y.; Li, X. Transcriptomic and metabolomic insights into temperature-dependent changes in catechin and anthocyanin accumulation in tea plants with different leaf colors. *Plant Stress* **2024**, *14*, 100705.

59. Xiang, P.; Wilson, I. W.; Huang, J.; Zhu, Q.; Tan, M.; Lu, J.; Liu, J.; Gao, S.; Zheng, S.; Lin, D.; et al. Co-regulation of catechins biosynthesis responses to temperature changes by shoot growth and catechin related gene expression in tea plants (*Camellia sinensis L.*). *J. Hortic. Sci. Biotechnol.* **2021**, *96*, 228-238.

60. Wang, L. Y.; Wei, K.; Jiang, Y. W.; Cheng, H.; Zhou, J.; He, W.; Zhang, C. C. Seasonal climate effects on flavanols and purine alkaloids of tea (*Camellia sinensis* L.). *Eur. Food Res. Technol.* **2011**, *233*, 1049-1055.

61. Yao, L.; Caffin, N.; D'Arcy, B.; Jiang, Y.; Shi, J.; Singanusong, R.; Liu, X.; Datta, N.; Kakuda, Y.; Xu, Y. Seasonal Variations of Phenolic Compounds in Australia-Grown Tea (*Camellia sinensis*). *J. Agric. Food Chem.* **2005**, *53*, 6477-6483.

62. Velásquez, A. C.; Castroverde, C. D. M.; He, S. Y. Plant–Pathogen Warfare under Changing Climate Conditions. *Curr. Biol.* **2018**, *28*, 619-634.

63. Beckers, G. J. M.; Spoel, S. H. Fine-Tuning Plant Defence Signalling: Salicylate versus Jasmonate. *Plant Biol.* **2006**, *8*, 1-10.

64. Zhao, S.; Mi, X.; Guo, R.; Xia, X.; Liu, L.; An, Y.; Yan, X.; Wang, S.; Guo, L.; Wei, C. The Biosynthesis of Main Taste Compounds Is Coordinately Regulated by miRNAs and Phytohormones in Tea Plant (*Camellia sinensis*). *J. Agric. Food Chem.* **2020**, *68*, 6221-6236.

65. Wang, J.; Song, L.; Gong, X.; Xu, J.; Li, M. Functions of Jasmonic Acid in Plant Regulation and Response to Abiotic Stress. *Int. J. Mol. Sci.* **2020**, *21*, 1446.

66. Neugart, S.; Krumbein, A.; Zrenner, R. Influence of Light and Temperature on Gene Expression Leading to Accumulation of Specific Flavonol Glycosides and Hydroxycinnamic Acid Derivatives in Kale (Brassica oleracea var. sabellica). *Front. Plant Sci.* **2016**, *7*, 326.

67. Teixeira, A.; Eiras-Dias, J.; Castellarin, S. D.; Gerós, H. Berry phenolics of grapevine under challenging environments. *Int. J. Mol. Sci.* **2013**, *14*, 18711-18739.

68. Hong, G.; Wang, J.; Zhang, Y.; Hochstetter, D.; Zhang, S.; Pan, Y.; Shi, Y.; Xu, P.; Wang, Y. Biosynthesis of catechin components is differentially regulated in dark-treated tea (*Camellia sinensis* L.). *Plant Physiol. Biochem.* **2014**, *78*, 49-52.

69. Sheng, Y.; Sun, Y.; Tang, Y.; Yu, Y.; Wang, J.; Zheng, F.; Li, Y. Catechins: Protective mechanism of antioxidant stress in atherosclerosis. *Front. Pharmacol.* **2023**, *14*, 1144878.

70. Teng, R.-M.; Wu, Z.-J.; Ma, H.-Y.; Wang, Y.-X.; Zhuang, J. Differentially Expressed Protein Are Involved in Dynamic Changes of Catechins Contents in Postharvest Tea Leaves under Different Temperatures. *J. Agric. Food Chem.* **2019**, *67*, 7547-7560.

CONCLUSÃO

A conclusão desta pesquisa permitiu o desenvolvimento de uma abordagem metabolômica capaz de avaliar a influência da sazonalidade no perfil metabólico e nas propriedades farmacológicas das folhas de *Eugenia punicifolia*. A aplicação da espectroscopia de ressonância magnética nuclear (RMN), associada a análises multivariadas, possibilitou a identificação de variações sazonais na composição química dos diferentes extratos das folhas de *E. punicifolia*, fornecendo insights fundamentais sobre o impacto dos fatores ambientais na biossíntese de metabólitos secundários, reforçando a aplicabilidade da metabolômica no estudo de plantas medicinais.

Além disso, os resultados evidenciaram que a sazonalidade exerce um papel determinante na produção de compostos fenólicos, demonstrando que as variações nos níveis de ácido gálico, catequina, epigalocatequina, quercetina e miricetina influenciam diretamente as atividades antioxidante, antiglicante e antiviral dos extratos. Os ensaios farmacológicos indicaram que os extratos obtidos no período chuvoso, utilizando o sistema de extração metanol:etanol:água (MEA), apresentaram maior concentração de compostos bioativos e melhor desempenho nas atividades avaliadas. A identificação de ácido gálico, catequina e quercetina como prováveis marcadores químicos sazonais, por meio das análises de PCA e PLS-DA, destaca a relevância dos fatores climáticos na otimização da colheita e no uso racional dessa espécie para aplicações fitoterápicas.

Portanto, além de sua contribuição científica, esta tese fortalece a valorização de uma matriz natural da biodiversidade amazônica, fornecendo uma base sólida para o desenvolvimento de produtos fitoterápicos derivados de *Eugenia punicifolia*. Dessa maneira, este estudo não apenas expande o conhecimento sobre a composição química e o potencial farmacológico dessa espécie, mas também abre novas perspectivas para investigações futuras. Entre elas, destacam-se estudos complementares sobre a regulação da biossíntese de metabólitos em resposta a fatores ambientais específicos, bem como a validação de suas aplicações farmacológicas em modelos biológicos mais complexos.

REFERÊNCIAS

1. SOBRAL, M. et al. Myrtaceae. In: *Lista de espécies da flora do Brasil*. Rio de Janeiro: Jardim Botânico do Rio de Janeiro. Disponível em: http://floradobrasil.jbrj.gov.br. Acesso em: 28 dez. 2023.

2. LORENZI, H. Frutas brasileiras e exóticas cultivadas: de consumo in natura. Nova Odessa: Instituto Plantarum de Estudos da Flora, 2006. ISBN 8586714232.

3. JORGE, U.; AGUIAR, J.; SILVA, M. Anatomia foliar de pedra-hume-caá (*Myrcia sphaerocarpa*, *Myrcia guianensis*, *Eugenia punicifolia* - Myrtaceae). Acta Amazonica, v. 30, p. 49-49, 2000.

4. RAMOS, A. *et al*. Pedra-ume caá fruit: An Amazon cherry rich in phenolic compounds with antiglycant and antioxidant properties. Food Research International, v. 123, p. 674-683, 2019.

5. KÉSIA, F. *et al*. Levantamento das espécies conhecidas como pedra-ume-caá (Myrtaceae), com ênfase nas comercializadas na cidade de Belém, Pará, Brasil. **Biota,** v. 5, p. 7-15, 2015.

6. ALBUQUERQUE, R. *et al*. Quantitative determination of pentacyclic triterpenic acids in Amazonian species *Eugenia punicifolia* DC by ATR-FTIR. Natural Product Research, v. 35, p. 2574-2578, 2019.

7. BASTING, R. T. *et al*. Antinociceptive, anti-inflammatory and gastroprotective effects of a hydroalcoholic extract from the leaves of *Eugenia punicifolia* (Kunth) DC. in rodents. Journal of Ethnopharmacology, v. 157, p. 257-267, 2014.

8. RIBEIRO, D. A. *et al*. Influence of seasonal variation on phenolic content and in vitro antioxidant activity of *Secondatia floribunda* A. DC. (Apocynaceae). Food Chemistry, v. 315, p. 126277, 2020.

9. GORI, A. *et al*. Seasonal and Diurnal Variation in Leaf Phenolics of Three Medicinal Mediterranean Wild Species: What Is the Best Harvesting Moment to Obtain the Richest and the Most Antioxidant Extracts? Molecules, v. 25, p. 956, 2020.

10. SHARMA, A. *et al*. Response of Phenylpropanoid Pathway and the Role of Polyphenols in Plants under Abiotic Stress. Molecules, v. 24, p. 2452, 2019.

11. PATIL, J. R. *et al*. Flavonoids in plant-environment interactions and stress responses. Discover Plants**,** v. 1, p. 68, 2024.

12. AKULA, R.; RAVISHANKAR, G. A. Influence of abiotic stress signals on secondary metabolites in plants. Plant Signaling & Behavior, v. 6, p. 1720-1731, 2011/.

13. ZAHRA, M.; ABRAHAMSE, H.; GEORGE, B. P. Flavonoids: Antioxidant Powerhouses and Their Role in Nanomedicine. Antioxidants (Basel), v. 13, p. 922, 2024.

14. SCOGNAMIGLIO, M. *et al*. Chemical Composition and Seasonality of Aromatic Mediterranean Plant Species by NMR-Based Metabolomics. Journal of Analytical Methods in Chemistry, v. 2015, p. 258570, 2015.

15. GOWDA, N.; RAFTERY, D. Recent Advances in NMR-Based Metabolomics. Analytical Chemistry, v. 89, p. 490-510, 2016.

16. EMWAS, A. H. *et al*. NMR Spectroscopy for Metabolomics Research. Metabolites, v. 9, p. 123, 2019.

17. ZANATTA, A.; VILEGAS, W.; EDRADA-EBEL, R. UHPLC-(ESI)-HRMS and NMR-Based Metabolomics Approach to Access the Seasonality of *Byrsonima intermedia* and *Serjania marginata* From Brazilian Cerrado Flora Diversity. Frontiers in Chemistry, v. 9, p. 710025, 2021.

18. YAN, K. J. *et al*. Qualitative and quantitative analyses of Compound Danshen extract based on 1H NMR method and its application for quality control Journal of Pharmaceutical and Biomedical Analysis, v. 131, p. 183-187, 2016.

19. ZHOU, X. *et al*. Spectrum-effect relationship between UPLC fingerprints and anti-lung cancer effect of Panax ginseng. Phytochem Anal, v. 32, p. 339-346, 2021.

20. JOLLIFFE, I. T.; CADIMA, J. Principal component analysis: a review and recent developments. Philosophical Transactions of the Royal Society A, v. 374, n. 2065, p. 20150202, 2016.

21. SZYMAŃSKA, E. *et al*. Double-check: validation of diagnostic statistics for PLS-DA models in metabolomics studies. Metabolomics, v. 8, p. 3-16, 2012.

22. LEE, L. C.; LIONG, C. Y.; JEMAIN, A. A. Partial least squares-discriminant analysis (PLS-DA) for classification of high-dimensional (HD) data: a review of contemporary practice strategies and knowledge gaps. Analyst, v. 143, p. 3526-3539, 2018.

23. CASCAES, M. M. *et al*. Constituents and Pharmacological Activities of *Myrcia* (Myrtaceae): A Review of an Aromatic and Medicinal Group of Plants. International Journal of Molecular Sciences, v. 16, p. 23881-23904, 2015.

24. YOSHIKAWA, M. *et al*. Antidiabetic principles of natural medicines. II. Aldose reductase and alpha-glucosidase inhibitors from Brazilian natural medicine, the leaves of *Myrcia multiflora* DC. (Myrtaceae): structures of myrciacitrins I and II and myrciaphenones A and B. Chemical and Pharmaceutical Bulletin (Tokyo), v. 46, p. 113-119, 1998.

25. SOUSA, W.; DE SOUZA CASTRO, C. F.; FILHO, A. Composição química, físico-química e atividade antifúngica dos óleos essenciais da flor e do fruto de *Myrcia guianensis* (Aubl.) DC. Revista Principia - Divulgação Científica e Tecnológica do IFPB, v. 52, p. 92-104, 2020.

26. RIBEIRO, C. L.; PAULA, J. A. M. D.; PEIXOTO, J. D. C. Pharmacological properties of species of the genres: *Myrcia*, *Eugenia* and *Psidium* – Myrtaceae-, typical of the Cerrado: A scope review. Research, Society and Development, v. 11, p. e44711830356, 2022.

27. DEXHEIMER, G. M.; POZZOBON, A. Atividade biológica de plantas da família Myrtaceae: revisão sistemática de artigos entre 1989 e 2015. Revista Cubana de Plantas Medicinales, v. 22, p. 1-22, 2017.

28. SANTOS, C. V. D. *et al*. Chemical composition, antimicrobial and antioxidant activity of leaves essential oil the *Myrcia palustris* DC. (MYRTACEAE). Research, Society and Development, v. 10, p. e20510313303, 2021.

29. ARRUDA, R.; VICTÓRIO, C. Leaf Secretory Structure and Volatile Compounds of *Eugenia copacabanensis* Kiaersk. (Myrtaceae). Journal of Essential Oil Research, v. 23, p. 1-6, 2011.

30. SOUZA, A. *et al*. Traditional Uses, Phytochemistry, and Antimicrobial Activities of *Eugenia* Species - A Review. Planta medica, v. 84, p. 1232-1248, 2018.

31. SOUSA, R. M. F. *et al*. Chemical composition, cytotoxic, and antibacterial activity of the essential oil from *Eugenia calycina* Cambess. leaves against oral bacteria. Industrial Crops and Products, v. 65, p. 71-78, 2015.

32. OLIVEIRA, E. S. C. *et al*. Hypoglycemic effect and toxicity of the dry extract of *Eugenia biflora* (L.) DC. leaves. Journal of Ethnopharmacology, v. 293, p. 115276, 2022.

33. OLIVEIRA, E. S. C. *et al*. NMR and multivariate methods: Identification of chemical markers in extracts of pedra-ume-caá and their antiglycation, antioxidant, and enzymatic inhibition activities. Phytochemical Analysis, v. 35, p. 552-566, 2024.

34. MAIA, J. G. S.; ZOGHBI, M. D. G. B.; DE AGUILAR ANDRADE, E. H. Plantas aromáticas na Amazônia e seus óleos essenciais. Belém: Museu Paraense Emílio Goeldi, 2001. ISBN 8570980698.

35. TEIXEIRA, R. G. S. *et al*. In vitro and in silico studies for barbinervic acid, a triterpene isolated from *Eugenia punicifolia* that inhibits vasopressor tone. ***Natural Product Research,*** v. 35, p. 4870-4875, 2021

36. TEIXEIRA, L. D. L. *et al*. Identification of Ellagitannins and Flavonoids from *Eugenia brasilienses* Lam. (Grumixama) by HPLC-ESI-MS/MS. Journal of Agricultural and Food Chemistry, v. 63, p. 5417-5427, 2015.

37. ARAÚJO, F. *et al*. Wild Brazilian species of *Eugenia* genera (Myrtaceae) as an innovation hotspot for food and pharmacological purposes. Food Research International, v. 121, p. 57-72, 2019.

38. WINDARSIH, A.; ROHMAN, A.; SWASONO, R. Application of H-NMR metabolite fingerprinting and chemometrics for the authentication of *Curcuma longa* adulterated with *Curcuma manga*. Journal of Applied Pharmaceutical Science, v. 8, p. 75-81, 2018.

39. LI, H. *et al*. Chemical Fingerprint for Identification and Quality Control of Saccharides in Danhong Injection Based on HPLC-ELSD with Chemometrics. Chemical Research in Chinese Universities, v. 35, p. 782-787, 2019.

40. ARU, V. *et al*. The Effect of Season on the Metabolic Profile of the European Clam *Ruditapes decussatus* as Studied by 1 H-NMR Spectroscopy. Metabolites, v. 7, p. 36, 07/26 2017.

41. ALVES FILHO, E. *et al*. ^{1}H NMR and LC-MS-based metabolomic approach for evaluation of the seasonality and viticultural practices in wines from São Francisco River Valley, a Brazilian semi-arid region. Food Chemistry, v. 289, p. 558-567, 2019.

42. SANTOS, M. F. C. *et al*. ^{1}H HR-MAS NMR chemical profile and chemometric analysis as a tool for quality control of different cultivars of green tea (*Camellia sinensis*). Food Chemistry, v. 408, p. 135016, 2023.

43. BUEDENBENDER, L. *et al*. HSQC-TOCSY Fingerprinting-Directed Discovery of Antiplasmodial Polyketides from the Marine Ascidian-Derived Streptomyces sp. (USC-16018). Marine Drugs, v. 16, p. 189, 2018.

44. DASHTI, H. *et al*. Spin System Modeling of NMR Spectra for Applications in Metabolomics and Small Molecule Screening. Analytical Chemistry, v. 89, p. 12201-12208, 2017.

45. LARIVE, C.; BARDING, G.; DINGES, M. NMR Spectroscopy for Metabolomics and Metabolic Profiling. Analytical chemistry, v. 87, p. 133-146, 2015.

46. CLARIDGE, T. D. W. High-resolution NMR techniques in organic chemistry. 3. ed. Boston: Elsevier, 2016. ISBN 9780080999869.

47. NASCIMENTO, C. Ressonância magnética nuclear. São Paulo: Edgard Blücher, 2016. ISBN 9788521210184.

48. ARAÚJO, C. S. *et al*. Total content of kaurene diterpenes in *Annona vepretorum* stems via ^{1}H qNMR: A method for speeding the identification of bioactive extracts. Phytochemical Analysis, v. 30, p. 83-88, 2019.

49. BHARTI, S. K.; ROY, R. Quantitative ^{1}H NMR spectroscopy. TrAC Trends in Analytical Chemistry, v. 35, p. 5-26, 2012.

50. OLIVEIRA, E. S. C. *et al*. qNMR quantification of phenolic compounds in dry extract of *Myrcia multiflora* leaves and its antioxidant, anti-AGE, and enzymatic inhibition activities. Journal of Pharmaceutical and Biomedical Analysis, v. 201, p. 114109, 2021.

51. RAVAGLIA, L. M. *et al*. qNMR in natural products: practical approaches. What nobody tells you before starting your qNMR study! Frontiers in Natural Products, v. 3, p. 1416195, 2024.

52. HONG, R. *et al*. Survey of ERETIC2 NMR for quantification. Journal of the Korean Magnetic Resonance Society, v. 17, p. 98-104, 2013.

53. WATANABE, R. *et al*. Quantitative Nuclear Magnetic Resonance Spectroscopy Based on PULCON Methodology: Application to Quantification of Invaluable Marine Toxin, Okadaic Acid. Toxins, v. 8, p. 294, 2016.

54. WATANABE, R. *et al*. Quantitative Nuclear Magnetic Resonance Spectroscopy Based on PULCON Methodology: Application to Quantification of Invaluable Marine Toxin, Okadaic Acid. Toxins, v. 8, p. 294, 2016.

55. MAK, J. Y. W. Determination of Sample Concentrations by PULCON NMR Spectroscopy. Australian Journal of Chemistry, v. 75, p. 160-164, 2022.

56. FERREIRA, M. M. C. Quimiometria: conceitos, métodos e aplicações. Campinas: Editora da Unicamp, 2015. ISBN 8526814710.

57. AMINU, M.; AHMAD, N. A. Complex Chemical Data Classification and Discrimination Using Locality Preserving Partial Least Squares Discriminant Analysis. ACS Omega, v. 5, p. 26601-26610, 2020.

58. KIM, H. K.; CHOI, Y. H.; VERPOORTE, R. NMR-based metabolomic analysis of plants. Nature Protocols, v. 5, p. 536-49, 2010.

59. BRERETON, R. G.; LLOYD, G. R. Partial least squares discriminant analysis: taking the magic away. Journal of Chemometrics, v. 28, p. 213-225, 2014.

60. TAWFIKE, A. F.; VIEGELMANN, C.; EDRADA-EBEL, R. Metabolomics and dereplication strategies in natural products. Methods in Molecular Biology, v. 1055, p. 227-44, 2013.

61. DAOLIO, C. *et al*. Classification of Commercial Catuaba Samples by NMR, HPLC and Chemometrics. Phytochemical Analysis, v. 17, p. 218–228, 2008.

62. SEHLAKGWE, P. F.; LALL, N.; PRINSLOO, G. ^{1}H-NMR metabolomics and LC-MS analysis to determine seasonal variation in a cosmeceutical plant *Leucosidea sericea*. Frontiers in Pharmacology, v. 11, p. 219, 2020.

63. SOUSA, C. M. D. M. *et al*. Total phenolics and antioxidant activity of five medicinal plants. Quimica Nova, v. 30, p. 351-355, 2007.

64. HUANG, D. J.; OU, B. X.; PRIOR, R. L. The chemistry behind antioxidant capacity assays. Journal of Agricultural and Food Chemistry, v. 53, p. 1841-1856, 2005.

65. MAGINA, M. D. A. *Estudo fitoquímico e biológico de espécies do gênero Eugenia*. 2008. 178 f. Tese (Doutorado em Química) – Departamento de Química, Universidade Federal de Santa Catarina, Florianópolis, 2008.

66. MAGALHAES, L. M. *et al*. Methodological aspects about in vitro evaluation of antioxidant properties. Analytica Chimica Acta**,** v. 613, p. 1-19, 2008.

67. RE, R. *et al*. Antioxidant activity applying an improved ABTS radical cation decolorization assay. Free Radical Biology and Medicine, v. 26, p. 1231-1237, 1999.

68. ALVES, C. Q. et al. Métodos para determinação de atividade antioxidante in vitro em substratos orgânicos. Química Nova**,** v. 33, p. 2202-2210, 2010.

69. MAGALHAES, L. M. *et al*. Methodological aspects about in vitro evaluation of antioxidant properties. Analytica Chimica Acta, v. 613, p. 1-19, 2008.

70. TRESINA, P. S.; KALA, S. M. J.; MOHAN, V. R. HPTLC finger print analysis of phytocompounds and in vitro antioxidant activity of *Eugenia singampattiana* Bedd. Journal of Applied Pharmaceutical Science**,** v. 2, p. 112-124, 2012.

71. DUDONNE, S. *et al*. Comparative Study of Antioxidant Properties and Total Phenolic Content of 30 Plant Extracts of Industrial Interest Using DPPH, ABTS, FRAP, SOD, and ORAC Assays. Journal of Agricultural and Food Chemistry, v. 57, p. 1768-1774, 2009.

72. RUFINO, M. S. M. *et al*. *Metodologia científica: determinação da atividade antioxidante total em frutas pela captura do radical livre DPPH*. Fortaleza: Embrapa, 2007.

73. RUFINO, M. S. M. *et al*. *Metodologia científica: determinação da atividade antioxidante total em frutas pela captura do radical livre* $ABTS^{\bullet+}$. Fortaleza: Embrapa, 2007.

74. BORGES, L. L. *et al*. Uma abordagem sobre métodos analíticos para determinação da atividade antioxidante em produtos naturais. Enciclopédia Biosfera, v. 7, p. 20, 2011.

75. KHALID, M.; PETROIANU, G.; ADEM, A. Advanced Glycation End Products and Diabetes Mellitus: Mechanisms and Perspectives. Biomolecules, v. 12, p. 542, 2022.

76. VISTOLI, G. *et al*. Advanced glycoxidation and lipoxidation end products (AGEs and ALEs): an overview of their mechanisms of formation. Free Radical Research, v. 47, p. 3-27, 2013.

77. ROCK, C. A. *et al*. Model studies of advanced glycation end product modification of heterograft biomaterials: The effects of in vitro glucose, glyoxal, and serum albumin on collagen structure and mechanical properties. Acta Biomaterialia, v. 123, p. 275-285, 2021.

78. ADEOSUN, W. B.; LOOTS, D. T. Medicinal Plants against Viral Infections: A Review of Metabolomics Evidence for the Antiviral Properties and Potentials in Plant Sources. Viruses, v. 16, p. 218, 2024.

79. SANTOS, C. *et al*. Optimization of *Eugenia punicifolia* (Kunth) D. C. leaf extraction using a simplex centroid design focused on extracting phenolics with antioxidant and antiproliferative activities. BMC Chemistry**,** v. 14, p. 34, 2020.

80. KHALEF, L. *et al*. Cell viability and cytotoxicity assays: Biochemical elements and cellular compartments. Cell Biochemistry and Function, v. 42, p. e4007, 2024.

81. CASTILHO, A. R. *et al*. Bioactive Compounds Enhance the Biocompatibility and the Physical Properties of a Glass Ionomer Cement. Journal of Functional Biomaterials, v. 15, p. 332, 2024.

82. RAIOLA, A. *et al*. Bioactive Compound Content and Cytotoxic Effect on Human Cancer Cells of Fresh and Processed Yellow Tomatoes. Molecules, v. 21, p. 33, 2016.

83. MAHAJAN, S. et al. Antiviral strategies targeting host factors and mechanisms obliging +ssRNA viral pathogens. Bioorganic & Medicinal Chemistry**,** v. 46, p. 116356, 2021.

84. RAJESH, N. *et al*. Antiviral Activity of Phytochemicals: A Comprehensive Review. Mini-Reviews in Medicinal Chemistry**,** v. 8, p. 1106-1133, 2008.

85. GOMES, E. O. *et al*. Detection of Zika Virus in *Aedes aegypti* and *Aedes albopictus* Mosquitoes Collected in Urban Forest Fragments in the Brazilian Amazon. Viruses**,** v. 15, p. 1356, 2023.

86. DONALD, C. L. *et al*. Full Genome Sequence and sfRNA Interferon Antagonist Activity of Zika Virus from Recife, Brazil. PLOS Neglected Tropical Diseases**,** v. 10, p. e0005048, 2016.

87. RAMOS, P. R. *et al*. Natural Compounds as Non-Nucleoside Inhibitors of Zika Virus Polymerase through Integration of In Silico and In Vitro Approaches. Pharmaceuticals, v. 15, p. 1493, 2022.

ANEXO

Artigo 1.

Supplementary Information

^{1}H NMR Chemical Profile and Antioxidant Activity of *Eugenia punicifolia* Extracts Over Seasons: A Metabolomic Pilot Study

Kidney O. G. Neves,[a] Maria F. C. Santos,[b] Josiana M. Mar,[c] Flávia L. D. Pontes,[d] Claudio F. Tormena,[b] Francisco C. M. Chaves,[e] Francinete R. Campos,[d] Edgar Aparecido Sanches,[c] Jaqueline A. Bezerra,[f] Marcos B. Machado *,[a] and Alan D. C. Santos *,[a]

[a]*Núcleo de Estudos Químicos de Micromoléculas da Amazônia (NEQUIMA), Universidade Federal do Amazonas, 69067-005 Manaus-AM, Brazil*

[b]*Instituto de Química, Universidade Estadual de Campinas, 13083-862 Campinas-SP, Brazil*

[c]*Laboratório de Polímeros Nanoestruturados (NANOPOL), Departamento de Física de Materiais, Universidade Federal do Amazonas, 69067-005 Manaus-AM, Brazil*

[d]*Departamento de Farmácia, Universidade Federal do Paraná, 80210-170 Curitiba-PR, Brazil*

[e]*Empresa Brasileira de Pesquisa Agropecuária - Embrapa Amazônia Ocidental, 69010-970 Manaus-AM, Brazil*

[f]*Centro Analítico, Instituto Federal de Educação, Ciência e Tecnologia do Amazonas, 69020-120 Manaus-AM, Brazil*

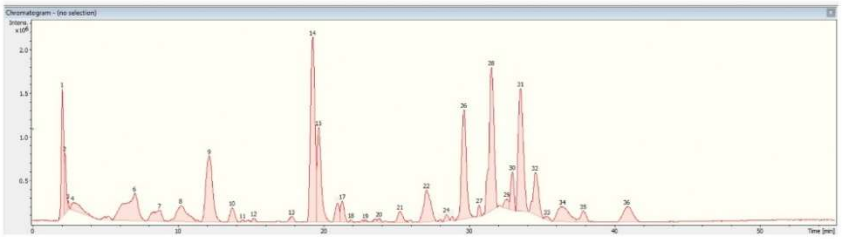

Figure S1. HPLC-DAD-HRMS spectrum of DMSO-d_6 extract from *E. punicifolia*.

*e-mail: alandiegormn@gmail.com.br; marcosmachado@ufam.edu.br

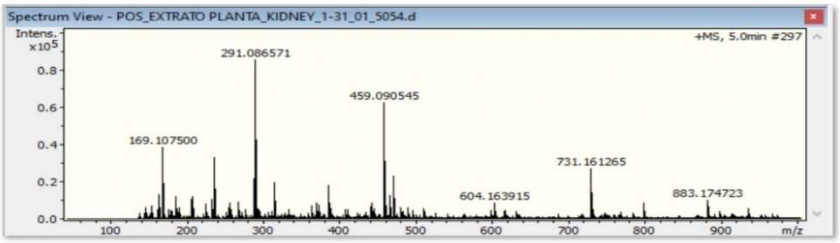

Figure S2. Full scan mass spectrum of the retention time of 5.0 min.

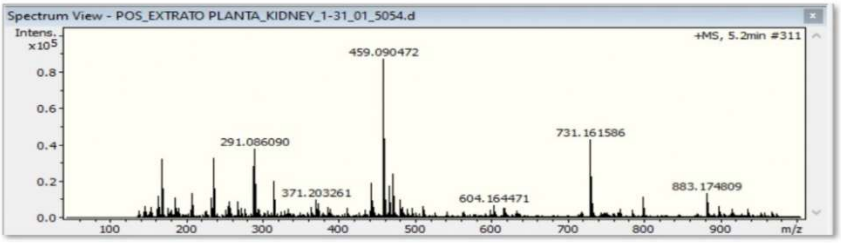

Figure S3. Full scan mass spectrum of the retention time of 5.2 min.

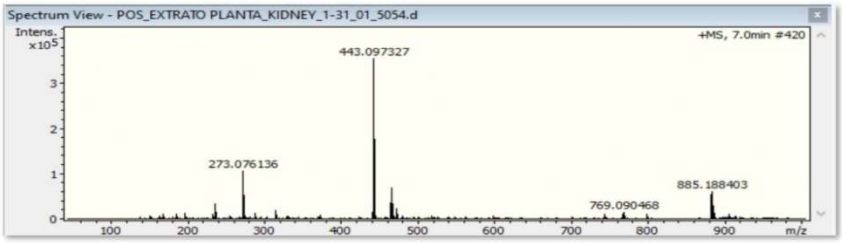

Figure S4. Full scan mass spectrum of the retention time of 7.0 min.

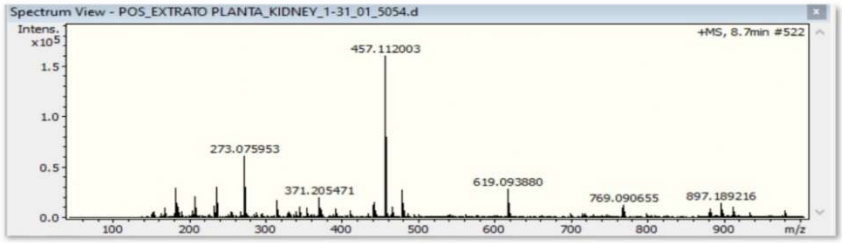

Figure S5. Full scan Mass spectrum of the retention time of 8.7 min.

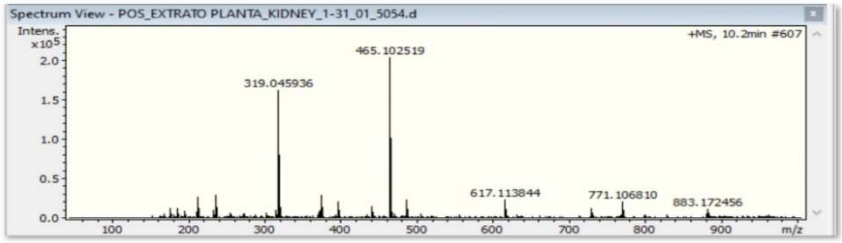

Figure S6. Full scan mass spectrum of the retention time of 10.2 min.

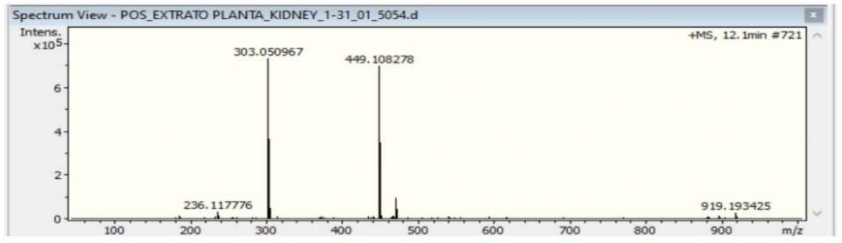

Figure S7. Full scan mass spectrum of the retention time of 12.1 min.

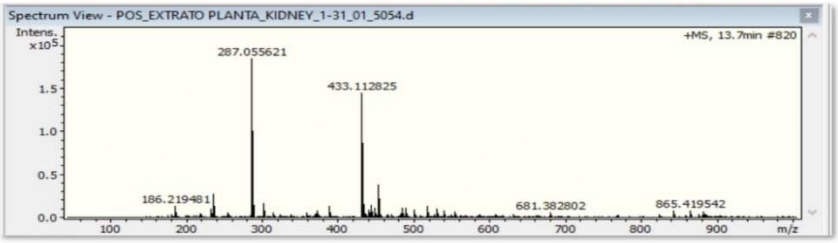

Figure S8. Full scan mass spectrum of the retention time of 13.7 min.

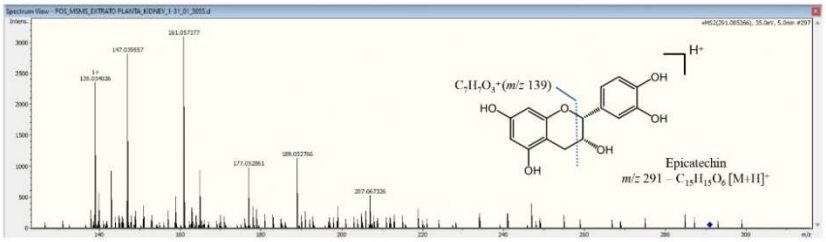

Figure S9. MS/MS spectrum of the ion at *m/z* 291 $[M + H]^+$, epicatechin (**6**).

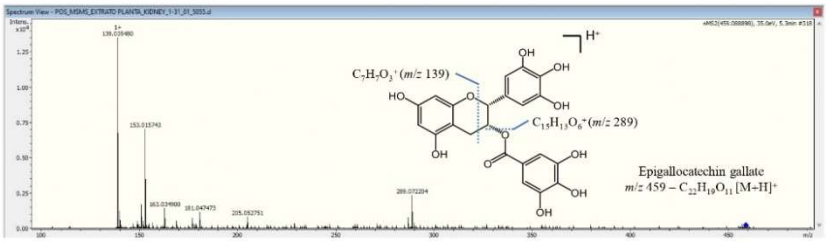

Figure S10. MS/MS spectrum of the ion at *m/z* 459 [M + H]$^+$, epigallocatechin gallate (**9**).

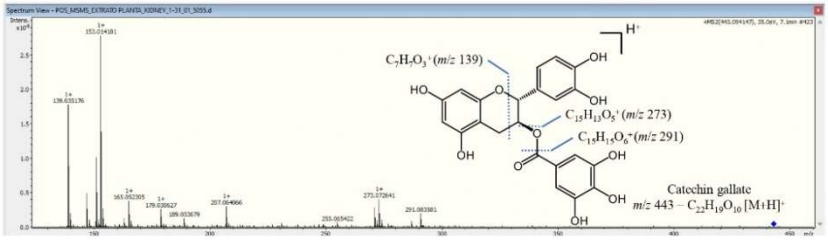

Figure S11. MS/MS spectrum of the ion at *m/z* 443 [M + H]$^+$, catechin gallate (**10**).

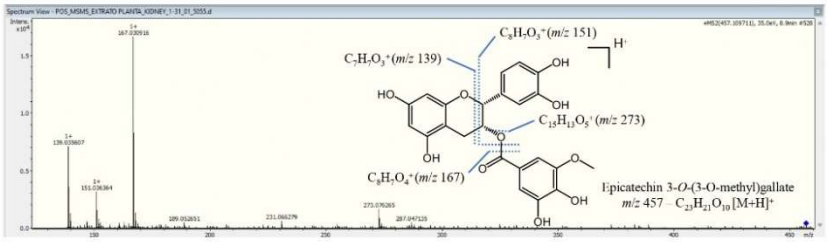

Figure S12. MS/MS spectrum of the ion at *m/z* 457 [M + H]$^+$, epicatechin 3-*O*-(3-*O*-methyl)gallate (**11**).

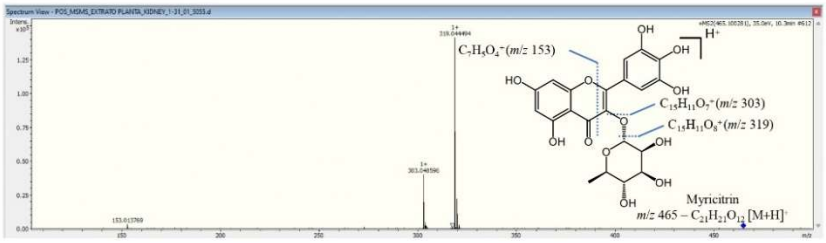

Figure S13. MS/MS spectrum of the ion at *m/z* 465 $[M + H]^+$, myricitrin (**12**).

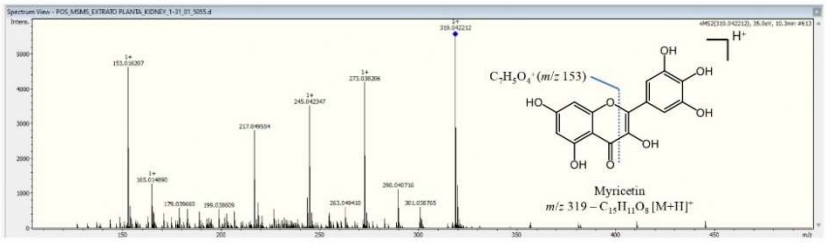

Figure S14. MS/MS spectrum of the ion at *m/z* 319 $[M + H]^+$, myricetin (**13**).

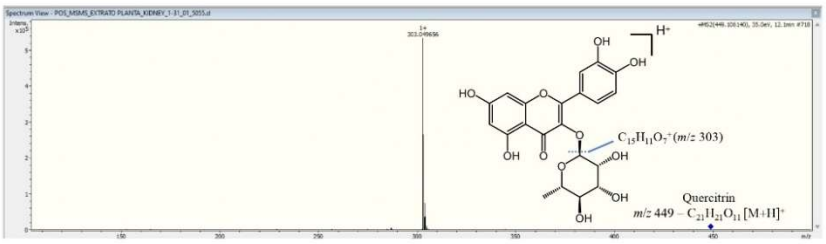

Figure S15. MS/MS spectrum of the ion at *m/z* 449 $[M + H]^+$, quercitrin (**14**).

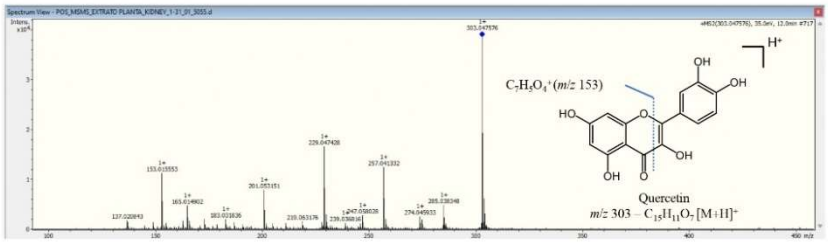

Figure S16. MS/MS spectrum of the ion at *m/z* 303 $[M + H]^+$, quercetin (**7**).

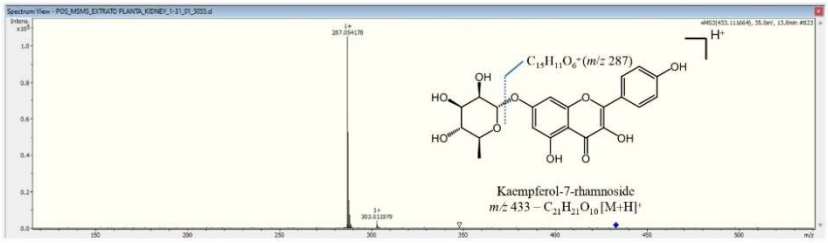

Figure S17. MS/MS spectrum of the ion at *m/z* 433.1075 $[M + H]^+$, kaempferol-7-rhamnoside (15).

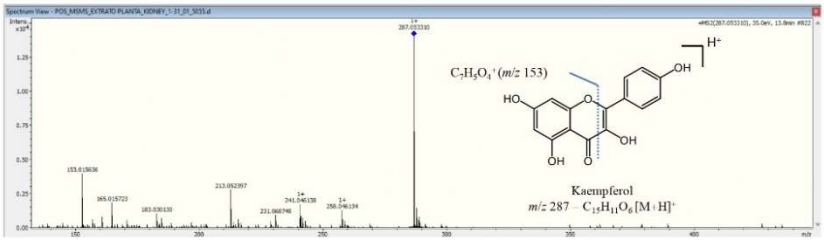

Figure S18. MS/MS spectrum of the ion at *m/z* 287.0527 $[M + H]^+$, kaempferol (**16**).

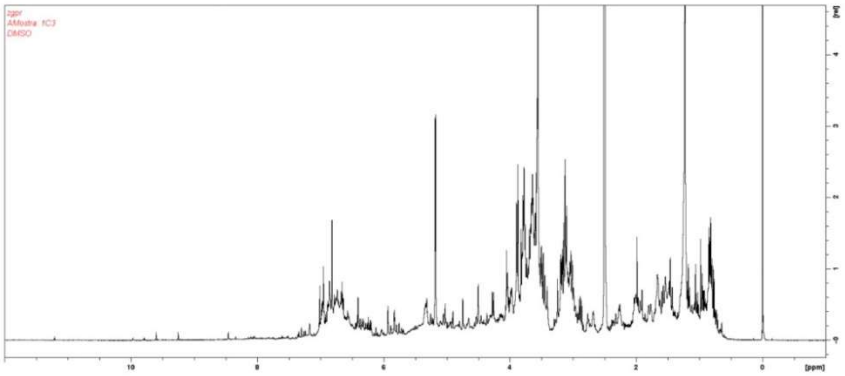

Figure S19. ^{1}H NMR spectrum of *Eugenia punicifolia* DMSO-d_6 extract (−1.00 to 12.00 ppm region).

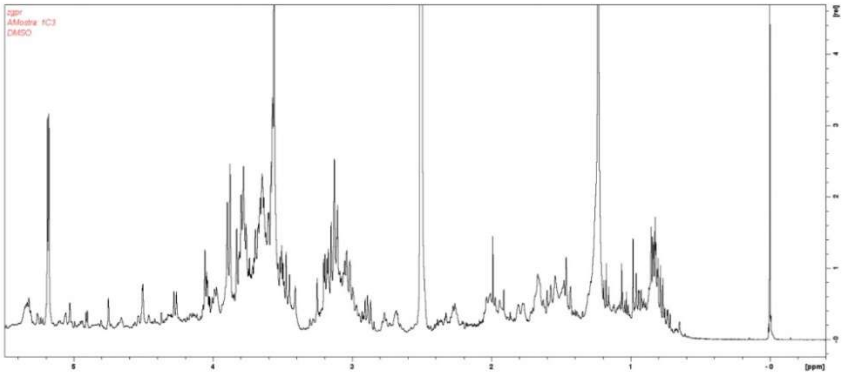

Figure S20. ^{1}H NMR spectrum of *Eugenia punicifolia* DMSO-d_6 extract (range magnification from −0.40 to 5.50 ppm).

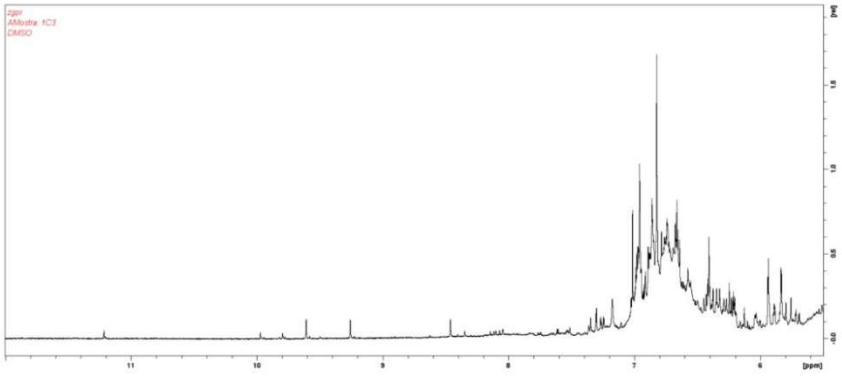

Figure S21. ^{1}H NMR spectrum of *Eugenia punicifolia* DMSO-d_6 extract (range magnification from 5.50 to 12.00 ppm).

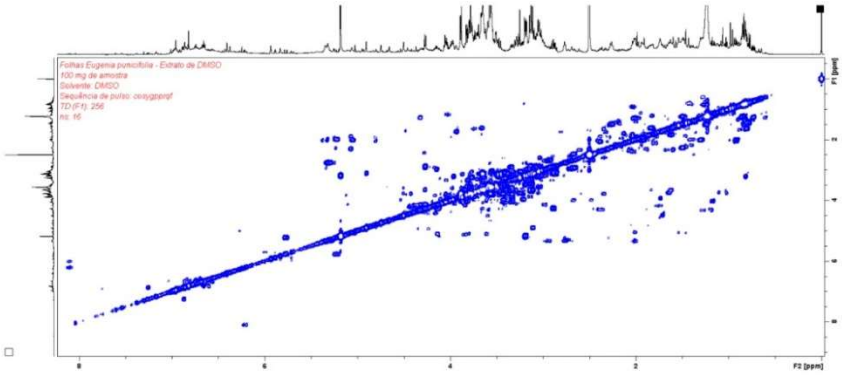

Figure S22. COSY spectrum of *Eugenia punicifolia* DMSO-d_6 extract.

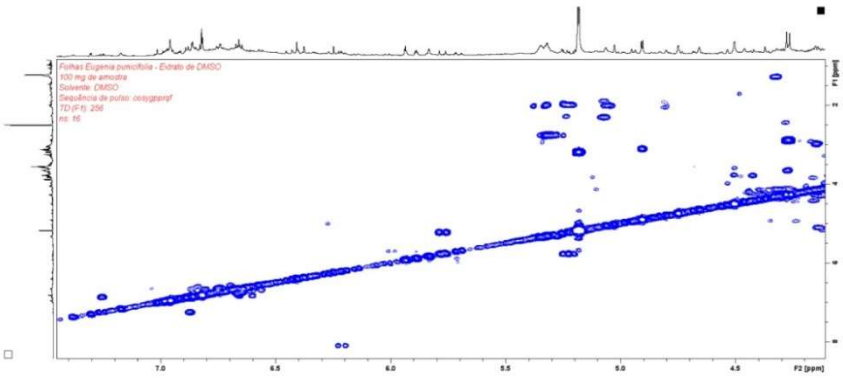

Figure S23. COSY spectrum of *Eugenia punicifolia* DMSO-d_6 extract (range magnification from 4.10 to 7.45 ppm).

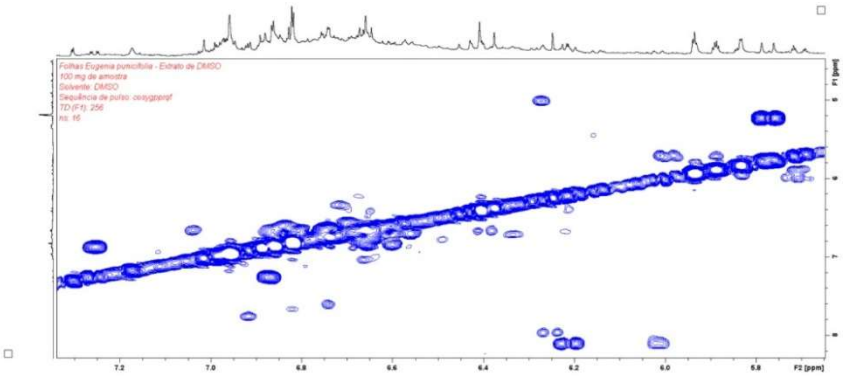

Figure S24. COSY spectrum of *Eugenia punicifolia* DMSO-d_6 extract (range magnification from 5.65 to 7.35 ppm).

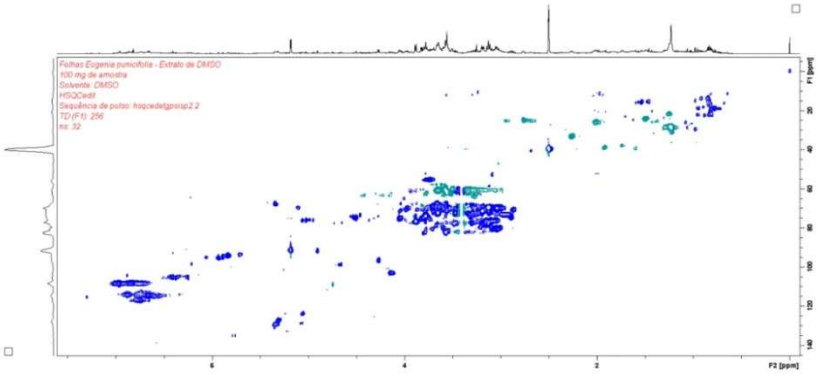

Figure S25. HSQCedit spectrum of *Eugenia punicifolia* DMSO-d_6 extract.

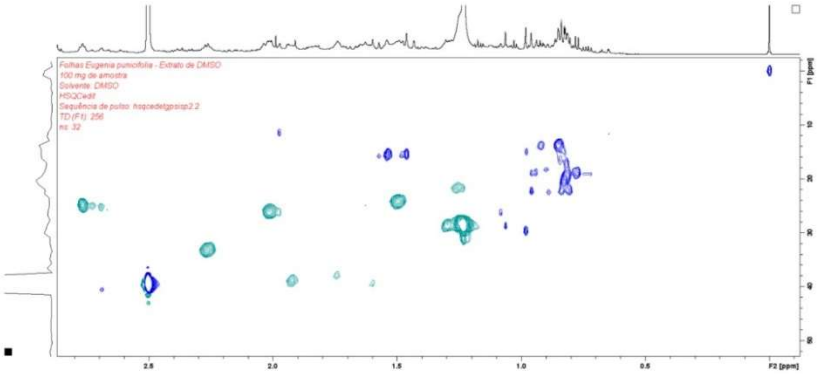

Figure S26. HSQCedit spectrum of *Eugenia punicifolia* DMSO-d_6 extract (range magnification from ^{1}H: –0.10 to 2.86 ppm, ^{13}C: –2.50 to 53.00 ppm).

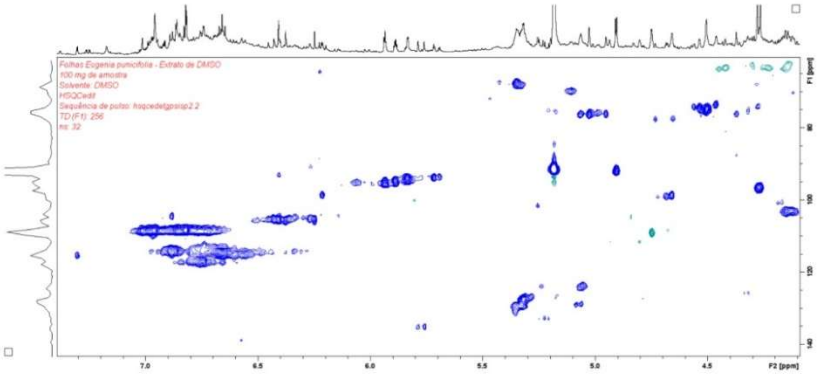

Figure S27. HSQCedit spectrum of *Eugenia punicifolia* DMSO-d_6 extract (range magnification from ^{1}H: 4.10 to 7.40 ppm, ^{13}C: 60.00 to 143.00 ppm).

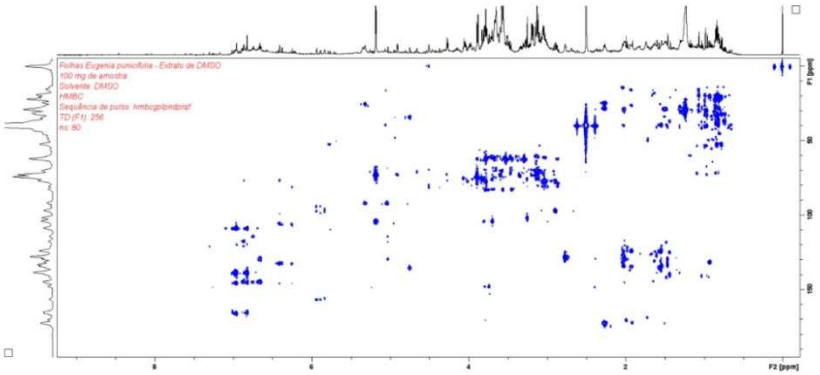

Figure S28. HMBC spectrum of *Eugenia punicifolia* DMSO-d_6 extract.

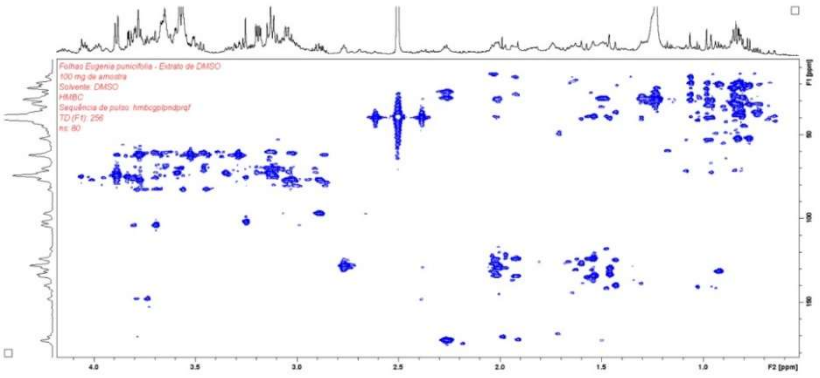

Figure S29. HMBC spectrum of *Eugenia punicifolia* DMSO-d_6 extract (range magnification from ^{1}H: 0.50 to 4.20 ppm, ^{13}C: 5.30 to 182.20 ppm).

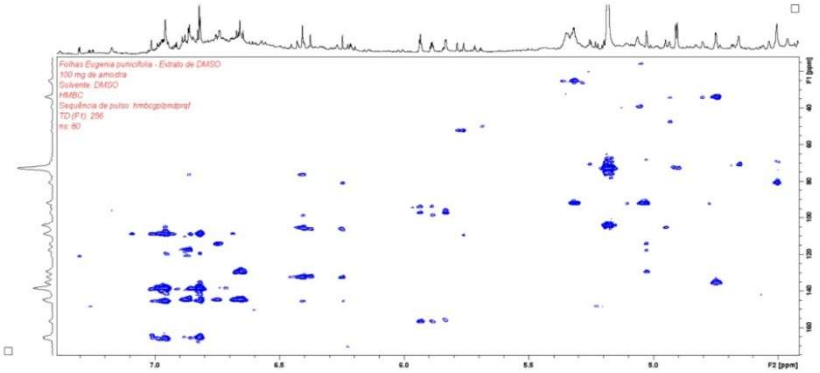

Figure S30. HMBC spectrum of *Eugenia punicifolia* DMSO-d_6 extract (range magnification from ^{1}H: 4.40 to 7.40 ppm, ^{13}C: 13.20 to 175.50 ppm).

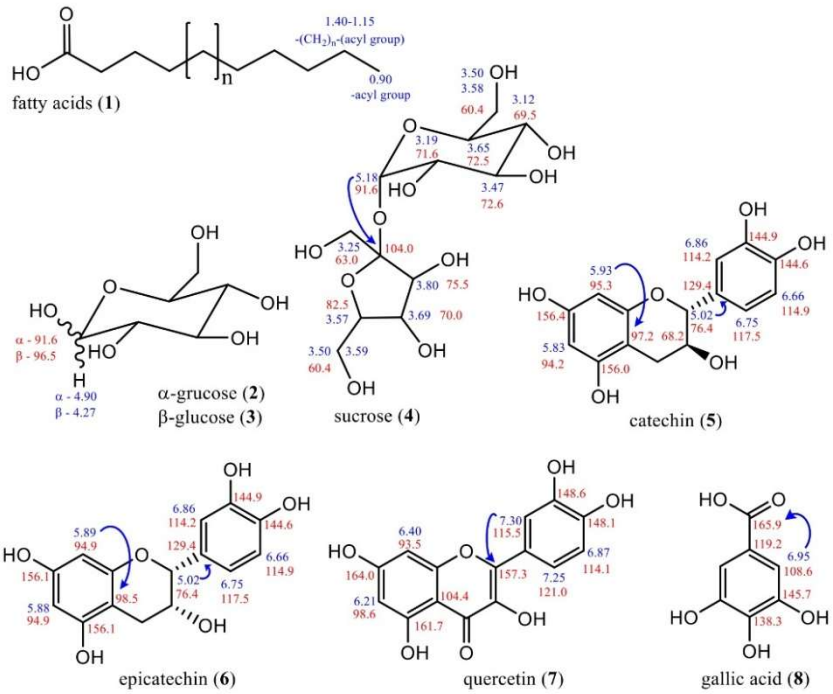

Figure S31. Compounds identified by 1D and 2D NMR in the DMSO-d_6 extract from *E. punicifolia* leaves. The blue arrows represent the key correlations observed in the (^{1}H-^{13}C) HMBC spectrum.

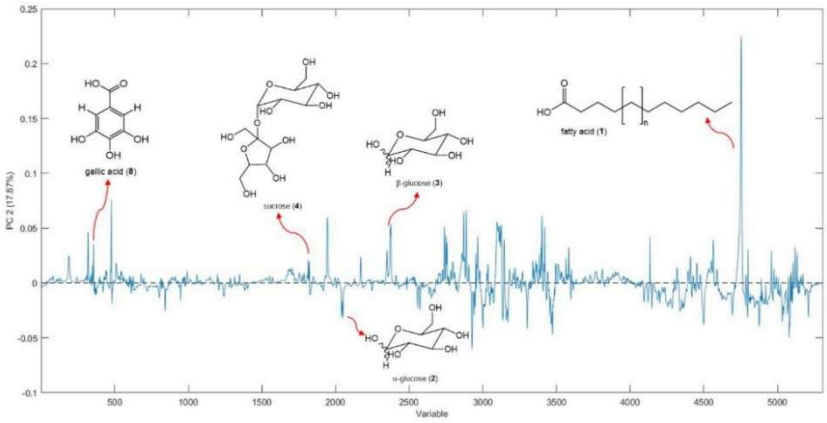

Figure S32. Loadings plot of PC2 discriminating the compounds responsible for the grouping of samples of *E. punicifolia*. Data obtained by ^{1}H NMR (400 MHz, DMSO-d_6).

Artigo 2.

Supplementary Information

Investigation of the Influence of the Extraction System and Seasonality on the Pharmacological Potential of *Eugenia punicifolia* Leaves

Kidney O. G. Neves[1], Samuel O. Silva[1], Marinildo S. Cruz[1], Josiana M. Mar[2], Jaqueline A. Bezerra[2], Edgar A. Sanches[2], Natasha M. Cassani[3], Giovanna A. Antoniucci[3], Ana C. G. Jardim[3], Francisco C. M. Chaves[4], Leonard D. R. Acho[5], Emerson S. Lima[5], Marcos B. Machado[1,*], Alan D. C. Santos[1,6,#]

[1]Núcleo de Estudos Químicos de Micromoléculas da Amazônia - NEQUIMA, Universidade Federal do Amazonas, 69067-005, Manaus-AM, Brazil

[2]Laboratório de Polímeros Nanoestruturados (NANOPOL), Departamento de Física de Materiais, Universidade Federal do Amazonas, 69067-005, Manaus-AM, Brazil

[3]Laboratory of Antiviral Research, Federal University of Uberlândia, 38408-100, Uberlândia - MG, Brazil

[4]Empresa Brasileira de Pesquisa Agropecuária - Embrapa Amazônia Ocidental, 69010-970, Manaus-AM, Brazil

[5]Laboratório de Atividade Biológica, Faculdade de Ciências Farmacêuticas, Universidade Federal do Amazonas, 69067-005, Manaus - AM, Brazil

[6]Núcleo de Pesquisa de Produtos Naturais, Universidade Federal de Santa Maria, Santa Maria - RS, 97105-900, Brazil

*marcosmachado@ufam.edu.br, #alandiegormn@gmail.com.br

Marcos B. Machado: https://orcid.org/0000-0002-8791-4803

Alan D. C. Santos: https://orcid.org/0000-0002-3877-0313

Figure S1. Effect of extract of *Eugenia punicifolia* leaves on viability of Vero E6 cells. Vero E6 cells were treated with each compound at the highest non-cytotoxic concentration. After 72 h, cell viability was measured via the MTT assay. Viability was measured by absorbance (560 nm). DMSO was used as the untreated control. Mean values of two independent experiments, each measured in triplicate including the standard error of the mean, are shown. P values < 0.05 were considered significant. (**) $p < 0.01$, (***) $p < 0.001$, and (****) $p < 0.0001$.

2

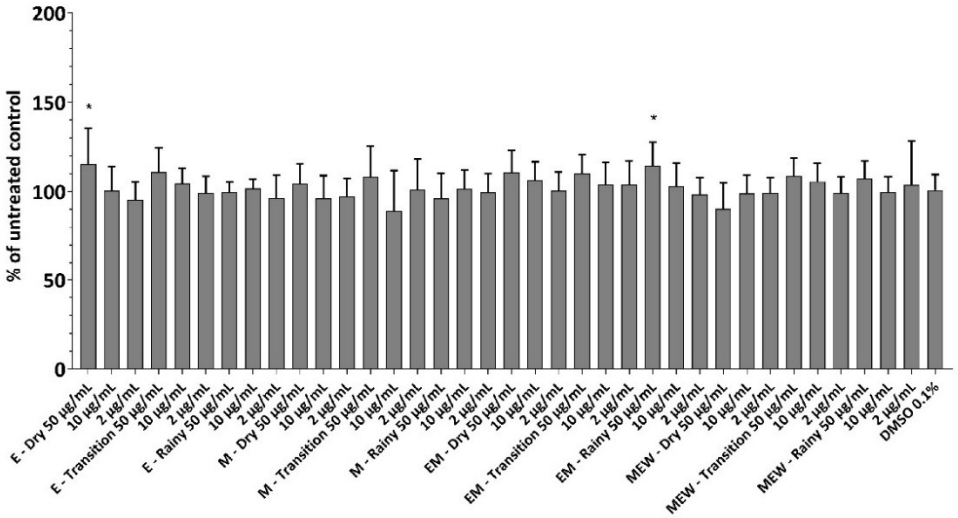

3

Figure S2. ^{1}H NMR spectrum (500 MHz, DMSO-d_6) of MEW extract of *Eugenia punicifolia* leaves collected during the dry season (− 1.00 to 10.00 ppm).

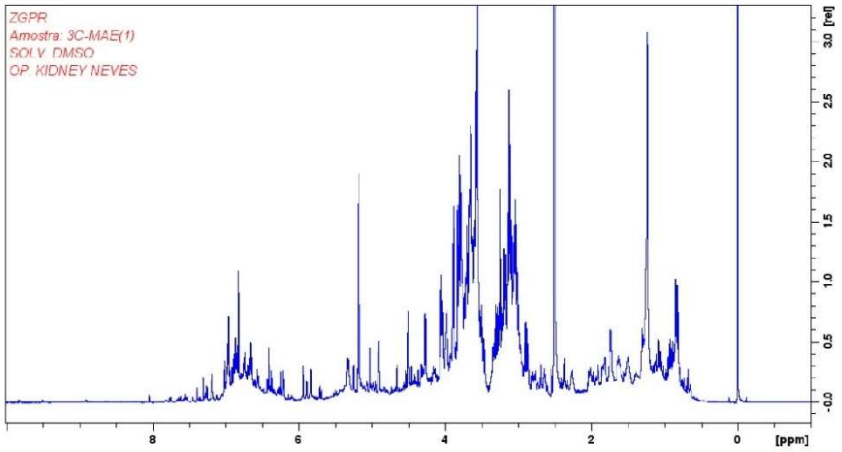

Figure S3. HSQC spectrum (500 MHz, DMSO-d_6) of MEW extract of *Eugenia punicifolia* leaves collected during the dry season (range magnification of ^{1}H: - 0.50 to 8.30 ppm - 13C: - 3.0 to 158.0 ppm).

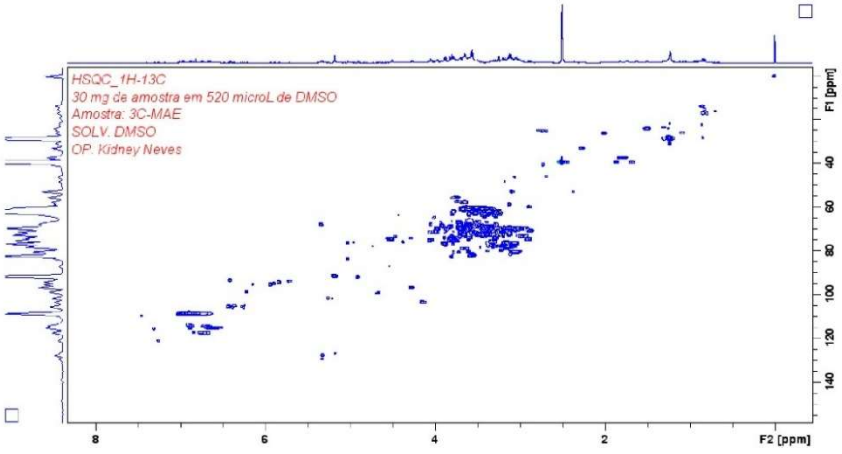

4

Figure S4. HSQC spectrum (^{1}H: 500 MHz, ^{13}C: 125 MHz DMSO-d_6) of MEW extract of *Eugenia punicifolia* leaves collected during the dry season (range magnification of ^{1}H: 5.50 to 7.80 ppm - ^{13}C: 96.0 to 128.0 ppm). Signals corresponding to gallic acid (**1**: δ 6.95 - δ 108.6), quercetin (**2**: δ 7.30 - δ 115.5), myricetin (**3**: δ 7.01 - δ 108.7), catechin (**4**: δ 5.93 - δ 95.4) and epigallocatechin (**5**: δ 5.89 - δ 95.1)].

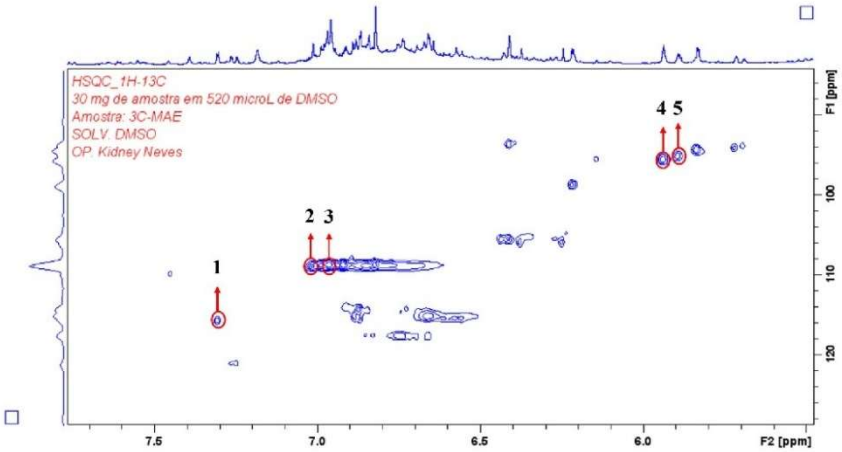

Figure S5. HMBC spectrum (^{1}H: 500 MHz, ^{13}C: 125 MHz DMSO-d_6) of MEW extract of *Eugenia punicifolia* leaves collected during the dry season (range magnification of ^{1}H: - 0.50 to 8.50 ppm - 13C: - 4.7 to 193.3 ppm),.

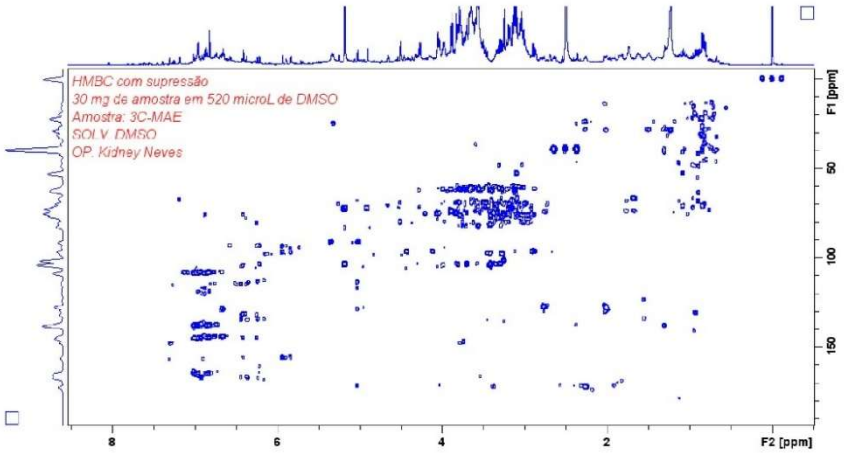

Figure S6. HMBC spectrum (^{1}H: 500 MHz, ^{13}C: 125 MHz DMSO-d_6) of MEW extract of *Eugenia punicifolia* leaves collected during the dry season (range magnification of ^{1}H: 5.55 to 7.40 ppm - ^{13}C: 50.7 to 180.2 ppm).

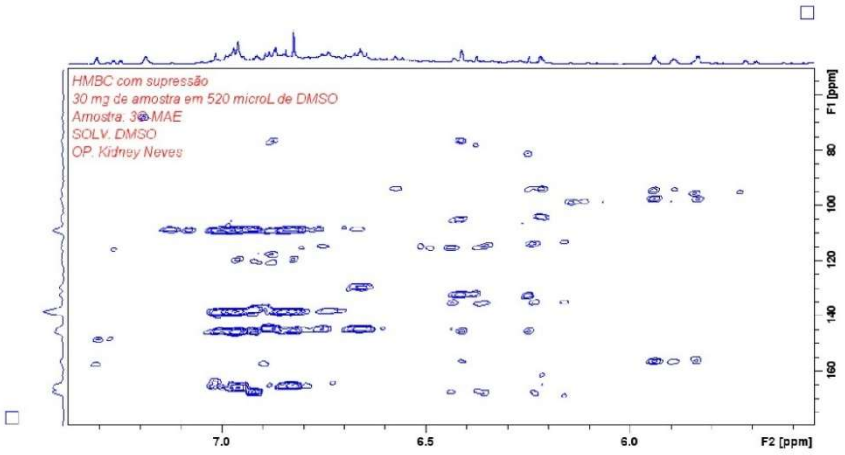

Figure S7. ^{1}H NMR spectrum (500 MHz, DMSO-d_6) of extracts of *Eugenia punicifolia* leaves collected during the dry season (- 1.00 to 10.00 ppm).

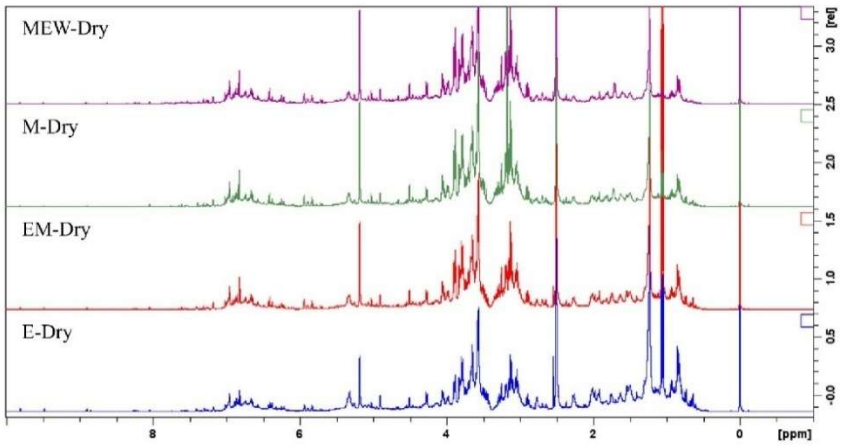

Figure S8. ^{1}H NMR spectrum (500 MHz, DMSO-d_6 - range magnification from 8.00 to 5.50 ppm) of extracts of *Eugenia punicifolia* leaves collected during the dry season. Signals corresponding to gallic acid (**1**: δ 6.95), quercetin (**2**: δ 7.30), myricetin (**3**: δ 7.01), catechin (**4**: δ 5.93) and epigallocatechin (**5**: δ 5.89)]. Extract acronyms: MEW – methanol:ethanol:water; M – methanol; EM – ethanol:methanol; and E – ethanol.

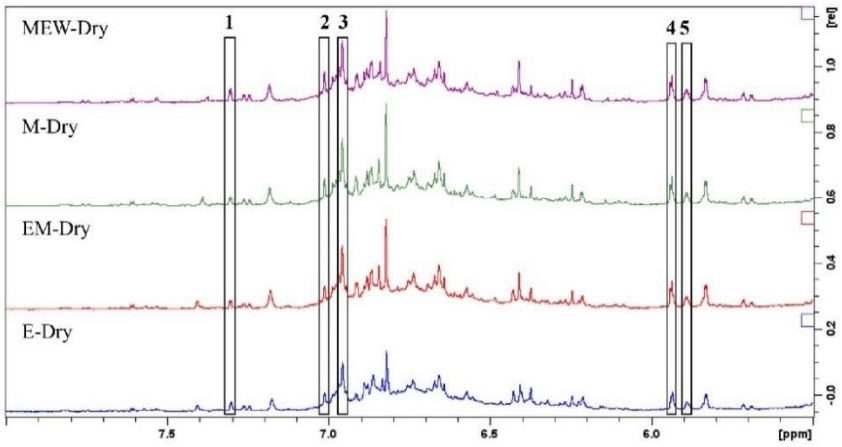

Figure S9. ^{1}H NMR spectrum (500 MHz, DMSO-d_6) of extracts of *Eugenia punicifolia* leaves collected during the transition season (- 1.00 to 10.00 ppm region).

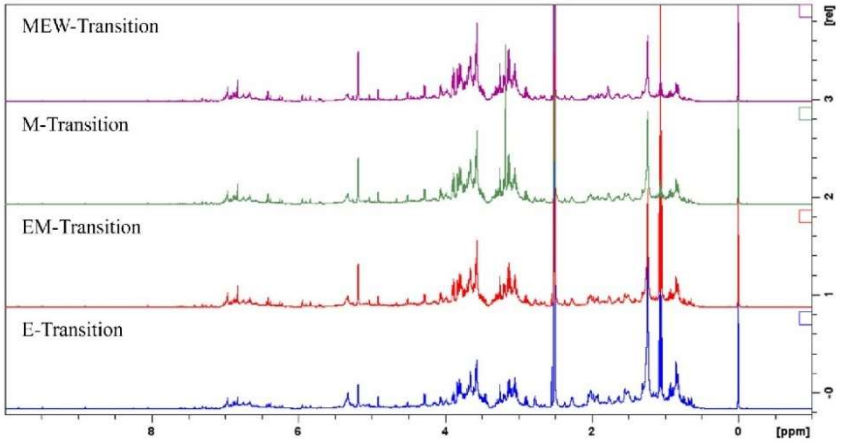

Figure S10. ^{1}H NMR spectrum (500 MHz, DMSO-d_6 - range magnification from 8.00 to 5.50 ppm) of extracts of *Eugenia punicifolia* leaves collected during the transition season. Signals corresponding to gallic acid (**1**: δ 6.95), quercetin (**2**: δ 7.30), myricetin (**3**: δ 7.01), catechin (**4**: δ 5.93) and epigallocatechin (**5**: δ 5.89)]. Extract acronyms: MEW – methanol:ethanol:water; M – methanol; EM – ethanol:methanol; and E – ethanol.

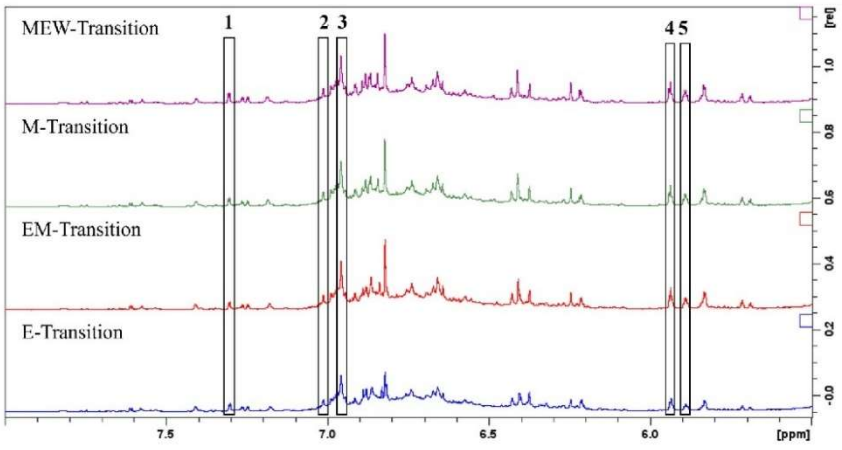

Figure S11. ^{1}H NMR spectrum (500 MHz, DMSO-d_6) of extracts of *Eugenia punicifolia* leaves collected during the rainy season (- 1.00 to 10.00 ppm).

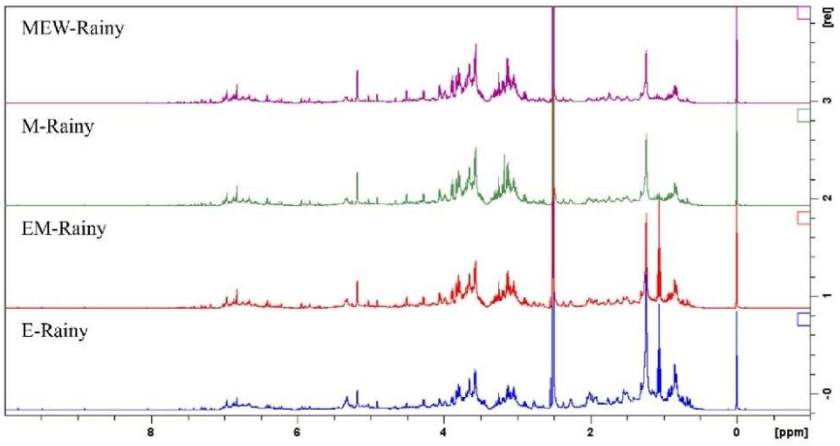

Figure S12. ^{1}H NMR spectrum (500 MHz, DMSO-d_6 - range magnification from 8.00 to 5.50 ppm) of extracts of *Eugenia punicifolia* collected during the transition season. Signals corresponding to gallic acid (**1**: δ 6.95), quercetin (**2**: δ 7.30), myricetin (**3**: δ 7.01), catechin (**4**: δ 5.93) and epigallocatechin (**5**: δ 5.89). Extract acronyms: MEW – methanol:ethanol:water; M – methanol; EM – ethanol:methanol; and E – ethanol.

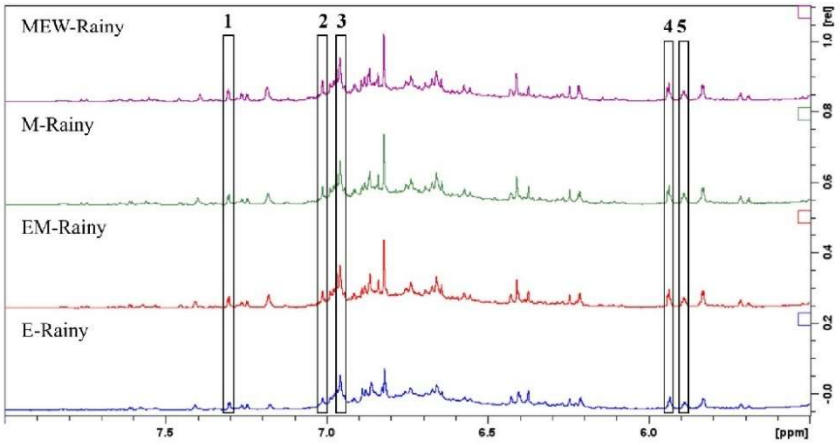

9

Table S1. Pearson correlation coefficient between the concentration determined by ^{1}H NMR and the scavenging capacity of the DPPH radical, the ABTS radical cation, and inhibition of AGE formation. **1** - gallic acid, **2** - epigallocatechin, **3** - catechin, **4** - quercetin, and **5** - myricetin.

	(**1**)	(**2**)	(**3**)	(**4**)	(**5**)	DPPH$^{\bullet}$	ABTS$^{\bullet+}$	AGEs inhibition
(**1**)	1.00	0.54	0.25	0.22	0.32	− 0.01	0.32	0.60
(**2**)	0.54	1.00	0.73	0.66	0.85	0.41	0.67	0.50
(**3**)	0.25	0.73	1.00	0.29	0.70	0.05	0.16	0.16
(**4**)	0.22	0.66	0.29	1.00	0.78	0.85	0.87	0.33
(**5**)	0.32	0.85	0.70	0.78	1.00	0.58	0.65	0.48
DPPH$^{\bullet}$	− 0.01	0.41	0.05	0.85	0.58	1.00	0.90	0.42
ABTS$^{\bullet+}$	0.32	0.67	0.16	0.87	0.65	0.90	1.00	0.56
AGEs inhibition	0.60	0.50	0.16	0.33	0.48	0.42	0.56	1.00

Artigo 3.

Supplementary Information

How seasonality shapes key phenolic compounds of *Eugenia punicifolia*: a metabolomic approach to abiotic stress

Kidney O. G. Neves [1], Samuel O. Silva [1], Marinildo S. Cruz [1], Francisco C. M. Chaves[2], Marcos B. Machado [1,*] and Alan D. C. Santos [1,3,#]

[1]Núcleo de Estudos Químicos de Micromoléculas da Amazônia - NEQUIMA, Universidade Federal do Amazonas, 69067-005, Manaus, AM, Brazil

[2]Empresa Brasileira de Pesquisa Agropecuária - Embrapa Amazônia Ocidental, 69010-970, Manaus, AM, Brazil

[3]Núcleo de Pesquisa de Produtos Naturais, Universidade Federal de Santa Maria, Santa Maria, RS, 97105-900, Brazil

Correspondence: #alandiegormn@gmail.com.br, marcosmachado@ufam.edu.br,

Alan D. C. Santos: https://orcid.org/0000-0002-3877-0313

Marcos B. Machado: https://orcid.org/0000-0002-8791-4803

Table S1. Climatic data collected monthly over the 12-month study period. Air temperature and relative humidity were reported as monthly mean values, while precipitation, number of rainy days, evaporation, and insolation were expressed as the cumulative totals for each month.

Months	Temperature (˚C)			Relative humidity (%)	Rainfall (mm)	Rainy days	Evaporation (mm)	Insolation (hour)
	Maximum	Minimum	Average					
January	30.7	22.4	25.6	88.8	345.1	23	47.5	70.9
February	31.2	22.5	26.1	88.8	460.0	22	40.7	64.8
March	31.8	23.0	26.6	87.6	384.3	20	54.5	92.9
April	32.9	23.2	27.0	88.6	297.1	25	53.1	97.7
May	33.6	23.6	27.7	86.5	183.4	19	56.8	123.2
June	32.4	22.7	26.8	86.4	101.6	16	55.9	140.9
July	34.1	22.8	27.8	79.6	61.9	6	93.6	208.9
August	35.3	23.2	28.6	77.1	85.1	8	112.0	212.2
September	36.1	23.3	28.9	79.1	46.4	8	124.5	171.9
October	36.3	23.8	29.3	74.3	67.5	7	140.2	143.7
November	35.0	23.9	28.8	79.4	114.8	7	105.2	134.5
December	31.8	23.2	27.0	89.2	268.6	21	54.0	67.1

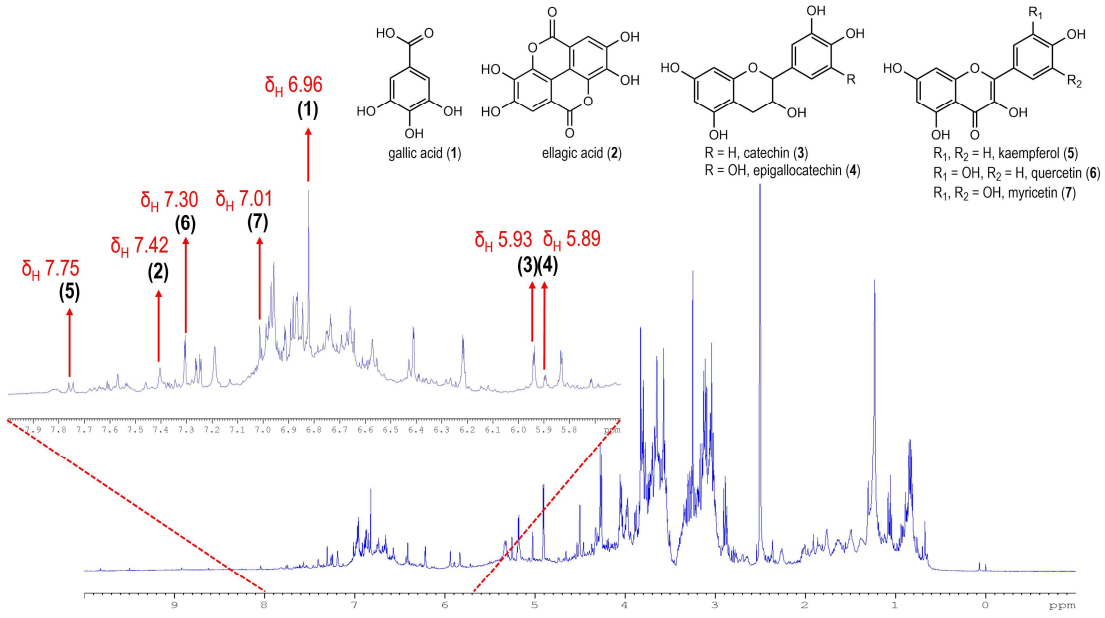

Figure S1. Expanded aromatic region (5.70 to 8.00 ppm) of the ^{1}H NMR spectrum of the MEW extract from *Eugenia punicifolia* leaves (500MHz, DMSO-d6).

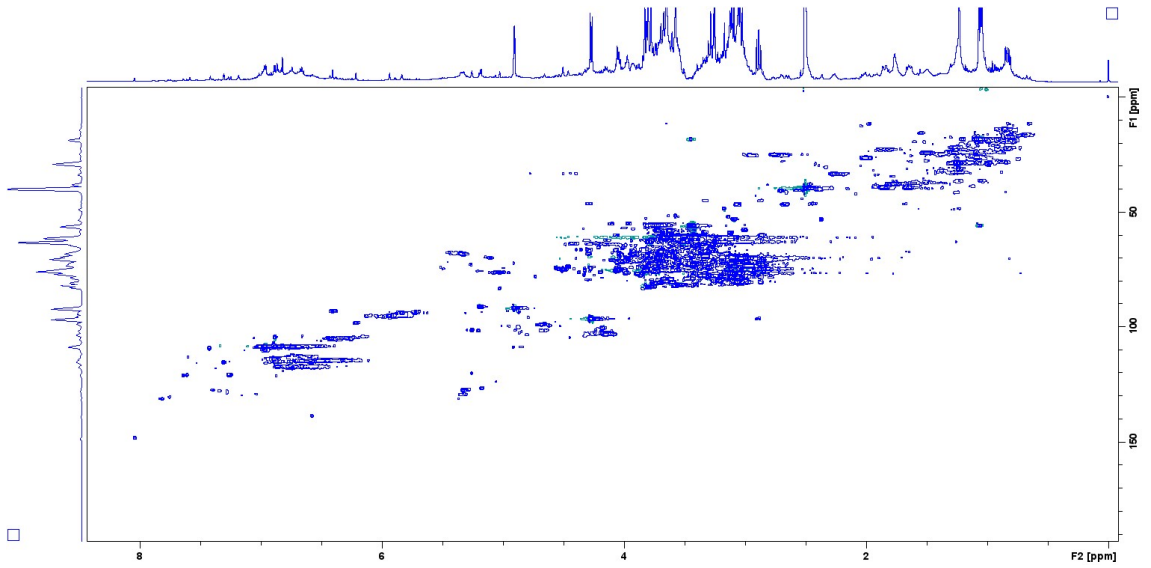

Figure S2. ^{1}H-^{13}C HSQC spectrum of the MEW extract from *Eugenia punicifolia* leaves (500MHz, DMSO-d6).

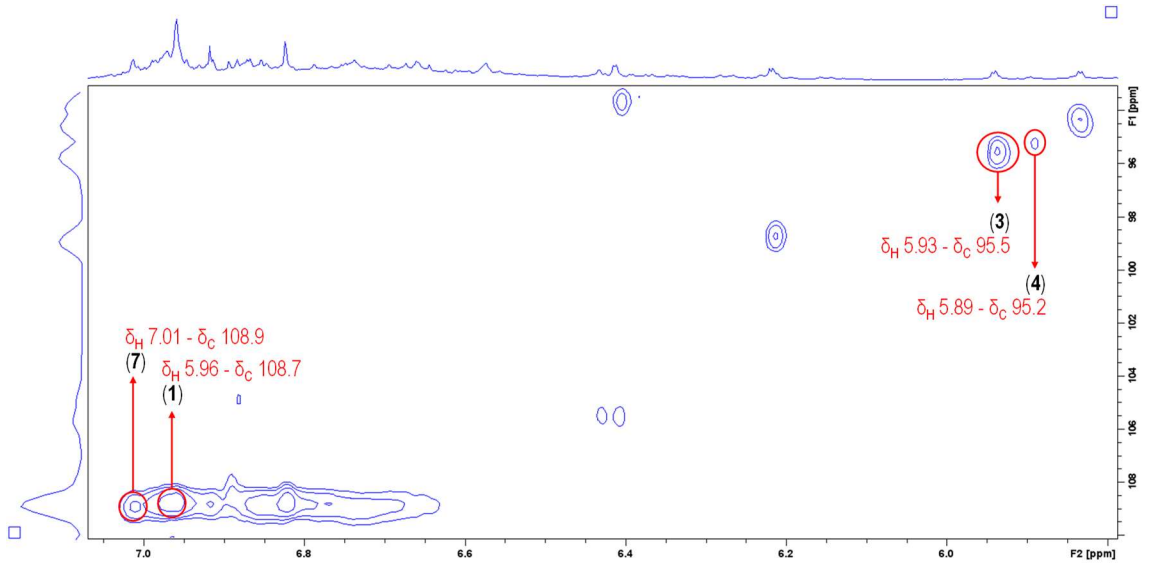

Figure S3. Expansion of the aromatic region of the ^{1}H-^{13}C HSQC spectrum of the MEW extract from *Eugenia punicifolia* leaves (500MHz, DMSO-d6).

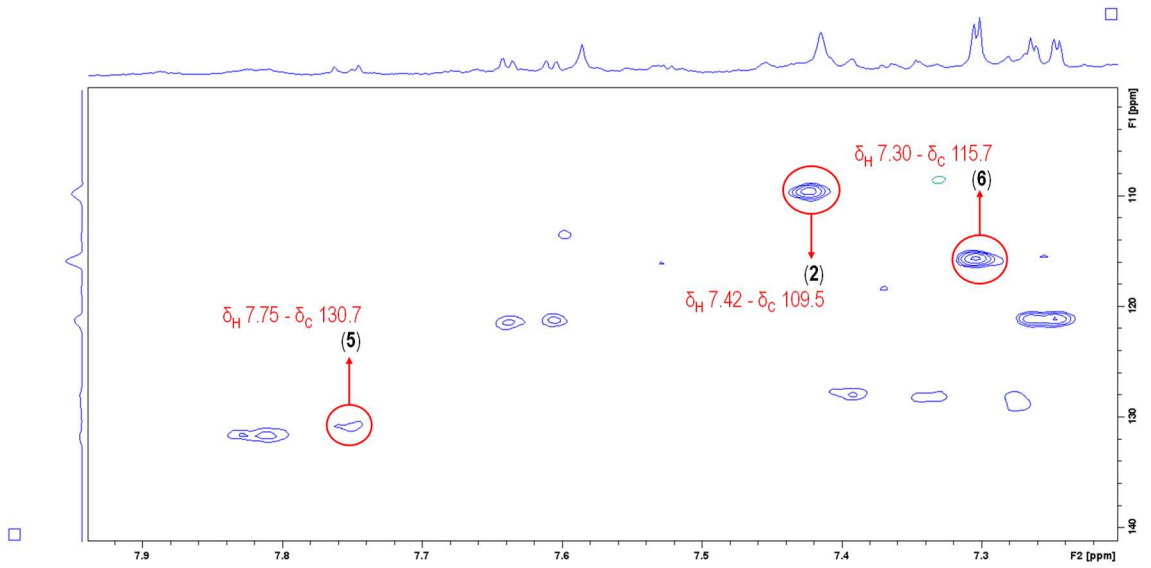

Figure S4. Expansion of the aromatic region of the ^{1}H-^{13}C HSQC spectrum of the MEW extract from *Eugenia punicifolia* leaves (500MHz, DMSO-d6).

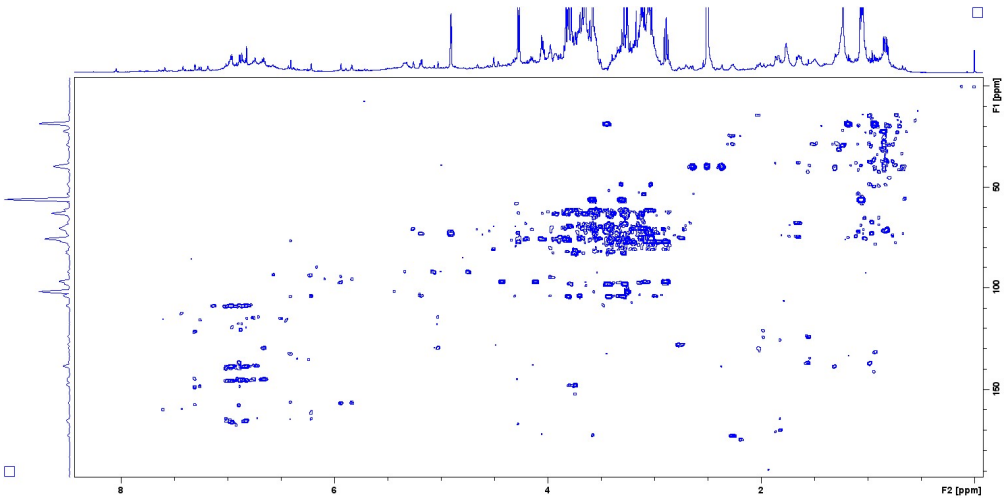

Figure S5. ^{1}H-^{13}C HMBC spectrum of the MEW extract from *Eugenia punicifolia* leaves (500MHz, DMSO-d6).

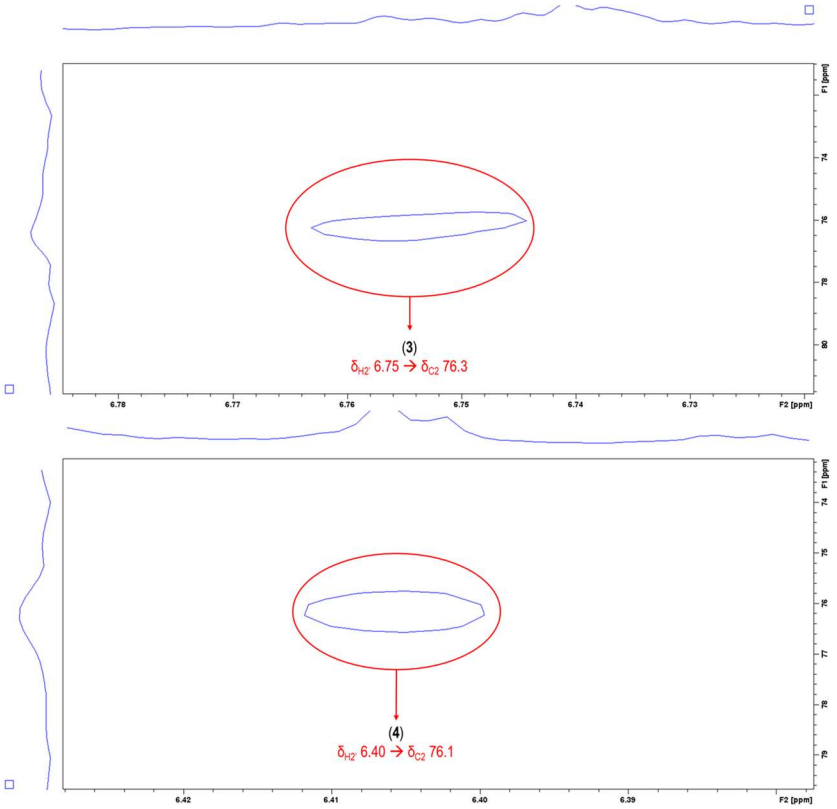

Figure S6. Expansion of the aromatic region of the ^{1}H-^{13}C HMBC spectrum of the MEW extract from *Eugenia punicifolia* leaves. Key correlation for confirmation of binding between catechin and epigallocatechin B and C rings (500MHz, DMSO-d6).

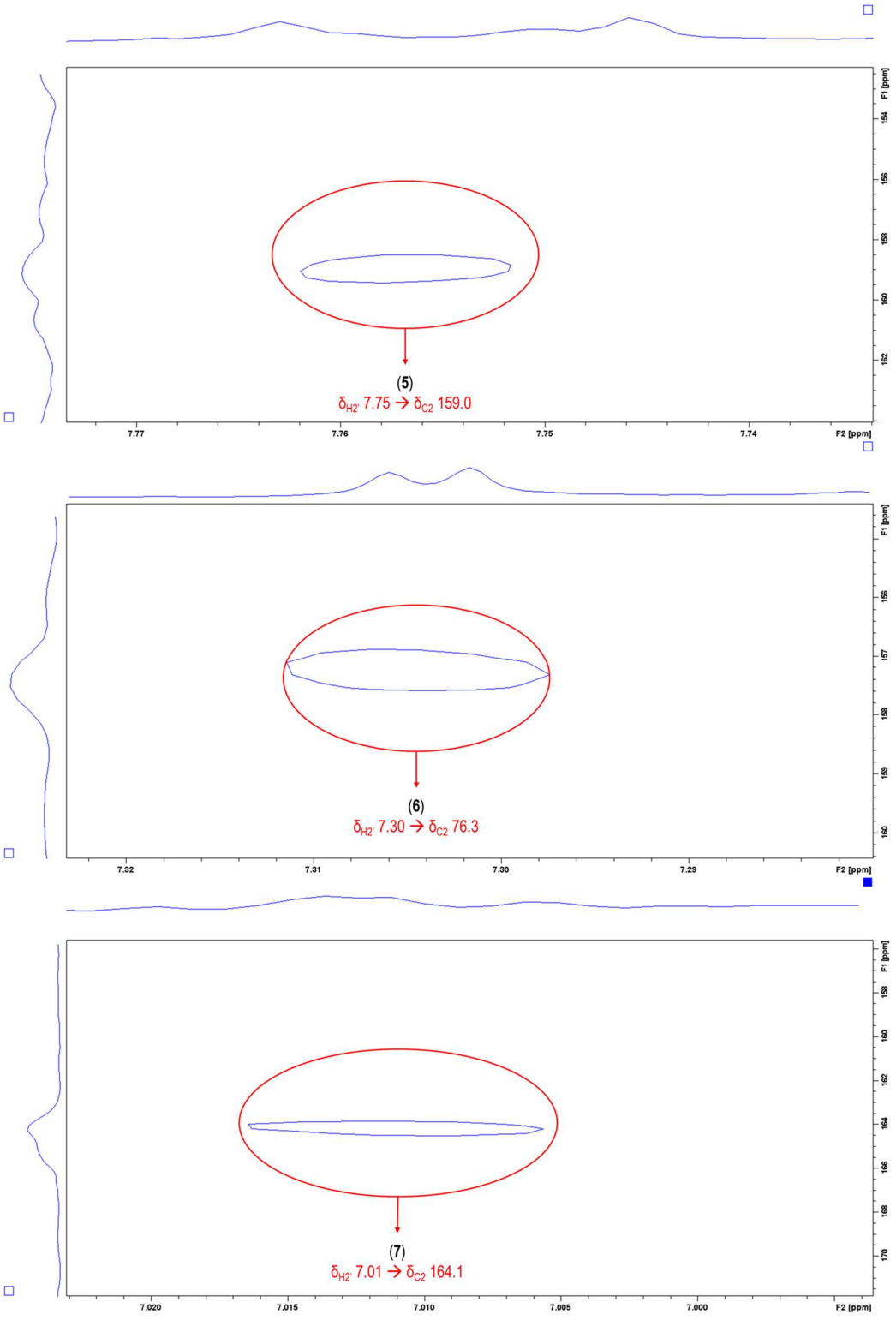

Figure S7. Expansion of the aromatic region of the ^{1}H-^{13}C HMBC spectrum of the MEW extract from *Eugenia punicifolia* leaves. Key correlation for confirmation of binding between apigen, myricetin and quercetin B and C rings (500MHz, DMSO-d6).

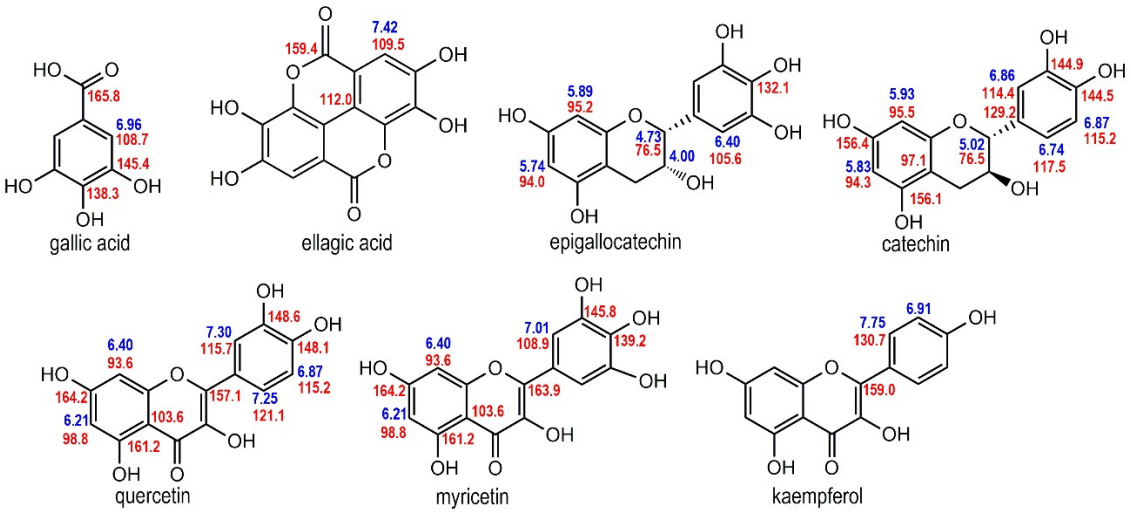

Figure S8. Main chemical shifts (ppm) observed in ^{1}H NMR, ^{1}H-^{13}C HSQC and ^{1}H-^{13}C HMBC spectra (500 MHz, DMSO-d_6).

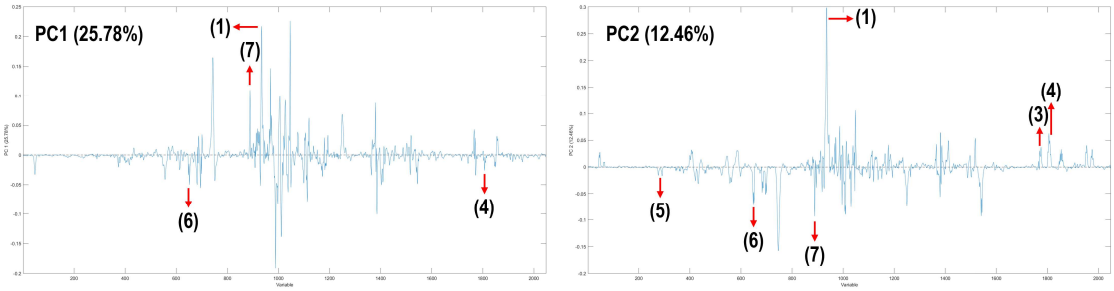

Figure S9. Loadings plot of PC1 and PC2 discriminating the compounds responsible for the grouping of samples of *E. punicifolia* (500MHz, DMSO-d6).

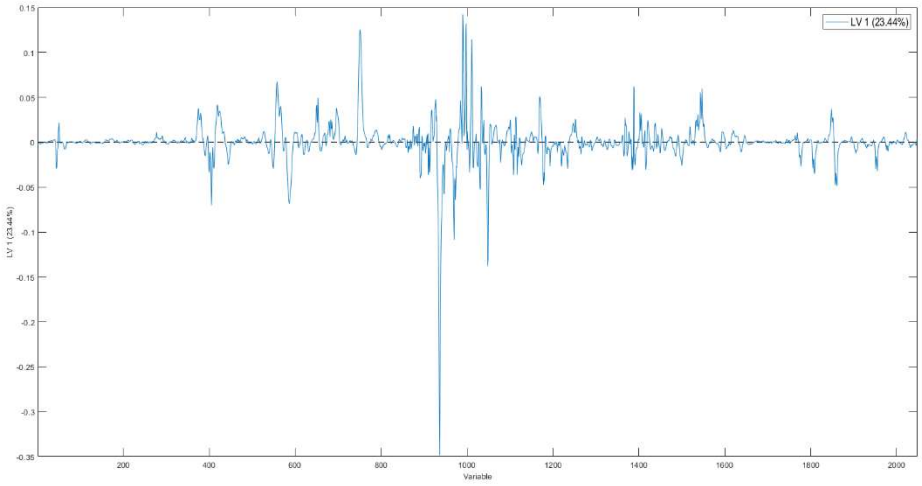

Figure S10. Loadings plot of LV1 illustrating the compounds responsible for the classification of **Groups 1** and **2** in the PLS-DA model (500MHz, DMSO-d6).

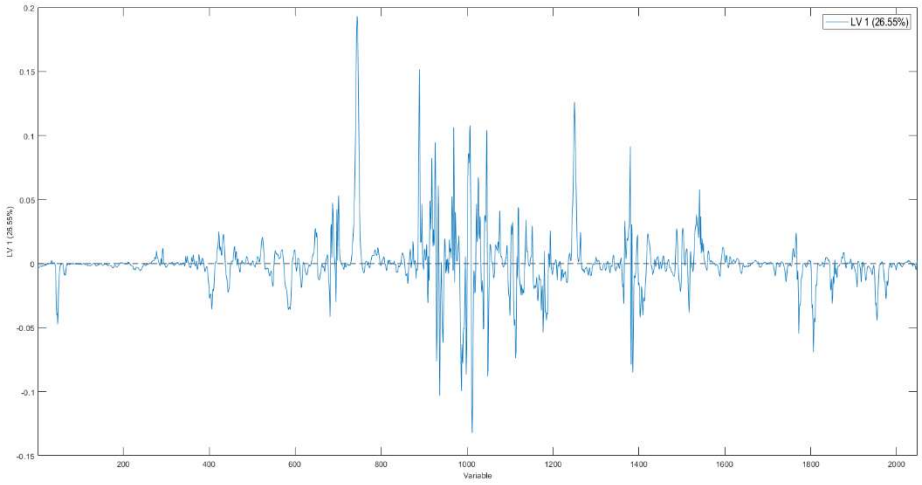

Figure S11. Loadings plot of LV1 illustrating the compounds responsible for the classification of **Groups 1** and **3** in the PLS-DA model (500MHz, DMSO-d6).

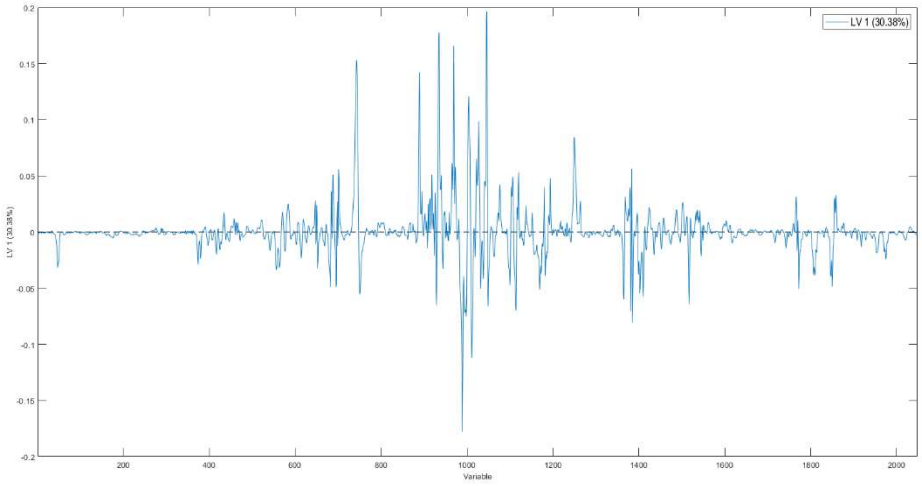

Figure S12. Loadings plot of LV1 illustrates the compounds responsible for the classification of **Groups 2** and **3** in the PLS-DA model (500MHz, DMSO-d6).

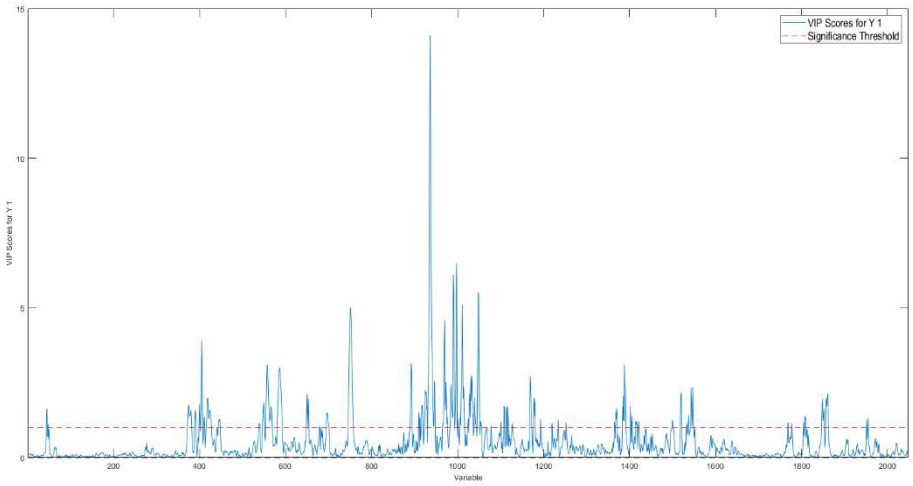

Figure S13. Vip scores plot of classification of **Groups 1** and **2** in the PLS-DA model (500MHz, DMSO-d6).

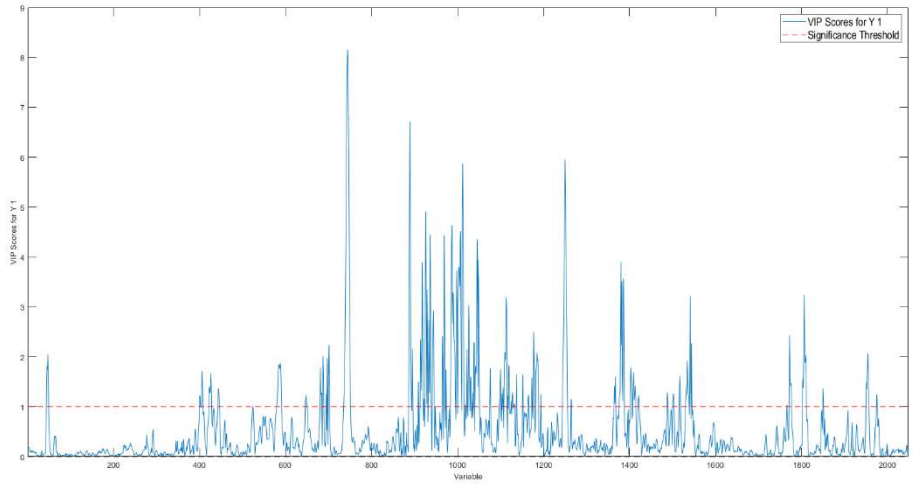

Figure S14. Vip scores plot of classification of **Groups 1** and **3** in the PLS-DA model (500MHz, DMSO-d6).

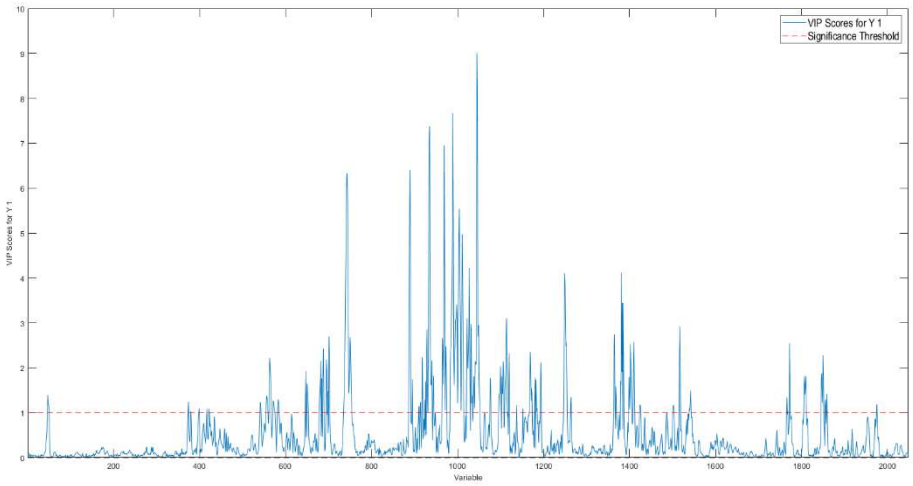

Figure S15. Vip scores plot of classification of **Groups 2** and **3** in the PLS-DA model (500MHz, DMSO-d6).